Analysis Procedures for Evaluating Superheavy Load Movement on Flexible Pavements, Volume III: Appendix B, Superheavy Load Configurations and Nucleus of Analysis Vehicle

PUBLICATION NO. FHWA-HRT-18-051

DECEMBER 2018

U.S. Department of Transportation
Federal Highway Administration

Research, Development, and Technology
Turner-Fairbank Highway Research Center
6300 Georgetown Pike
McLean, VA 22101-2296

FOREWORD

The movement of superheavy loads (SHLs) on the Nation's highways is an increasingly common, vital economic necessity for many important industries, such as chemical, oil, electrical, and defense. Many superheavy components are extremely large and heavy (gross vehicle weights in excess of a few million pounds), and they often require specialized trailers and hauling units. At times, SHL vehicles have been assembled to suit the load being transported, and therefore, the axle configurations have not been standard or consistent. Accommodating SHL movements without undue damage to highway infrastructure requires the determination of whether the pavement is structurally adequate to sustain the SHL movement and protect any underground utilities. Such determination involves analyzing the likelihood of instantaneous or rapid load-induced shear failure of the pavement structure.

The goal of this project was to develop a comprehensive analysis process for evaluating SHL movement on flexible pavements. As part of this project, a comprehensive mechanistic-based analysis approach consisting of several analysis procedures was developed for flexible pavement structures and documented in a 10-volume series of Federal Highway Administration reports—a final report and 9 appendices.[1–9] This report is *Analysis Procedures for Evaluating Superheavy Load Movement on Flexible Pavements, Volume III: Appendix B, Superheavy Load Configurations and Nucleus of Analysis Vehicle*, and it details the approach developed to identify a segment of the SHL configuration that can be regarded as representative of the entire vehicle. Pavement responses under the entire SHL configuration can then be estimated by superimposing stresses calculated under the proposed element, eliminating the need to model the entire vehicle. This report is intended for use by highway agency pavement engineers responsible for assessing the structural adequacy of pavements in the proposed route and identifying mitigation strategies, where warranted, in support of the agency's response to SHL-movement permit requests.

Cheryl Allen Richter, P.E., Ph.D.
Director, Office of Infrastructure
Research and Development

TECHNICAL REPORT DOCUMENTATION PAGE

1. Report No. FHWA-HRT-18-051	2. Government Accession No.	3. Recipient's Catalog No.
4. Title and Subtitle Analysis Procedures for Evaluating Superheavy Load Movement on Flexible Pavements, Volume III: Appendix B, Superheavy Load Configurations and Nucleus of Analysis Vehicle		5. Report Date December 2018 6. Performing Organization Code
7. Author(s) Mohamed Nimeri (ORCID: 0000-0002-3328-4367), Hadi Nabizadeh (ORCID: 0000-0001-8215-1299), Elie Y. Hajj (ORCID: 0000-0001-8568-6360), Raj V. Siddharthan (ORCID: 0000-0002-3847-7934), and Sherif Elfass (ORCID: 0000-0003-3401-6513)		8. Performing Organization Report No. WRSC-UNR-201710-01B
9. Performing Organization Name and Address Department of Civil and Environmental Engineering University of Nevada 1664 North Virginia Street Reno, NV 89557		10. Work Unit No. 11. Contract or Grant No. DTFH61-13-C-00014
12. Sponsoring Agency Name and Address U.S. Department of Transportation Federal Highway Administration Turner-Fairbank Highway Research Center 6300 Georgetown Pike McLean, VA 22101		13. Type of Report and Period Covered Final Report; August 2013–July 2018 14. Sponsoring Agency Code HRDI-20
15. Supplementary Notes Nadarajah Sivaneswaran (HRDI-20; ORCID: 0000-0003-0287-664X), Office of Infrastructure Research and Development, Turner-Fairbank Highway Research Center, served as the Contracting Officer's Representative.		
16. Abstract The movement of superheavy loads (SHLs) has become more common over the years since it is a vital necessity for many important industries, such as chemical, oil, electrical, and defense. SHL hauling units are much larger in size and weight compared to standard trucks. SHL gross vehicle weights may be in excess of a few million pounds, so they often require specialized trailers and components with nonstandard spacing between the tires and axles. Accommodating SHL movement requires the determination of whether the pavement is structurally adequate and involves the analysis of the likelihood of instantaneous or rapid load-induced shear failure. As part of this Federal Highway Administration project, Analysis Procedures for Evaluating Superheavy Load Movement on Flexible Pavements, a procedure was developed to identify a segment (or element) of the SHL configuration that can be regarded as representative of the entire SHL vehicle. This element is referred to as the nucleus. The vertical stress distribution (or any other pavement response) under the entire SHL configuration can then be estimated by superimposing the stresses calculated under the nucleus, eliminating the need to model the entire SHL vehicle. A sensitivity analysis was conducted to assess the procedure's accuracy and sensitivity to different pavement structures, SHL cases, and pavement analysis temperatures. Procedures for handling uniform axle and tire spacing of SHL vehicles as well as special SHL cases were also considered.		
17. Key Words Load nucleus, flexible pavement, superheavy load, pavement analysis, permits, axle group	18. Distribution Statement No restrictions. This document is available to the public through the National Technical Information Service, Springfield, VA 22161. http://www.ntis.gov	

19. Security Classif. (of this report)	20. Security Classif. (of this page)	21. No. of Pages	22. Price
Unclassified	Unclassified	90	N/A

Form DOT F 1700.7 (8-72) Reproduction of completed page authorized.

SI* (MODERN METRIC) CONVERSION FACTORS

APPROXIMATE CONVERSIONS TO SI UNITS

Symbol	When You Know	Multiply By	To Find	Symbol
		LENGTH		
in	inches	25.4	millimeters	mm
ft	feet	0.305	meters	m
yd	yards	0.914	meters	m
mi	miles	1.61	kilometers	km
		AREA		
in^2	square inches	645.2	square millimeters	mm^2
ft^2	square feet	0.093	square meters	m^2
yd^2	square yard	0.836	square meters	m^2
ac	acres	0.405	hectares	ha
mi^2	square miles	2.59	square kilometers	km^2
		VOLUME		
fl oz	fluid ounces	29.57	milliliters	mL
gal	gallons	3.785	liters	L
ft^3	cubic feet	0.028	cubic meters	m^3
yd^3	cubic yards	0.765	cubic meters	m^3
		NOTE: volumes greater than 1000 L shall be shown in m^3		
		MASS		
oz	ounces	28.35	grams	g
lb	pounds	0.454	kilograms	kg
T	short tons (2000 lb)	0.907	megagrams (or "metric ton")	Mg (or "t")
		TEMPERATURE (exact degrees)		
^oF	Fahrenheit	5 (F-32)/9 or (F-32)/1.8	Celsius	^oC
		ILLUMINATION		
fc	foot-candles	10.76	lux	lx
fl	foot-Lamberts	3.426	candela/m^2	cd/m^2
		FORCE and PRESSURE or STRESS		
lbf	poundforce	4.45	newtons	N
lbf/in^2	poundforce per square inch	6.89	kilopascals	kPa

APPROXIMATE CONVERSIONS FROM SI UNITS

Symbol	When You Know	Multiply By	To Find	Symbol
		LENGTH		
mm	millimeters	0.039	inches	in
m	meters	3.28	feet	ft
m	meters	1.09	yards	yd
km	kilometers	0.621	miles	mi
		AREA		
mm^2	square millimeters	0.0016	square inches	in^2
m^2	square meters	10.764	square feet	ft^2
m^2	square meters	1.195	square yards	yd^2
ha	hectares	2.47	acres	ac
km^2	square kilometers	0.386	square miles	mi^2
		VOLUME		
mL	milliliters	0.034	fluid ounces	fl oz
L	liters	0.264	gallons	gal
m^3	cubic meters	35.314	cubic feet	ft^3
m^3	cubic meters	1.307	cubic yards	yd^3
		MASS		
g	grams	0.035	ounces	oz
kg	kilograms	2.202	pounds	lb
Mg (or "t")	megagrams (or "metric ton")	1.103	short tons (2000 lb)	T
		TEMPERATURE (exact degrees)		
^oC	Celsius	1.8C+32	Fahrenheit	^oF
		ILLUMINATION		
lx	lux	0.0929	foot-candles	fc
cd/m^2	candela/m^2	0.2919	foot-Lamberts	fl
		FORCE and PRESSURE or STRESS		
N	newtons	0.225	poundforce	lbf
kPa	kilopascals	0.145	poundforce per square inch	lbf/in^2

ANALYSIS PROCEDURES FOR EVALUATING SUPERHEAVY LOAD MOVEMENT ON FLEXIBLE PAVEMENTS PROJECT REPORT SERIES

This volume is the third of 10 volumes in this research report series. Volume I is the final report, and volume II through volume X consist of appendix A through appendix I. Any reference to a volume in this series will be referenced in the text as "Volume II: Appendix A," "Volume III: Appendix B," and so forth. The following list contains the volumes:

Volume	Title	Report Number
I	Analysis Procedures for Evaluating Superheavy Load Movement on Flexible Pavements, Volume I: Final Report	FHWA-HRT-18-049
II	Analysis Procedures for Evaluating Superheavy Load Movement on Flexible Pavements, Volume II: Appendix A, Experimental Program	FHWA-HRT-18-050
III	Analysis Procedures for Evaluating Superheavy Load Movement on Flexible Pavements, Volume III: Appendix B, Superheavy Load Configurations and Nucleus of Analysis Vehicle	FHWA-HRT-18-051
IV	Analysis Procedures for Evaluating Superheavy Load Movement on Flexible Pavements, Volume IV: Appendix C, Material Characterization for Superheavy Load Movement Analysis	FHWA-HRT-18-052
V	Analysis Procedures for Evaluating Superheavy Load Movement on Flexible Pavements, Volume V: Appendix D, Estimation of Subgrade Shear Strength Parameters Using Falling Weight Deflectometer	FHWA-HRT-18-053
VI	Analysis Procedures for Evaluating Superheavy Load Movement on Flexible Pavements, Volume VI: Appendix E, Ultimate and Service Limit Analyses	FHWA-HRT-18-054
VII	Analysis Procedures for Evaluating Superheavy Load Movement on Flexible Pavements, Volume VII: Appendix F, Failure Analysis of Sloped Pavement Shoulders	FHWA-HRT-18-055
VIII	Analysis Procedures for Evaluating Superheavy Load Movement on Flexible Pavements, Volume VIII: Appendix G, Risk Analysis of Buried Utilities Under Superheavy Load Vehicle Movements	FHWA-HRT-18-056
IX	Analysis Procedures for Evaluating Superheavy Load Movement on Flexible Pavements, Volume IX: Appendix H, Analysis of Cost Allocation Associated With Pavement Damage Under a Superheavy Load Vehicle Movement	FHWA-HRT-18-057
X	Analysis Procedures for Evaluating Superheavy Load Movement on Flexible Pavements, Volume X: Appendix I, Analysis Package for Superheavy Load Vehicle Movement on Flexible Pavement (SuperPACK)	FHWA-HRT-18-058

TABLE OF CONTENTS

LIST OF FIGURES

LIST OF TABLES

LIST OF ABBREVIATIONS AND SYMBOLS

Abbreviations

3D	three-dimensional
AC	asphalt concrete
ADOT	Arizona Department of Transportation
CAB	crushed aggregate base
CDOT	Colorado Department of Transportation
GVW	gross vehicle weight
HMA	hot-mix asphalt
LaDOTD	Louisiana Department of Transportation and Development
NDOT	Nevada Department of Transportation
No.	number
NYDOT	New York Department of Transportation
OS	oversize
ODV	over-dimensional vehicle
OW	overweight
PS	pavement structure
SG	subgrade
SHA	State highway agency
SHL	superheavy load

Symbols

$E*$	dynamic modulus
Nx	number of additional tires in *x*-direction that influence the point of interest
Ny	number of additional tires in *y*-direction that influence the point of interest
q_{ave}	average uniform vertical stress
σ_v	vertical stress
$\sigma_{v\ max}$	maximum vertical stress
z	depth from the pavement surface

CHAPTER 1. INTRODUCTION

Superheavy load (SHL) hauling units are much larger in size and weight compared to standard trucks. They often require specialized trailers and components that are assembled to suit their respective characteristics. Although the tires used are often conventional, which enables the use of existing methodologies in addressing critical issues such as pavement–tire interaction stresses etc., the axle and tire configurations are variable, which means the spacing between tires and axles is not standard, and the tire imprints as a whole can span more than the entire width of a lane. Therefore, it is imperative that the nongeneric nature of the axle and tire configurations is regarded in a realistic manner for studying the pavement subjected to an SHL-vehicle movement.

Initially, the research team planned on defining some general and common configurations for SHL hauling units. To this end, information regarding the tire and axle loads and configurations was collected from a select number of State highway agencies (SHAs). However, the research team found that existing tire and axle configurations of SHL hauling units cannot be grouped into one or more identical and generic categories.

In this report, the collected information regarding SHL-movement permits issued by SHAs is presented first. Afterward, the entire SHL vehicle–load configuration is divided into individual axle groups depending on the interaction between tires that are present in the axle groups. The interaction between the groups is minimal because of the wider spacing between them. The procedure to determine the axle groups that make the entire SHL vehicle is presented in chapter 4. A methodology capable of specifying a representative segment (or element) of the axle-load configuration for each of the axle groups is elaborated on in chapter 2. This element, referred to as the nucleus, can be treated as a representative segment of the axle group under consideration and is eventually used to determine the required pavement responses under SHL movements (i.e., stress, strain, and displacement).

1.1. OBJECTIVES AND SCOPE OF WORK

As part of this Federal Highway Administration project, Analysis Procedures for Evaluating Superheavy Load Movement on Flexible Pavements, a comprehensive mechanistic-based analysis approach consisting of several analysis procedures was developed. This report (Volume III: Appendix B) is the third of 10 volumes and presents a methodology to identify a segment(s) of the SHL configuration that can be regarded as representative of the entire SHL vehicle.[1–9] The analysis procedures developed in this study and associated objectives (including related volume numbers) are summarized in table 1.

Table 1. Developed analysis procedures to evaluate SHL movement on flexible pavements.

Procedure	Objective
SHL analysis vehicle	Identify segment(s) of the SHL-vehicle configuration that can be regarded as representative of the entire SHL vehicle (Volume III: Appendix B)
Flexible pavement structure	Characterize representative material properties for existing pavement layers (Volume IV: Appendix C and Volume V: Appendix D)[3,4]
Subgrade bearing failure analysis	Investigate instantaneous ultimate shear failure in pavement SG (Volume VI: Appendix E)[5]
Sloped-shoulder failure analysis	Examine the stability of sloped pavement shoulder under SHL-vehicle movement (Volume VII: Appendix F)[6]
Buried utility risk analysis	Perform risk analysis of existing buried utilities (Volume VIII: Appendix G)[7]
Localized shear failure analysis	Inspect the likelihood of localized failure (yield) in the pavement SG (Volume VI: Appendix E)[5]
Deflection-based service limit analysis	Investigate the development of premature surface distresses (Volume VI: Appendix E)[5]
Cost allocation analysis	Determine pavement damage–associated cost attributable to SHL-vehicle movement (Volume IX: Appendix H)[8]

1.2. SHL TYPES AND AXLE CONFIGURATIONS

A select number of SHAs that experienced SHL-vehicle movements exceeding 250,000 lb were contacted in an attempt to gain knowledge and acquire information regarding State definitions of SHL, get an estimate of the annual number of SHL permits, and most importantly, view typical tire and axle loads and configurations. The information received from five of the contacted SHAs (Arizona, Colorado, Louisiana, Nevada, and New York) is summarized in the following sections. Though the requests to the SHAs were the same and indicated a uniform format for reporting, the responses were not consistent and did not cover all the inquiries. It should be noted that the collected information was not meant to cover all the existing and possible SHL permit types in the Nation. Instead, the presented information should be viewed as a sample of typically observed tire and axle loads and configurations for SHL vehicles.

1.2.1. Arizona Department of Transportation

In Arizona, SHL vehicles are classified as “Class C oversize/overweight” (OS/OW).[10] An SHL vehicle is defined as any vehicle that is greater than 250,000 lb, over axle weight, or in excess of posted bridge weights. The Maintenance Permits Services office at the Arizona Department of Transportation (ADOT) is responsible for issuing permits. The Class C SHL permit fee is $40 for loads no greater than 18 ft in height and width. For SHL-vehicle movements with heights and widths greater than 18 ft, the fee is $100. Class C permits are valid on State and interstate highways only.[1]

Four different SHL permit forms were received from the ADOT Maintenance Permits Services office. Figure 1 illustrates an example of information pertinent to SHL movement from the received forms. Based on the SHL-vehicle permitting information, gross vehicle weights (GVWs) ranged from 647,855 to 1,180,000 lb. The total weight per axle ranged from 46,305 to 51,687 lb. The axle width (measured from the out-to-out edges of the outside tires) ranged from 18 ft 4 inches to 20 ft 4 inches. The center-to-center distance between each adjacent axle ranged from 6 ft to 12 ft 1 inch. Eight tires existed on each axle with an individual tire load ranging from 5,000 to 6,460 lb. The edge-to-edge width of each tire ranged from 8.25 to 11 inches. One major tire configuration within each axle was observed with three different tire distances, as shown in figure 2 (note that drawings are not to scale).

[1]Hajj, E.Y., Siddharthan, R., Elfass, S., Nabizadeh, H., and Souliman, M. (2014). *Analysis Procedures for Evaluating Superheavy Load Movement on Flexible Pavements*, Unpublished Interim Report, Federal Highway Administration, Washington, DC.

Gross Vehicle Weight = 959,000 lb

	Axle 1 (Steering Axle)	Axle 2	Axle 3	Axle 4	Axle 5	Axle 6	Axle 7	Axle 8	Axle 9	Axle 10	Axle 11	Axle 12
Axle Spacing (Center-to-Center)	18 feet-6 inches	5 feet-0 inch	14 feet-9 inches	6 feet-0 inch	12 feet-1 inch	6 feet-0 inch	12 feet-1 inch	6 feet-0 inch	12 feet-1 inch	6 feet-0 inch	59 feet-8 inches	
Total Weight per Axle (lb)	20,000	23,000	23,000	51,687	51,688	51,687	51,688	51,687	51,688	51,687	51,688	51,687
Number of Tires per Axle	2	4	4	8	8	8	8	8	8	8	8	8
*Axle Width**	8 feet-0 inch	8 feet-9 inches	8 feet-9 inches	20 feet-0 inch	20 feet-0 inch	20 feet-0 inch	20 feet-0 inch	20 feet-0 inch	20 feet-0 inch	20 feet-0 inch	20 feet-0 inch	20 feet-0 inch
Tire Size	17 inches	12 inches	12 inches	11 inches	11 inches	11 inches	11 inches	11 inches	11 inches	11 inches	11 inches	11 inches

*Measured out-to-out excluding the tire bulge.

	Axle 12	Axle 13	Axle 14	Axle 15	Axle 16	Axle 17	Axle 18	Axle 19	Axle 20	Axle 21	Axle 22	Axle 23
Axle Spacing (Center-to-Center)	6 feet-0 inch	12 feet-1 inch	6 feet-0 inch	12 feet-1 inch	6 feet-0 inch	12 feet-1 inch	6 feet-0 inch	18 feet-10 inch	18 feet-1 inch	5 feet-5 inches	Not Applicable	
Total Weight per Axle (lb)		51,688	51,687	51,688	51,688	51,687	51,687	51,688	20,000	23,000	23,000	Not Applicable
Number of Tires per Axle		8	8	8	8	8	8	8	2	4	4	Not Applicable
*Axle Width**		20 feet-0 inch	20 feet-0 inch	20 feet-0 inch	20 feet-0 inch	20 feet-0 inch	20 feet-0 inch	20 feet-0 inch	8 feet-3 inches	9 feet-2 inches	9 feet-2 inches	Not Applicable
Tire Size		11 inches	11 inches	11 inches	11 inches	11 inches	11 inches	11 inches	17 inches	12 inches	12 inches	Not Applicable

*Measured out-to-out excluding the tire bulge.

Recreated from © 2016 ADOT.[2]

Figure 1. Picture. Example of relevant information from an SHL-vehicle permit in Arizona: axle configurations and loads.

[2]Unpublished source obtained through personal communication July 2018.

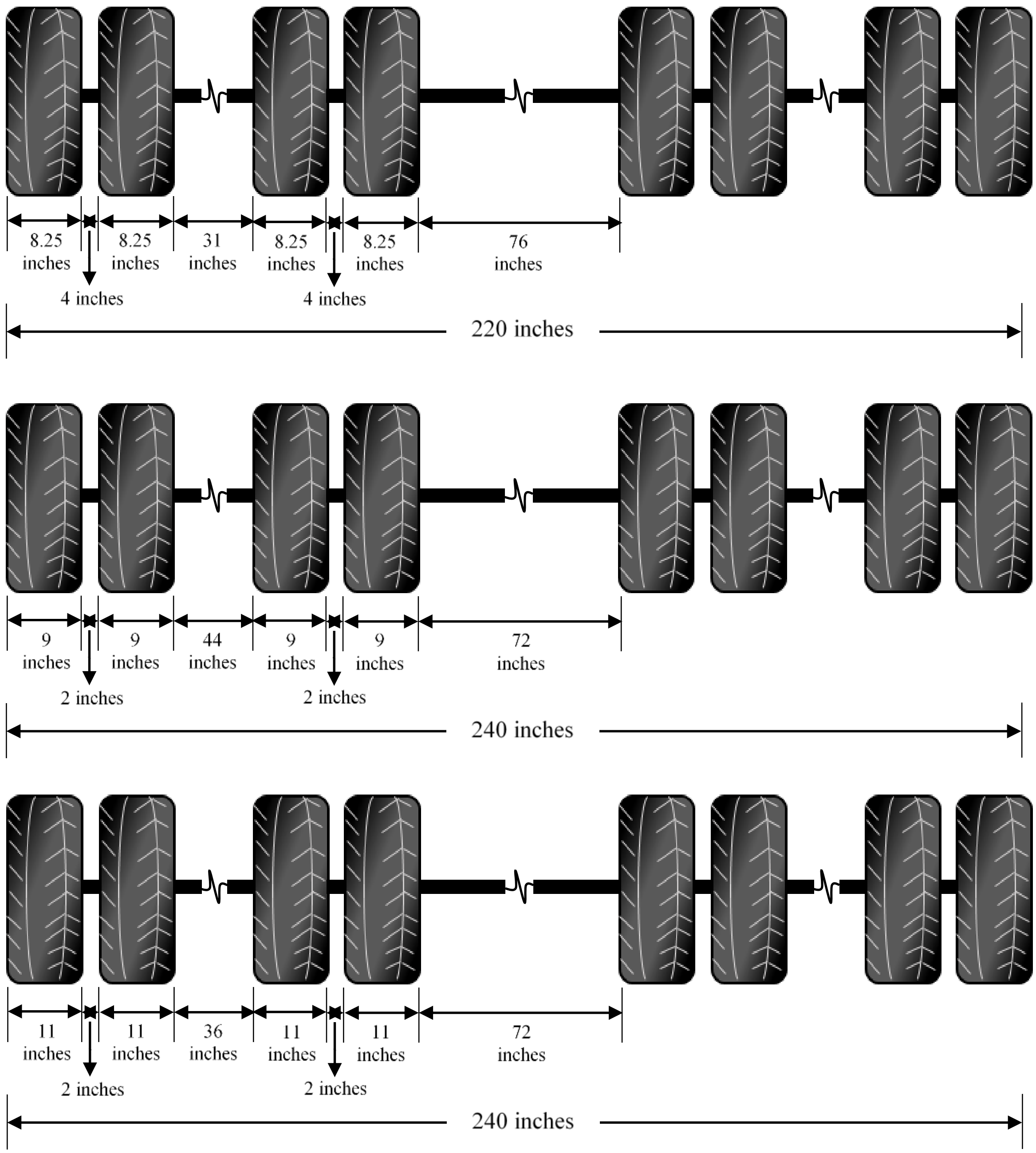

Figure 2. Illustration. Observed common tire configurations in Arizona (not to scale).

1.2.2. Colorado Department of Transportation

The Colorado Department of Transportation (CDOT) refers to SHL vehicles as double-dolly vehicles, which consist of two axles adjacent to one another with each axle line consisting of eight tires (figure 3). The double dolly is typically used for large and heavy loads, such as refinery equipment or electrical transformers. Table 2 through table 4 show CDOT weight-limit maps for different ranges of double-dolly axle-line widths and distances between the axle groups (figure 3). The data in table 2 through table 4 were compiled for permit writers and trucking companies to readily evaluate CDOT bridge weight limits for OS/OW vehicles.(11)[3]

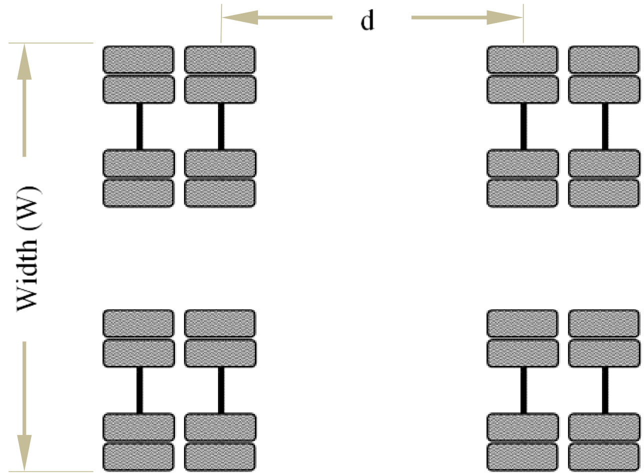

© 2018 UNR.
d = distance.

Figure 3. Illustration. Double-dolly configuration according to CDOT.

[3]Hajj, E.Y., Siddharthan, R., Elfass, S., Nabizadeh, H., and Souliman, M. (2014). *Analysis Procedures for Evaluating Superheavy Load Movement on Flexible Pavements*, Unpublished Interim Report, Federal Highway Administration, Washington, DC.

Table 2. CDOT bridge weight-limit map for double-dolly axles: maximum allowable permit weight per axle group for axle distances between 8 and 10 ft (data from CDOT 2015).[11]

Width	Axle Group	Orange Permit (×1,000 lb)	Yellow Permit (×1,000 lb)	White Permit (×1,000 lb)
≤10 ft 0 inch	Single axle	22.0	25.0	27.0
≤10 ft 0 inch	Tandem axle	36.0	39.0	43.0
≤10 ft 0 inch	Triple axle	49.0	53.0	58.0
≤10 ft 0 inch	Four or more axles	52.0	57.0	62.0
11 ft 0 inch	Single axle	23.3	26.4	28.5
11 ft 0 inch	Tandem axle	38.1	41.2	45.5
11 ft 0 inch	Triple axle	51.8	56.0	61.3
11 ft 0 inch	Four or more axles	55.0	60.3	65.5
12 ft 0 inch	Single axle	24.5	27.9	30.1
12 ft 0 inch	Tandem axle	40.1	43.5	47.9
12 ft 0 inch	Triple axle	54.6	59.1	64.6
12 ft 0 inch	Four or more axles	57.9	63.5	69.1
13 ft 0 inch	Single axle	25.8	29.3	31.6
13 ft 0 inch	Tandem axle	42.2	45.7	50.4
13 ft 0 inch	Triple axle	57.4	62.1	67.9
13 ft 0 inch	Four or more axles	60.9	66.8	72.6
14 ft 0 inch	Single axle	27.0	30.7	33.2
14 ft 0 inch	Tandem axle	44.2	47.9	52.8
14 ft 0 inch	Triple axle	60.2	65.1	71.2
14 ft 0 inch	Four or more axles	63.9	70.0	76.2
15 ft 0 inch	Single axle	28.3	32.2	34.7
15 ft 0 inch	Tandem axle	46.3	50.2	55.3
15 ft 0 inch	Triple axle	63.0	68.2	74.6
15 ft 0 inch	Four or more axles	66.9	73.3	79.7
16 ft 0 inch	Single axle	29.6	33.6	36.2
16 ft 0 inch	Tandem axle	48.4	52.4	57.8
16 ft 0 inch	Triple axle	65.8	71.2	77.9
16 ft 0 inch	Four or more axles	69.8	76.6	83.2
17 ft 0 inch	Single axle	30.8	35.0	37.8
17 ft 0 inch	Tandem axle	50.4	54.6	60.2
17 ft 0 inch	Triple axle	68.6	74.2	81.2
17 ft 0 inch	Four or more axles	72.8	79.8	86.8
18 ft 0 inch	Single axle	32.1	36.4	39.3
18 ft 0 inch	Tandem axle	52.5	56.8	62.7
18 ft 0 inch	Triple axle	71.4	77.2	84.5
18 ft 0 inch	Four or more axles	75.8	83.1	90.3
19 ft 0 inch	Single axle	33.3	37.9	40.9
19 ft 0 inch	Tandem axle	54.5	59.1	65.1
19 ft 0 inch	Triple axle	74.2	80.3	87.8
19 ft 0 inch	Four or more axles	78.7	86.3	93.9
≥20 ft 0 inch	Single axle	34.6	39.3	42.4
≥20 ft 0 inch	Tandem axle	56.6	61.3	67.6
≥20 ft 0 inch	Triple axle	77.0	83.3	91.1
≥20 ft 0 inch	Four or more axles	81.7	89.6	97.4

Table 3. CDOT bridge weight-limit map for double-dolly axles: maximum allowable permit weight per axle group for axle distances between 10 and 12 ft (data from CDOT 2015).[11]

Width	Axle Group	Orange Permit (×1,000 lb)	Yellow Permit (×1,000 lb)	White Permit (×1,000 lb)
≤10 ft 0 inch	Single axle	22.0	25.0	27.0
≤10 ft 0 inch	Tandem axle	39.0	43.0	47.0
≤10 ft 0 inch	Triple axle	53.0	58.0	63.0
≤10 ft 0 inch	Four or more axles	57.0	62.0	68.0
11 ft 0 inch	Single axle	23.3	26.4	28.5
11 ft 0 inch	Tandem axle	41.2	45.5	49.7
11 ft 0 inch	Triple axle	56.0	61.3	66.6
11 ft 0 inch	Four or more axles	60.3	65.5	71.9
12 ft 0 inch	Single axle	24.5	27.9	30.1
12 ft 0 inch	Tandem axle	43.5	47.9	52.4
12 ft 0 inch	Triple axle	59.1	64.6	70.2
12 ft 0 inch	Four or more axles	63.5	69.1	75.8
13 ft 0 inch	Single axle	25.8	29.3	31.6
13 ft 0 inch	Tandem axle	45.7	50.4	55.1
13 ft 0 inch	Triple axle	62.1	67.9	73.8
13 ft 0 inch	Four or more axles	66.8	72.6	79.7
14 ft 0 inch	Single axle	27.0	30.7	33.2
14 ft 0 inch	Tandem axle	47.9	52.8	57.8
14 ft 0 inch	Triple axle	65.1	71.2	77.4
14 ft 0 inch	Four or more axles	70.0	76.2	83.6
15 ft 0 inch	Single axle	28.3	32.2	34.7
15 ft 0 inch	Tandem axle	50.2	55.3	60.5
15 ft 0 inch	Triple axle	68.2	74.6	81.0
15 ft 0 inch	Four or more axles	73.3	79.7	87.5
16 ft 0 inch	Single axle	29.6	33.6	36.2
16 ft 0 inch	Tandem axle	52.4	57.8	63.1
16 ft 0 inch	Triple axle	71.2	77.9	84.6
16 ft 0 inch	Four or more axles	76.6	83.2	91.3
17 ft 0 inch	Single axle	30.8	35.0	37.8
17 ft 0 inch	Tandem axle	54.6	60.2	65.8
17 ft 0 inch	Triple axle	74.2	81.2	88.2
17 ft 0 inch	Four or more axles	79.8	86.8	95.2
18 ft 0 inch	Single axle	32.1	36.4	39.3
18 ft 0 inch	Tandem axle	56.8	62.7	68.5
18 ft 0 inch	Triple axle	77.2	84.5	91.8
18 ft 0 inch	Four or more axles	83.1	90.3	99.1
19 ft 0 inch	Single axle	33.3	37.9	40.9
19 ft 0 inch	Tandem axle	59.1	65.1	71.2
19 ft 0 inch	Triple axle	80.3	87.8	95.4
19 ft 0 inch	Four or more axles	86.3	93.9	103.0
≥20 ft 0 inch	Single axle	34.6	39.3	42.4
≥20 ft 0 inch	Tandem axle	61.3	67.6	73.9
≥20 ft 0 inch	Triple axle	83.3	91.1	99.0
≥20 ft 0 inch	Four or more axles	89.6	97.4	106.9

Table 4. CDOT bridge weight-limit map for double-dolly axles: maximum allowable permit weight per axle group for axle distances greater than 12 ft (data from CDOT 2015).[11]

Width	Axle Group	Orange Permit (×1,000 lb)	Yellow Permit (×1,000 lb)	White Permit (×1,000 lb)
≤10 ft 0 inch	Single axle	22.0	25.0	27.0
≤10 ft 0 inch	Tandem axle	42.0	46.0	50.0
≤10 ft 0 inch	Triple axle	55.0	60.0	65.0
≤10 ft 0 inch	Four or more axles	60.0	66.0	72.0
11 ft 0 inch	Single axle	23.3	26.4	28.5
11 ft 0 inch	Tandem axle	44.4	48.6	52.9
11 ft 0 inch	Triple axle	58.1	63.4	68.7
11 ft 0 inch	Four or more axles	63.4	69.8	76.1
12 ft 0 inch	Single axle	24.5	27.9	30.1
12 ft 0 inch	Tandem axle	46.8	51.3	55.7
12 ft 0 inch	Triple axle	61.3	66.9	72.4
12 ft 0 inch	Four or more axles	66.9	73.5	80.2
13 ft 0 inch	Single axle	25.8	29.3	31.6
13 ft 0 inch	Tandem axle	49.2	53.9	58.6
13 ft 0 inch	Triple axle	64.4	70.3	76.1
13 ft 0 inch	Four or more axles	70.3	77.3	84.3
14 ft 0 inch	Single axle	27.0	30.7	33.2
14 ft 0 inch	Tandem axle	51.6	56.5	61.4
14 ft 0 inch	Triple axle	67.6	73.7	79.8
14 ft 0 inch	Four or more axles	73.7	81.1	88.4
15 ft 0 inch	Single axle	28.3	32.2	34.7
15 ft 0 inch	Tandem axle	54.0	59.2	64.3
15 ft 0 inch	Triple axle	70.7	77.2	83.6
15 ft 0 inch	Four or more axles	77.2	84.9	92.6
16 ft 0 inch	Single axle	29.6	33.6	36.2
16 ft 0 inch	Tandem axle	56.4	61.8	67.2
16 ft 0 inch	Triple axle	73.8	80.6	87.3
16 ft 0 inch	Four or more axles	80.6	88.6	96.7
17 ft 0 inch	Single axle	30.8	35.0	37.8
17 ft 0 inch	Tandem axle	58.8	64.4	70.0
17 ft 0 inch	Triple axle	77.0	84.0	91.0
17 ft 0 inch	Four or more axles	84.0	92.4	100.8
18 ft 0 inch	Single axle	32.1	36.4	39.3
18 ft 0 inch	Tandem axle	61.2	67.0	72.9
18 ft 0 inch	Triple axle	80.1	87.4	94.7
18 ft 0 inch	Four or more axles	87.4	96.2	104.9
19 ft 0 inch	Single axle	33.3	37.9	40.9
19 ft 0 inch	Tandem axle	63.6	69.7	75.7
19 ft 0 inch	Triple axle	83.3	90.9	98.4
19 ft 0 inch	Four or more axles	90.9	99.9	109.0
≥20 ft 0 inch	Single axle	34.6	39.3	42.4
≥20 ft 0 inch	Tandem axle	66.0	72.3	78.6
≥20 ft 0 inch	Triple axle	86.4	94.3	102.1
≥20 ft 0 inch	Four or more axles	94.3	103.7	113.1

1.2.3. Louisiana Department of Transportation and Development

The Louisiana Department of Transportation and Development (LaDOTD) truck permit office issues all OS/OW permits that govern truck movement on State highways in Louisiana. SHL permits are determined by highway geometry and condition, gross and axle weights, day of the week and time of travel, escort (private or State police), curfews, and other conditions necessary to ensure safe travel. There are 27 different types of permits issued by this office. Currently, the truck permit office has a customer list of more than 33,000 companies, individuals, and State and Federal agencies.[4]

As presented in table 5, the research team received 16 different SHL permit forms from the LaDOTD truck permit office. Figure 4 and figure 5 are examples of information pertinent to SHL vehicle–movement analysis from the received forms. Based on the collected SHL permitting information, the GVW ranged from 485,736 to 4,073,472 lb. The total weight per axle ranged from 56,223 to 130,734 lb for 12- and 8-tire axles and from 25,639 to 37,368 lb for 4-tire axles. The axle width (measured out-to-out edges of the outside tires) ranged from 7 ft 11.6875 inches to 31 ft 3 inches. The center-to-center distance between each adjacent axle ranged from 4 ft 7 inches to 11 ft 0.75 inch. Typically, eight tires existed in each axle with an individual tire load ranging from 7,028 to 16,341 lb. The edge-to-edge width of each tire ranged from 1 ft 0.5 inch to 1 ft 2 inches. Three different tire arrangements within each axle were observed, as shown in figure 6.

[4]Hajj, E.Y., Siddharthan, R., Elfass, S., Nabizadeh, H., and Souliman, M. (2014). *Analysis Procedures for Evaluating Superheavy Load Movement on Flexible Pavements*, Unpublished Interim Report, Federal Highway Administration, Washington, DC.

Table 5. Summary of SHL characteristics from Louisiana sample permits.

ID	GVW (lb)	Axle Weight (lb)	No. of Axles	No. of Tires per Axle	Axle Width (Measured Out-to-Out Edges)	Minimum Center-to-Center Distance Between Adjacent Axles	Minimum Center-to-Center Distance Between Sets of Dual Tires	Tire Load (lb)	Tire Width
LA-4T-1	672,624	37,368	18	4	7 ft 11.6875 inches	4 ft 7 inches	4 ft 9.5 inches	9,342	1 ft 1.5625 inches
LA-4T-2	512,780	25,639	20	4	7 ft 11.6875 inches	4 ft 7 inches	4 ft 9.5 inches	6,410	1 ft 1.5625 inches
LA-8T-3	485,736	40,478	12	8	17 ft 5.8125 inches	4 ft 7 inches	4 ft 9.0625 inches	5,060	1 ft 1.5625 inches
LA-8T-4	589,821	56,223 and 65,420	10	8	17 ft 5.8125 inches	4 ft 7 inches	4 ft 9.0625 inches	7,028 and 8,178	1 ft 1.5625 inches
LA-8T-5	704,604	58,717	12	8	24 ft 7.375 inches	4 ft 7 inches	4 ft 9.5 inches	7,340	1 ft 1.5625 inches
LA-8T-6	717,821	70,193 and 75,490	10	8	17 ft 5.8125 inches	4 ft 7 inches	4 ft 9.0625 inches	8,774 and 9,436	1 ft 1.5625 inches
LA-8T-7	725,221	71,203 and 75,600	10	8	17 ft 5.8125 inches	4 ft 7 inches	4 ft 9.0625 inches	8,900 and 9,450	1 ft 1.5625 inches
LA-8T-8	784,164	65,347	12	8	24 ft 7.375 inches	4 ft 7 inches	4 ft 9.5 inches	8,168	1 ft 1.5625 inches
LA-8T-9	804,480	67,040	12	8	24 ft 7.375 inches	4 ft 7 inches	4 ft 9.5 inches	8,380	1 ft 1.5625 inches
LA-8T-10	1,415,660	63,057 and 78,509	20	8	17 ft 5.8125 inches	4 ft 7 inches	4 ft 9.0625 inches	9,814 and 7,882	1 ft 1.5625 inches
LA-8T-11	1,500,660	74,678 and 75,388	20	8	17 ft 5.8125 inches	4 ft 7 inches	4 ft 9.0625 inches	9,335 and 9,424	1 ft 1.5625 inches
LA-8T-12	1,833,960	74,460 and 115,600	18	8	17 ft 5.8125 inches	4 ft 7 inches	4 ft 9.0625 inches	14,450 and 9,308	1 ft 2 inches
LA-8T-13	3,634,092	129,789	28	8	17 ft 5.8125 inches	4 ft 7 inches	4 ft 9.0625 inches	16,224	1 ft 1.5625 inches
LA-8T-14	3,660,552	130,734	28	8	17 ft 5.8125 inches	4 ft 7 inches	4 ft 9.0625 inches	16,342	1 ft 1.5625 inches
LA-8T-15	4,073,472	113,152	36	8	17 ft 5.8125 inches	4 ft 7 inches	4 ft 9.0625 inches	14,144	1 ft 1.5625 inches
LA-12T-16	1,754,220	72,214 and 73,971	24	12	31 ft 3 inches	4 ft 7 inches	4 ft 8.5625 inches	6,164 and 6,018	1 ft 2 inches

ID = identification number; No. = number.

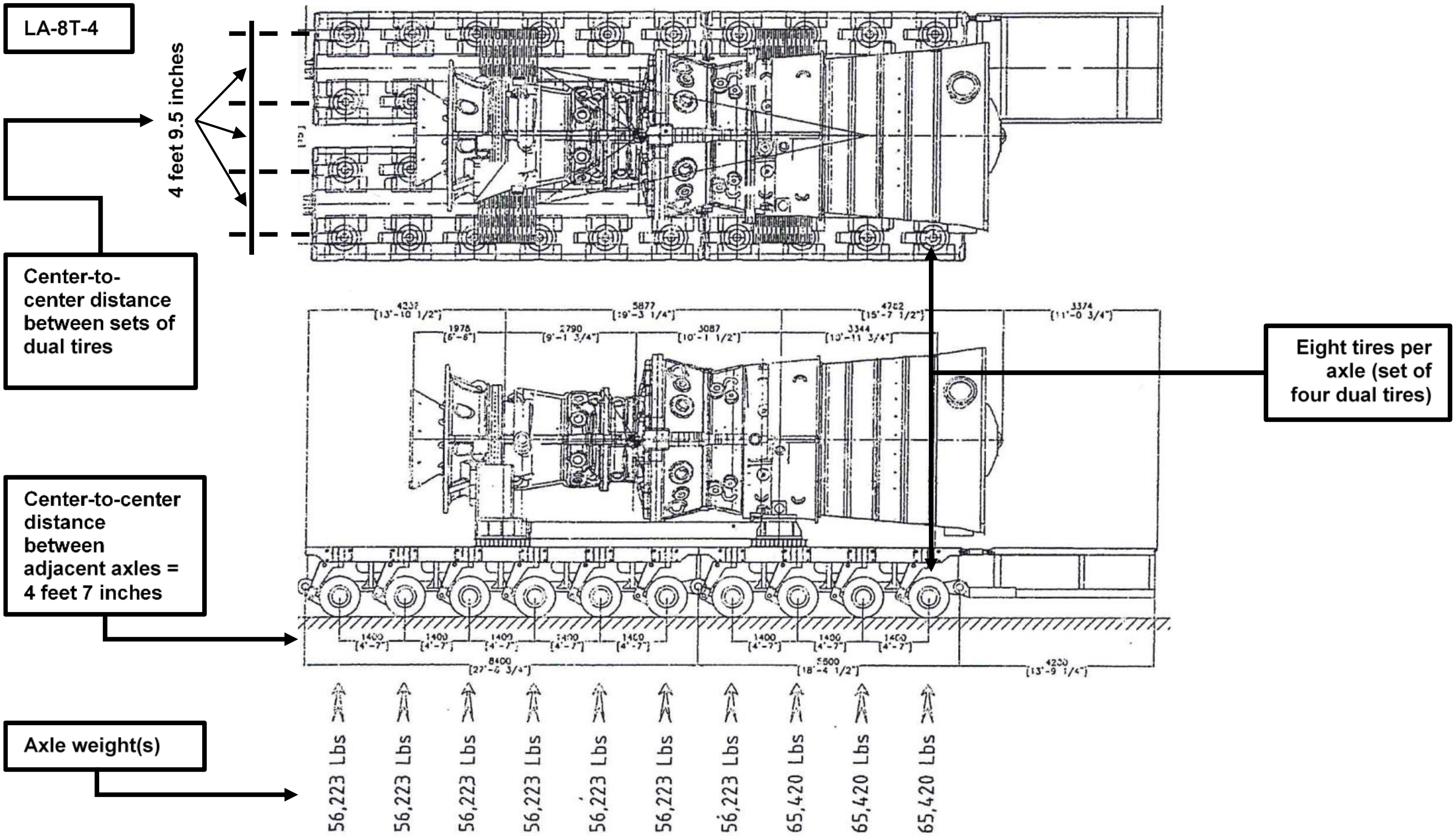

Modified from © 2016 LaDOTD.[5]

Figure 4. Picture. Example of relevant information from an SHL permit in Louisiana: transport configuration for gas-turbine package.

[5]Unpublished source obtained through personal communication August 2018.

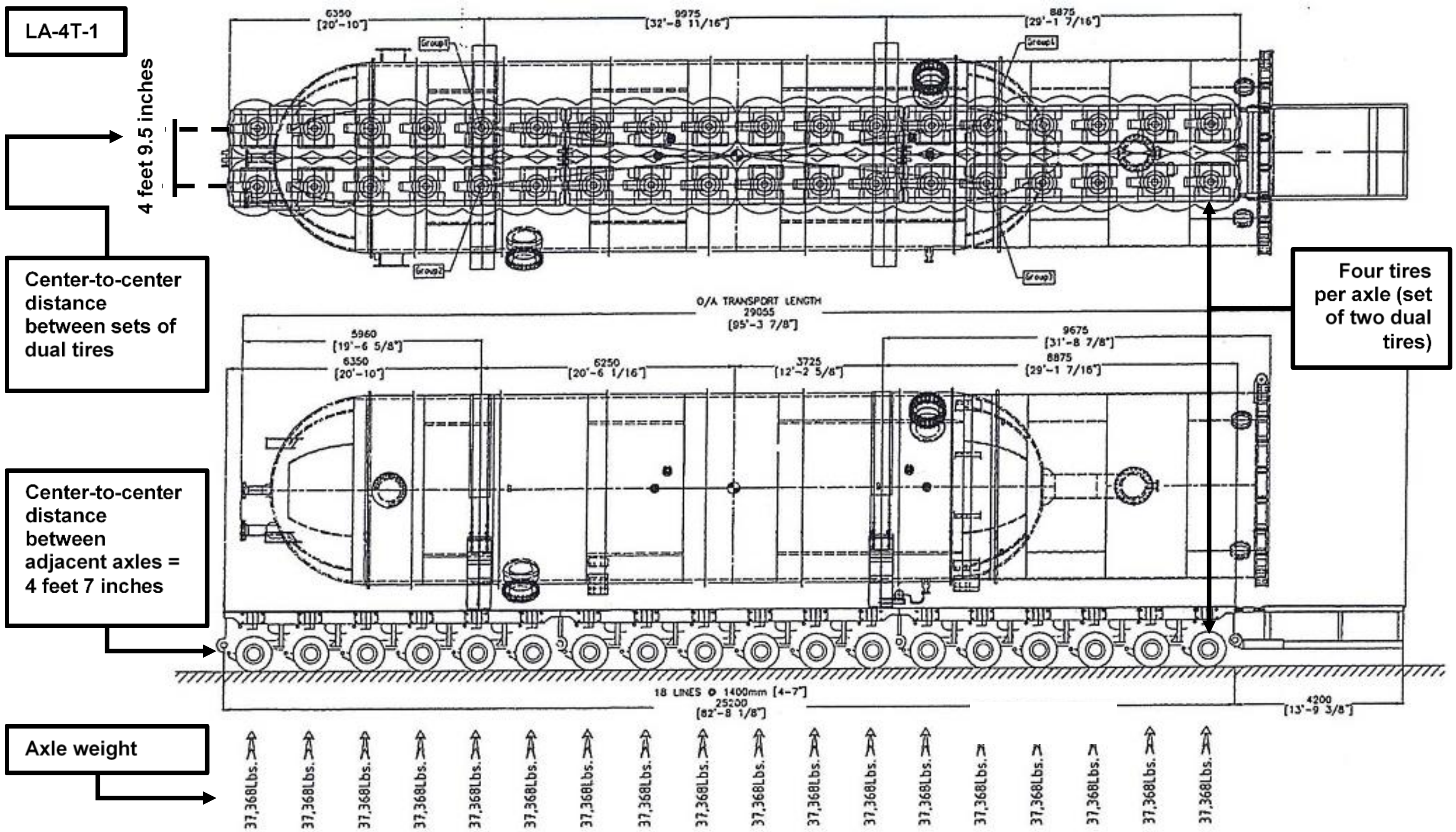

Modified from © 2016 LaDOTD.[6]

Figure 5. Picture. Example of relevant information from an SHL permit in Louisiana: transport configuration for D-943-004 (hot low-pressure separator) on 18 line axles.

---

[6]Unpublished source obtained through personal communication August 2018.

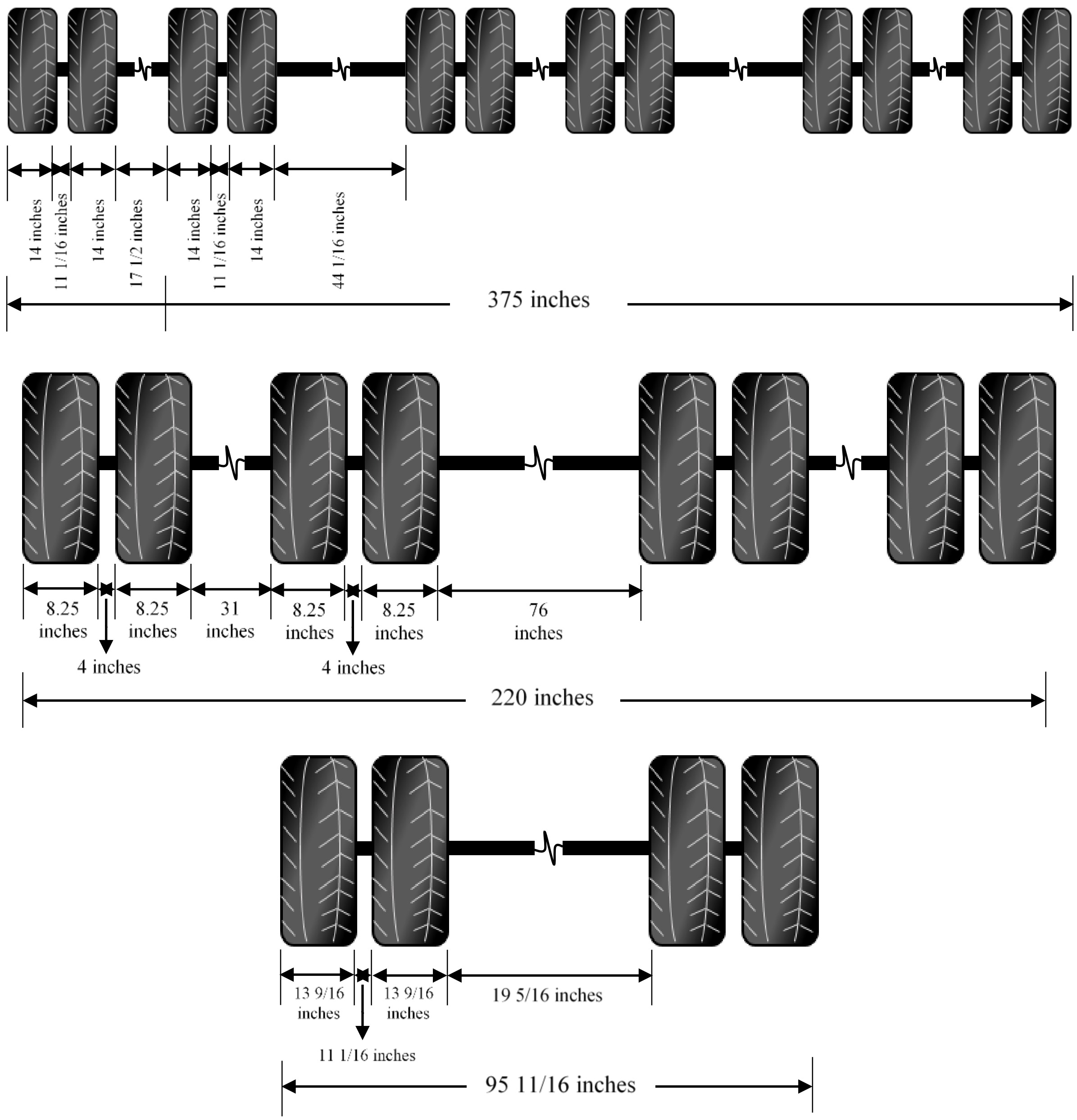

Figure 6. Illustration. Observed common tire configurations in Louisiana (not to scale).

1.2.4. Nevada Department of Transportation

In Nevada, SHL vehicles are classified as OS/OW. SHL vehicles are defined as those exceeding 250,000 lb. The Nevada Department of Transportation's (NDOT's) Over-Dimensional Vehicle (ODV) Permits Office is responsible for issuing permits. Three OS/OW fee categories exist: annual permit fee of $60, semiannual fee of $60, and 5 d–trip fee of $25.[7]

A Microsoft® Excel™–based database was received from NDOT's ODV Permits Office. This database contained a total of 1,398 permits for vehicles with GVWs greater than 250,000 lb, and the maximum recorded SHL-vehicle weight was 6,215,938 lb. Figure 7 illustrates the distribution of SHL permits based on GVW. Table 6 shows the distribution and load ranges of SHL permits based on usage purposes. Notably, movers of construction equipment had the highest number of permits issued in Nevada in the examined 10-yr period (approximately 74 percent of the total SHL permits).

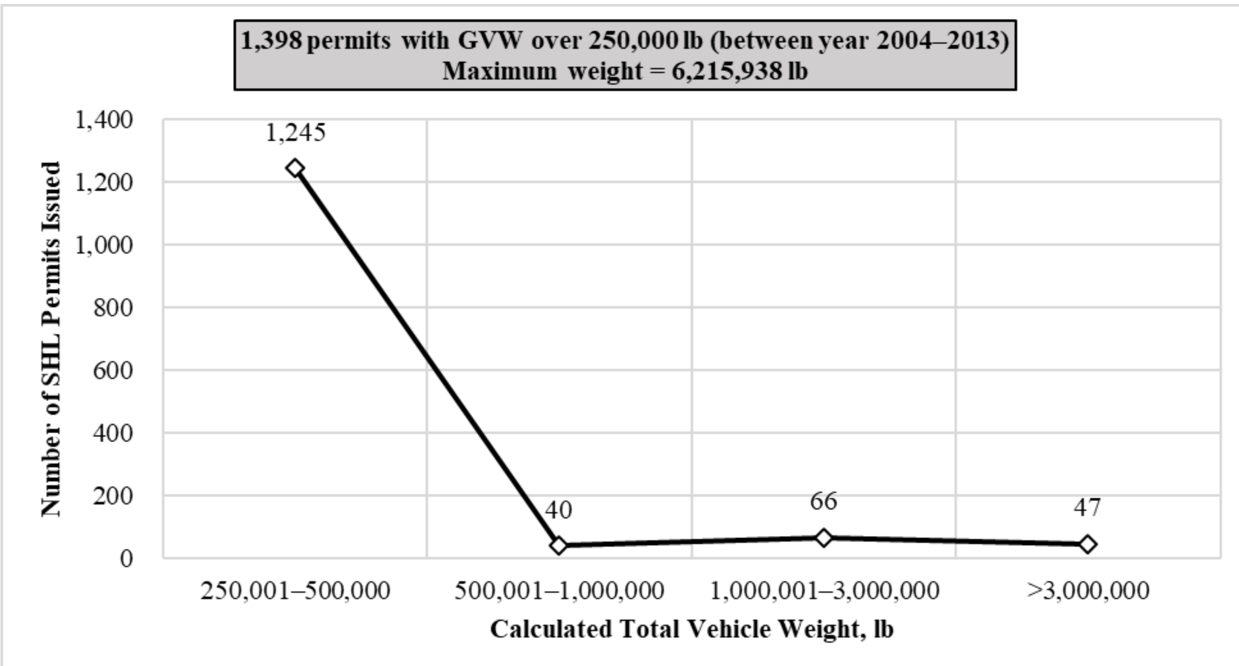

Figure 7. Graph. Distribution of SHL permits in Nevada based on GVW.

[7]Hajj, E.Y., Siddharthan, R., Elfass, S., Nabizadeh, H., and Souliman, M. (2014). *Analysis Procedures for Evaluating Superheavy Load Movement on Flexible Pavements*, Unpublished Interim Report, Federal Highway Administration, Washington, DC.

Table 6. Distribution and load ranges of SHL permits in Nevada.

Categories	No. of Permits	Minimum GVW (lb)	Maximum GVW (lb)	Average GVW (lb)	Median GVW (lb)
Construction	1,041	250,041	6,215,938	540,631	252,788
Mining and oil	53	250,041	6,112,775	525,728	254,325
Farming	4	294,170	1,572,971	1,135,136	1,336,701
Mechanical and electrical equipment	170	250,063	6,123,268	615,711	259,493
Other	130	250,150	2,094,013	348,317	283,170

No. = number.

Figure 8 shows a summary of information listed in a typical NDOT SHL permit. In this figure, the axle and load configurations are highlighted. It should be noted that axle and wheelbase spacing as well the total number of individual axles are included.

Route: From: North Las Vegas, NV – Rail Siding (6 Miles North East of Junction US 93 on Las Vegas Blvd)
To: North Las Vegas, NV – Harry Allen Generating Station

Travel: From: February 12, 2015
Thru: February 16, 2015

Authorized:
☐ Weekend ☐ Night ☐ Holiday [X] Workday Commute Hour

Description of Load: Haul Transformer

Dimensions: **Width:** 14 feet 0 inch | **Height:** 18 feet 0 inch | **Length:** 147 feet 2 inch

Gross Weight: 706,400 pounds **Total Axles:** 18 **Overhang:** **Front:** Legal **Rear:** Legal

Axle Spacing	1	17 feet 9 inch	2	4 feet 6 inch	3	19 feet 9 inch	4	4 feet 11 inch	5	4 feet 11 inch	6	4 feet 11 inch	7	4 feet 11 inch	8	4 feet 11 inch	9	4 feet 11 inch	10
Wheels	4		4		4		8		8		8		8		8		8		8
Weight (pounds)	13,000 (Steer weight)			34,000				50,950		50,950		50,950		50,950		50,950		50,950	

Axle Spacing	10	4 feet 11 inch	11	4 feet 11 inch	12	4 feet 11 inch	13	4 feet 11 inch	14	4 feet 11 inch	15	20 feet 4 inch	16	17 feet 9 inch	17	4 feet 6 inch	18		19
Wheels	8		8		8		8		8		8		4		4		4		
Weight (pounds)		50,950 (Steer weight)		50,950		50,950		50,950		50,950		50,950		14,000		34,000			

Recreated from © 2016 NDOT.[8]

Figure 8. Picture. Summary of relevant information from a typical NDOT SHL permit.

The permits provided by NDOT were scrutinized for the common axle groups used in SHL and OW vehicles. For example, although a single axle with single tires is always used as a steering axle, the analyzed SHL and OW vehicles might have different combinations of singles, single duals, tandems, tridems, quads, and/or trunnions for the remaining axles. Quads are identified as

[8]Unpublished source obtained through personal communication July 2018.

axles groups with 16 tires, and trunnion axles have different configurations with 16 or more tires. Figure 9 provides a schematic of the most common axle groups identified in the sample permits.

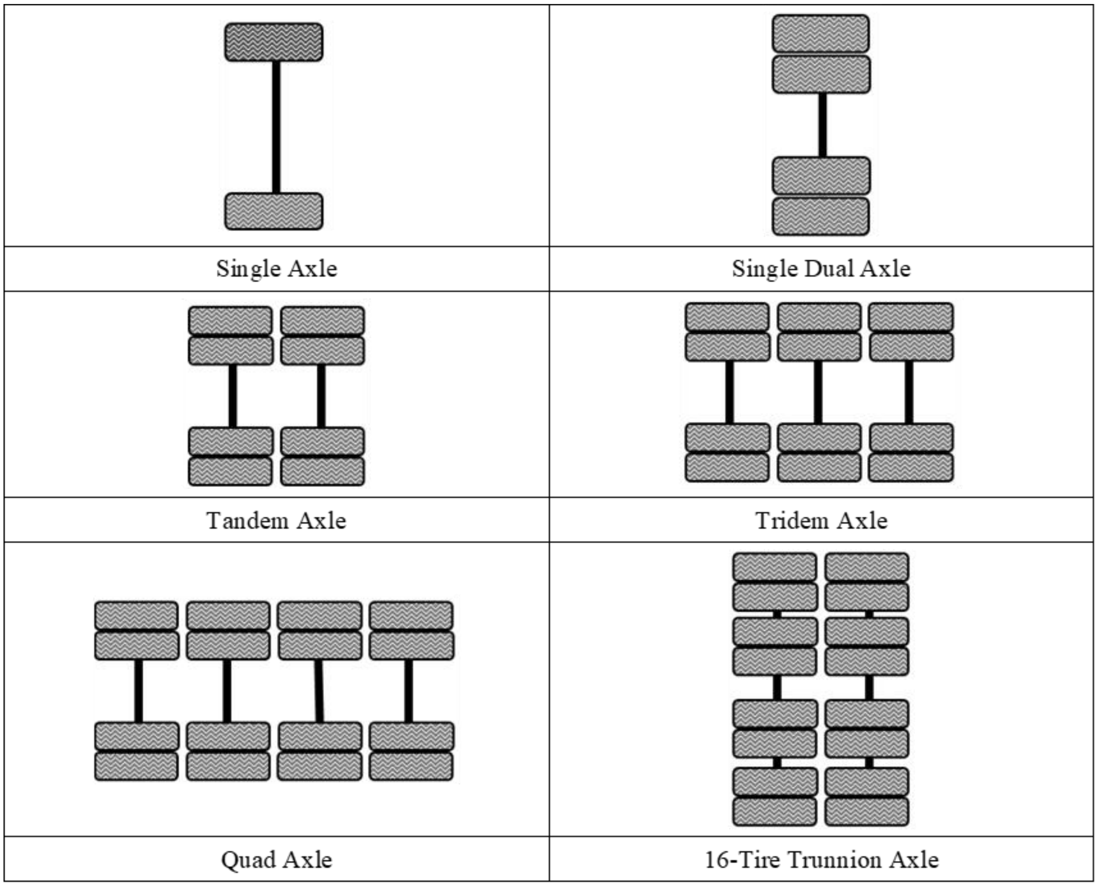

Figure 9. Picture. Identified axle-group types in NDOT SHL and OW vehicle sample permits.

To illustrate the identification of axle groups in SHL and OW vehicles, figure 10 presents a configuration of an SHL vehicle as obtained from an actual NDOT permit form. The GVW of the vehicle is 314,290 lb. The trucking company is required to provide the axle spacing and number of axles enabling the grouping. The vehicle presented in figure 10 contains seven axle groups. First, the steering axle is a single axle with single tires (axle group A). Then, a tridem axle (axle group B) is presented. Finally, a sequence of five tandem groups (axle groups C, D, E, F, and G) are presented.

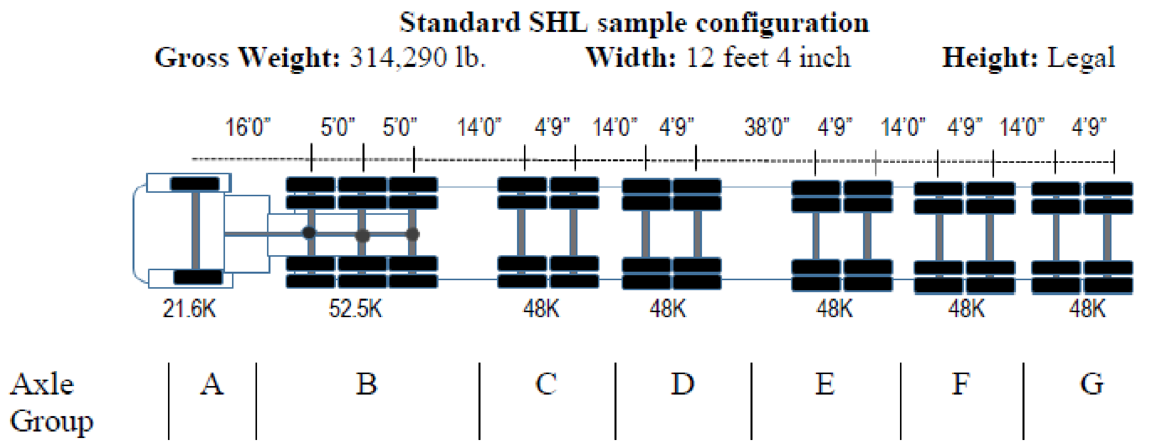

Figure 10. Illustration. Configurations of a permitted vehicle in Nevada.

NDOT permits contained data on the axle weight (figure 8). After identifing and classifying axle groups, a descriptive statistical analysis was conducted to identify statistical parameters that could describe the distributions of the axle groups. For instance, figure 11 presents a boxplot representation of these distributions. The single-axle group shows the minimum range with maximum values up to 23,000 lb. On the other hand, the quad- and trunnion-axle groups, which were grouped together, present the highest range with loads as high as 75,000 lb. Notably, the load range of the single-dual-axle group (four tires) is not much higher than the single axle. Similarly, the ranges of tandem and tridem groups containing 8 and 12 tires, respectively, are not far from each other. The horizontal bar inside the boxplot represents the median of the distributions. As expected, the median axle-group load increases from single axle to quad/trunnion. Table 7 presents a descriptive statistical summary of the axle-group loads. This table provides the minimum, maximum, median, mean, and first and third quartile values.

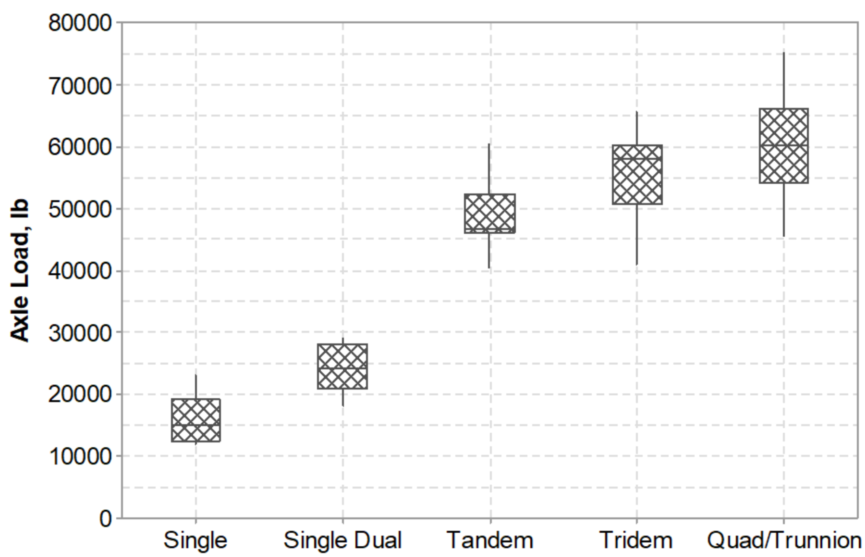

Figure 11. Chart. Boxplot representation of axle-group load distributions.

Table 7. Descriptive statistical summary of axle groups from SHL and OW permit samples.

Axle Group	Mean Axle Load (lb)	Minimum Axle Load (lb)	Quartile 1 Axle Load (lb)	Median Axle Load (lb)	Quartile 3 Axle Load (lb)	Maximum Axle Load (lb)
Single	16,519	12,000	12,500	15,000	19,200	23,000
Single dual	24,012	18,000	21,000	24,000	28,000	29,000
Tandem	46,442	22,000	46,200	46,725	52,041	65,000
Tridem	54,359	30,957	50,750	58,000	60,000	65,525
Quad/trunnion	60,242	45,500	54,167	60,000	66,000	75,000

The number of tires per individual axle is also provided in the permit forms. Using these data and the axle-group weights, the load corresponding to each tire in the group was identified. Figure 12 provides a boxplot representation of the tire load distributions. Counterintuitively, the research team found that the highest loads per tire corresponded to the single axle and the lowest to the quad- and trunnion-axle groups. This load distribution is due to the number of tires contained in each axle. For instance, the maximum 75,000 lb on the quad axle was distributed over 16 tires, which resulted in a tire load of 4,688 lb. On the other hand, the maximum single axle load was 23,000 lb (table 7). Thus, the load per tire was 11,500 lb, which is considerably higher than the quad axle tire load. Table 8 provides a descriptive statistical summary of the tire load distributions for the identified axle groups.

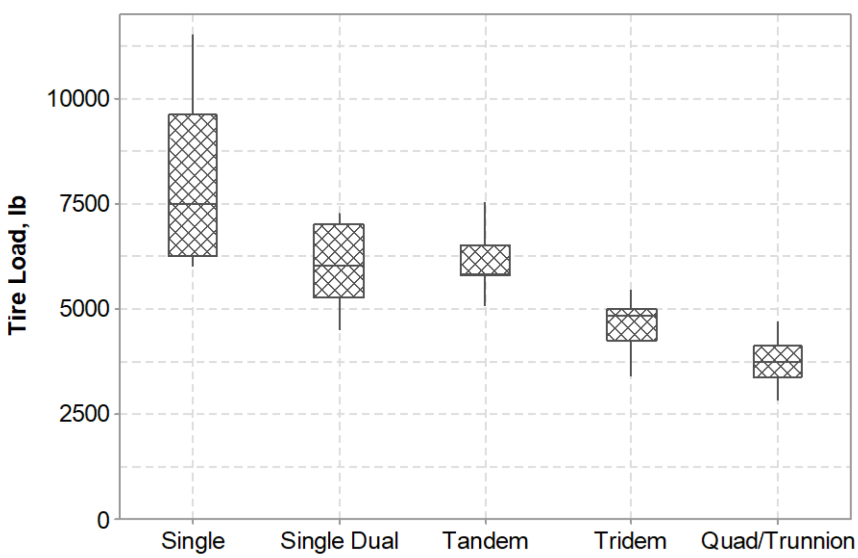

Figure 12. Chart. Boxplot representation of tire load distributions.

Table 8. Descriptive statistical summary of tire loads from SHL and OW permit samples.

Axle Group	Mean Tire Load (lb)	Minimum Tire Load (lb)	Quartile 1 Tire Load (lb)	Median Tire Load (lb)	Quartile 3 Tire Load (lb)	Maximum Tire Load (lb)
Single	8,260	6,000	6,250	7,500	9,600	11,500
Single dual	6,003	4,500	5,250	6,000	7,000	7,250
Tandem	5,760	2,750	5,775	5,841	6,505	8,125
Tridem	4,529	2,580	4,229	4,833	5,000	5,460
Quad/trunnion	3,765	2,844	3,385	3,750	4,125	4,688

1.2.5. New York Department of Transportation

The New York Department of Transportation (NYDOT) defines an SHL vehicle as any vehicle that exceeds 200,000 lb.[9] NYDOT's central permit office is responsible for issuing permits. Table 9 summarizes the number of SHL permits issued by NYDOT between 2011 and 2013 for various GVW ranges. A total of 1,961 SHL permits were issued between 2011 and 2013. It is clear that most of the issued permits were for vehicles with GVWs between 200,000 and 300,000 lb. Only 35 permits (approximately 1.8 percent of all permits issued between 2011 and 2013) were issued for vehicles with GVWs at or greater than 500,000 lb. Table 10 summarizes the minimum, maximum, average, and median GVWs for all 35 permits. The data show an increase in the average and median GVWs over the years.

[9]Hajj, E.Y., Siddharthan, R., Elfass, S., Nabizadeh, H., and Souliman, M. (2014). *Analysis Procedures for Evaluating Superheavy Load Movement on Flexible Pavements*, Unpublished Interim Report, Federal Highway Administration, Washington, DC.

Table 9. Number of SHL permits from 2011–2013 in New York.

Year	GVW	Number of SHL Permits	Percentage of SHL Permits (%)
2011	At or greater than 200,000 lb	535	78.8
2011	At or greater than 300,000 lb	126	18.6
2011	At or greater than 400,000 lb	15	2.2
2011	At or greater than 500,000 lb	3	0.4
2011	***Total permits for the year***	***679***	***100***
2012	At or greater than 200,000 lb	584	75.6
2012	At or greater than 300,000 lb	124	16.0
2012	At or greater than 400,000 lb	49	6.3
2012	At or greater than 500,000 lb	16	2.1
2012	***Total permits for the year***	***773***	***100***
2013	At or greater than 200,000 lb	346	68.0
2013	At or greater than 300,000 lb	105	20.6
2013	At or greater than 400,000 lb	42	8.3
2013	At or greater than 500,000 lb	16	3.1
2013	***Total permits for the year***	***509***	***100***
2011–2013	***Cumulative total permits***	***1,961***	—

Note: Bold, italic text indicates the row with subtotals for the given year in the first column.
—Not applicable.

Table 10. Statistics for SHL permits with GVWs at or greater than 500,000 lb from New York.

Year	No. of Permits	Minimum GVW (lb)	Maximum GVW (lb)	Average GVW (lb)	Median GVW (lb)
2011	3	509,500	660,076	559,692	509,500
2012	16	514,100	855,000	571,194	521,300
2013	16	535,000	855,000	673,850	645,300

Twenty-one different permit forms for SHL vehicles exceeding 500,000 lb were received from the NYDOT permit office. Figure 13 illustrates an example of information on axle and load configurations pertinent to an SHL-vehicle movement from an NYDOT sample form. Based on the collected SHL permitting information, the maximum recorded GVW was 855,000 lb. The total weight per axle ranged from 28,300 to 52,600 lb for eight-tire axles and from 22,700 to 24,700 lb for four-tire axles. The axle width (measured out-to-out edges of the outside tires) ranged from 12 ft 10 inches to 13 ft 6 inches. The center-to-center distance between each adjacent axle ranged between 4 ft 11 inches and 5 ft. Typically, eight tires per axle were used with an individual tire load ranging from 3,538 to 6,575 lb. The edge-to-edge width of each tire ranged from 1 ft 0.5 inch to 1 ft 2 inches. Tire arrangements within each axle were not provided.

Axle Number	Axle Weight (lb)	Number of Tires per Axle	Sum of Tire Widths (inch)	Axle Spacing	Feet	Inch
1	11,500	2	22	1-2	15	4
2	16,200	4	44	2-3	4	10
3	27,300	4	44	3-4	5	0
4	27,000	4	44	4-5	15	0
5	49,200	8	88	5-6	5	0
6	51,600	8	88	6-7	5	0
7	51,800	8	88	7-8	15	0
8	49,400	8	88	8-9	5	0
9	49,500	8	88	9-10	5	0
10	46,200	8	88	10-11	60	3
11	39,400	8	88	11-12	5	0
12	41,400	8	88	12-13	5	0
13	41,400	8	88	13-14	15	0
14	39,800	8	88	14-15	5	0
15	39,600	8	88	15-16	5	0
16	39,600	8	88	16-17	15	0
17	50,000	8	88	17-18	5	0
18	52,600	8	88	18-19	5	0
19	44,500	8	88	19-20	17	6
20	14,000	2	22	20-21	13	3
21	20,000	4	44	21-22	5	5
22	26,500	4	44	22-23	5	4
23	26,500	4	44			
Total	855,000	148	Not applicable	Not applicable	Not applicable	Not applicable

Figure 13. Photo. Summary of relevant information from a typical NYDOT SHL permit.

[10]Unpublished source obtained through personal communication August 2018.

1.2.6. Summary of Collected Information for SHL

The SHL-vehicle data collected from the various SHAs were reviewed, and a summary of the relevant information is shown in table 11. Based on the information received, the axle weights for the SHL vehicles were anywhere between 25,000 and 131,000 lb. An axle can have between 4 and 12 tires with an axle width anywhere between approximately 12 and 25 ft. The distance between the adjacent axles varied between 4 ft 7 inches and 12 ft 1 inch. Depending on the SHL configuration, the tire load was as low as 3,538 lb and as high as 16,341 lb. On the other hand, the tire width varied between 8.25 inches and 1 ft 2 inches.

Table 11. SHL axle and tire configurations from past SHA permits.

SHL Information	Arizona	Louisiana	Nevada	New York
GVW (lb)	647,855–1,180,000	485,736–4,073,472	250,041–6,215,938	200,000–855,000
Axle weight (lb)	46,305–51,687	25,639–130,734	18,000–75,000	28,300–52,600
Number of tires per axle	8	4, 8, and 12	4 and 8	4 and 8
Axle width (measured out-to-out edges of the outside tires)	18 ft 4 inches–20 ft 4 inches	17 ft 5 inches–31 ft 3 inches	—	12 ft 10 inches–13 ft 6 inches
Center-to-center distance between adjacent axles	6 ft–12 ft 1 inch	4 ft 7 inches–11 ft 0.75 inch	—	4 ft 11 inches–5 ft
Tire load (lb)	5,000–6,460	7,028–16,341	2,580–11,500	3,538–6,575
Tire width	8.25 inches–11 inches	1 ft 0.5 inch–1 ft 2 inches	—	1 ft 0.5 inch–1 ft 2 inches

—No data.

CHAPTER 2. NUCLEUS OF ANALYSIS VEHICLE

SHL hauling units require specialized trailers and components to suit the superheavy components being transported. According to the collected information regarding the tire and axle loads and configurations, which are presented in chapter 1, it was concluded that it is not possible to define one or more generic and common configurations for SHL hauling units. Therefore, a more involved procedure is required to model SHL movement on flexible pavement in order to consider the SHL axle and tire configurations that are nonstandard. To do so, a methodology was developed aiming to identify segments (or elements) of the axle-load configurations (or groups) that can be regarded as individual axle groups that make up the SHL vehicle. The axle groups are spaced far enough so that the interactions between them are minimal. Subsequently, the element referred to as the nucleus is determined for each of the axle groups. The vertical stress (σ_v) distribution (or any other pavement responses) under the entire SHL configuration can be estimated by superimposing the stresses calculated under the nucleus, eliminating the need to model the entire SHL.

2.1. METHODOLOGY

An important initial step to identifying a representative nucleus is to determine the load-induced σ_v distribution in the pavement structure. The σ_v resulting from surface tire loads of the SHL axle group is expected to overlap beyond a specific depth within the pavement structure. The extent of overlapping is highly affected by the surface load configuration and magnitude as well as the pavement-layer properties and thicknesses. As a representative example, the case of a five-line load model depicting an axle group is shown in figure 14 and figure 15. The surface load configuration consists of a uniform longitudinal (i.e., vehicle direction) spacing between the axles. On the other hand, spacing in the transverse direction is not uniform. The elevation plot (figure 15) shows the overlapping of σ_v at deeper locations within the pavement. These overlapping stresses at any interior plane can fall under one of the three cases shown in figure 16 through figure 18. Case 1 represents no overlapping (figure 16), whereas case 3 shows substantial overlapping of σ_v (figure 18).

Assuming a point of interest at a specific depth, the load-induced stress at this location is affected by the overlapped stress distributions from adjacent tires within the axle group. Therefore, the nucleus consists of the tires in both longitudinal (i.e., vehicle direction) and transverse directions that influence the point of interest at the specific depth. In other words, the representative nucleus should be determined based on σ_v influence zones of contributing tires.

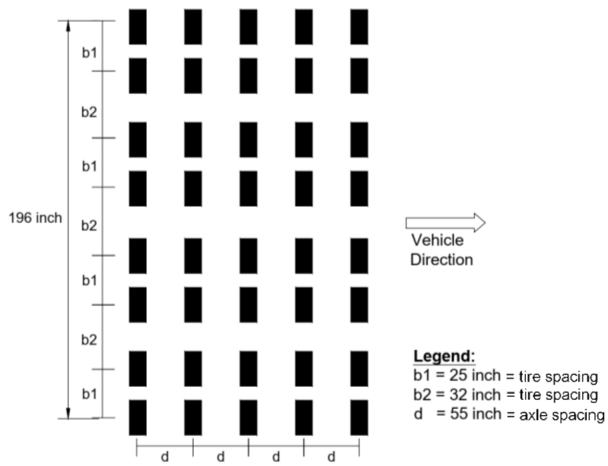

Figure 14. Illustration. Five-line model for SHL simulation—plan view.

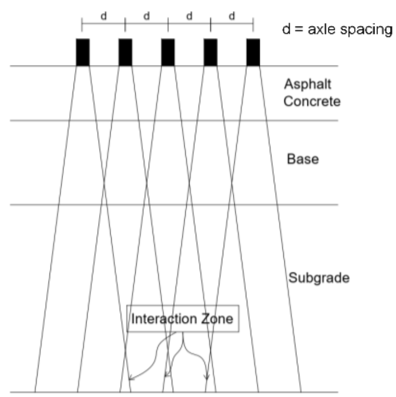

Figure 15. Illustration. Five-line model for SHL simulation—elevation view.

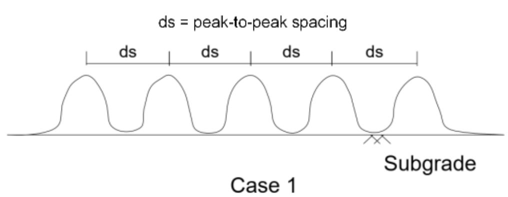

Figure 16. Illustration. σ_v distribution within pavement—case 1.

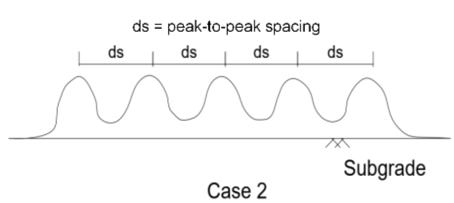

Figure 17. Illustration. σ_v distribution within pavement—case 2.

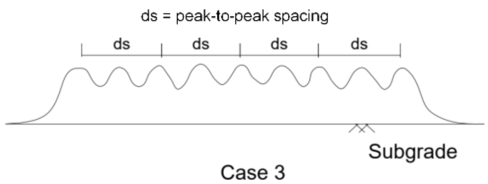

Figure 18. Illustration. σ_v distribution within pavement—case 3.

To identify a representative nucleus, an incremental tire-load approach is used. First, a single-tire load (figure 19) is applied at the surface of known pavement-layer thicknesses and properties. The σ_v response is then calculated at the point of interest (i.e., centerline of the tire load at the specific depth). Afterward, the next tire load in travel direction is added (figure 20), where the σ_v at the point of interest is observed. Additional tire loads are applied one at a time (figure 21 and figure 22), and the pavement σ_v values at the point of interest are monitored. The tire addition process continues until the last added tire does not influence the point of interest, which means that the load-induced σ_v at the interest point is not affected by adding a new tire in that direction. In a similar fashion, the number of tires in the transverse direction of the nucleus's configuration can be identified.

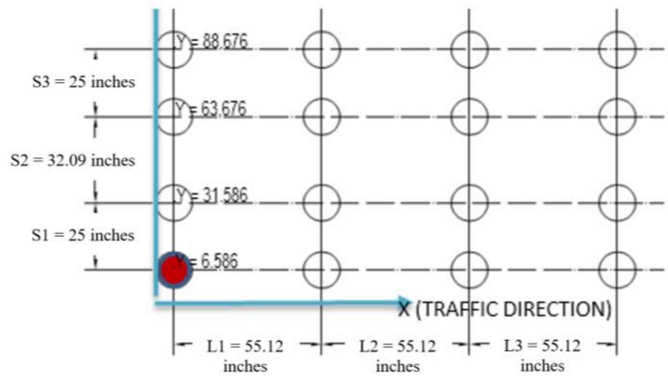

Figure 19. Illustration. Incremental tire-load approach—single tire (red-filled circle).

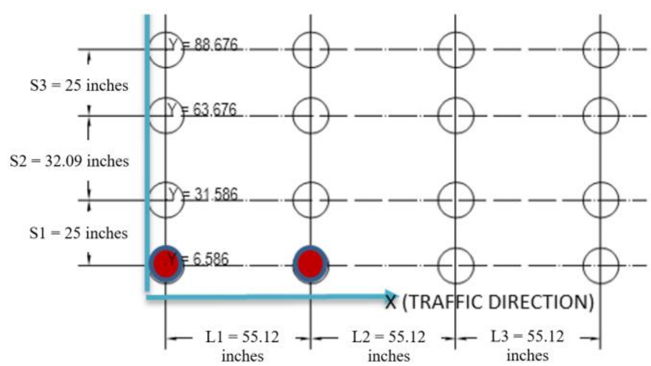

Figure 20. Illustration. Incremental tire-load approach—two tires (red-filled circles).

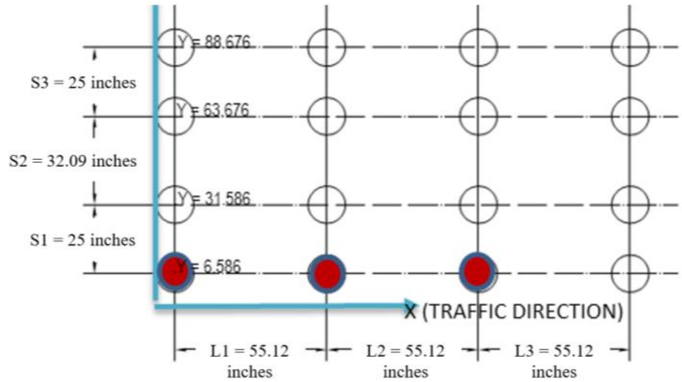

Figure 21. Illustration. Incremental tire-load approach—three tires (red-filled circles).

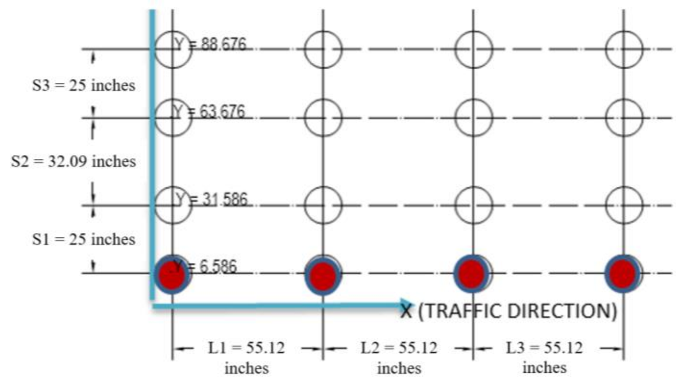

Figure 22. Illustration. Incremental tire-load approach—four tires (red-filled circles).

2.2. ILLUSTRATION FOR A REPRESENTATIVE NUCLEUS OF AN SHL CONFIGURATION

SHL case number (No.) LA-8T-14 axle-load configuration (table 5) is shown in figure 23. The vehicle had 28 line axles and 8 tires per axle. Since the entire SHL vehicle consisted of uniformly spaced axles, there was one axle group in this case. This case has been selected to illustrate the variety of the steps associated with the proposed approach for determining a representative nucleus.

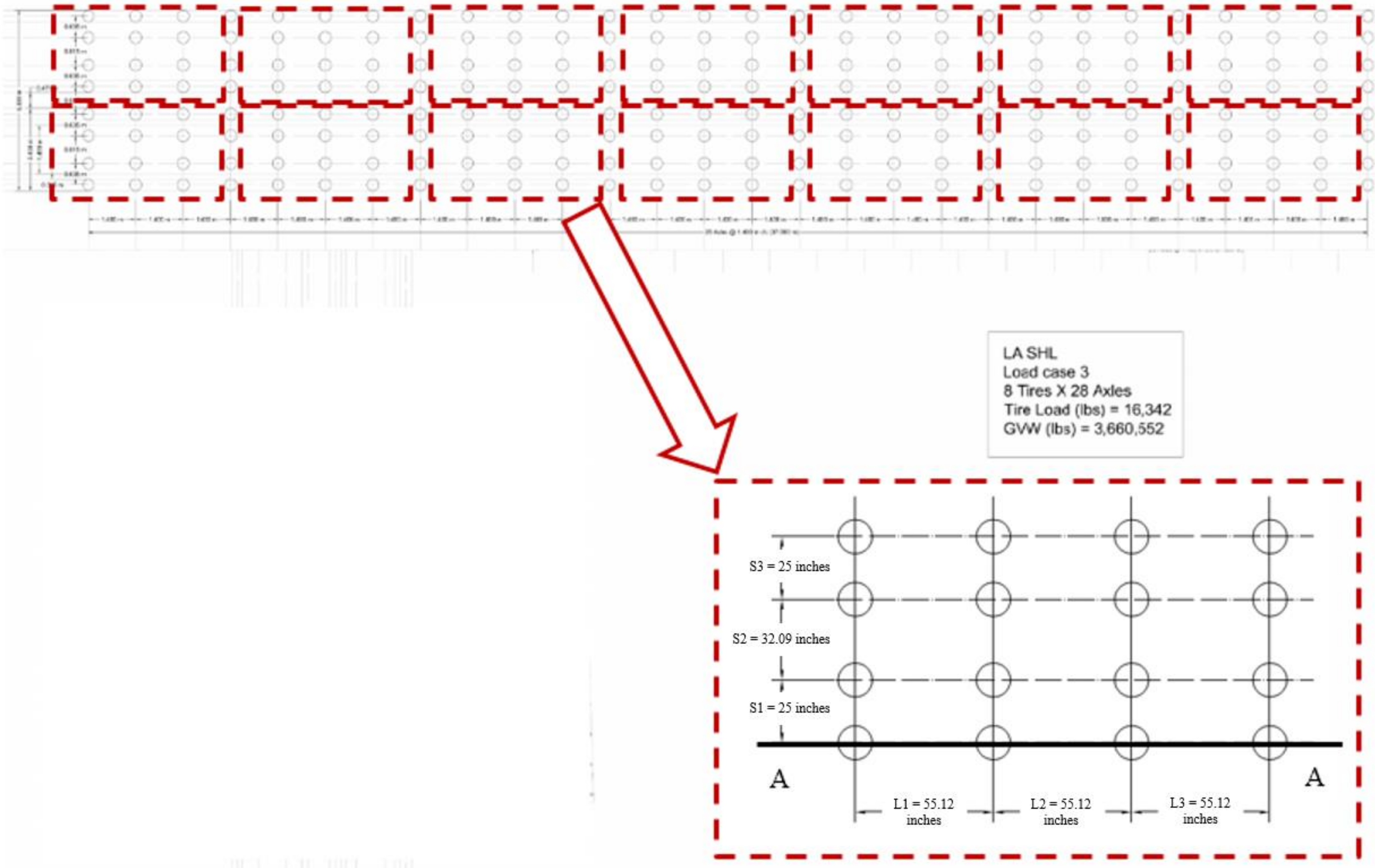

Figure 23. Illustration. SHL-vehicle axle configuration (case LA-8T-14) and nucleus of SHL configuration.

In this case, the GVW was greater than 3.6 million lb with a tire load of 16,342 lb, which was the maximum tire load among the 16 SHL permits received from LaDOTD.

2.2.1. 3D-Move Analysis Software

3D-Move Analysis software was chosen to compute the stress distributions within the pavement structure.(12) This software calculated the pavement responses at a selected pavement location as a function of different axle-load configurations, pavement structure, and material properties.

The 3D-Move Analysis software code uses a continuum-based finite layer approach to evaluate pavement responses resulting from surface loading.(12) The vehicle loading can be either static or moving on a pavement structure.(12,13) 3D-Move Analysis allows the user to define a multilayer pavement structure with the capability of handling a combination of viscoelastic asphalt concrete (AC) layer(s) and elastic unbound-material layer(s).(12) Each layer is defined as a horizontal layer with uniform properties.

2.2.2. 3D-Move Analysis—Inputs

3D-Move Analysis load input includes six options to specify the tire-contact stress distribution, covering most of the commonly used load configurations.(12) The software is capable of handling multiple load combinations with virtually any shape of contact area. In one of the input options, the user can upload a manual load input file that allows for any nonuniform tire-pavement, normal-contact stress distribution and nonuniform-interface shear stresses caused by braking and turning forces.

A uniformly distributed circular load configuration was used with a uniform tire pressure of 120 psi. However, when the tire load was changed from one load case to the other, the tire-imprint radius also changed. The various load cases considered are presented in section 3.2.

A total of three pavement structures were considered for this analysis, and they are shown in table 12. Pavement structure 2 (i.e., PS 2), which consisted of a 9-inch AC layer on top of 10 inches of crushed aggregate base (CAB) and a semi-infinite subgrade (SG) layer is presented in this section as a representative case of the pavement structures studied. Figure 24 shows a three-dimensional (3D) schematic of the pavement structure.

Table 12. Pavement Structures for 3D-Move Analysis.(12)

Pavement Structure ID	AC-Layer Thickness (Inches)	CAB-Layer Thickness (Inches)	SG-Layer Thickness (Inches)
PS 1	6	8	Semi-infinite
PS 2	9	10	Semi-infinite
PS 3	12	12	Semi-infinite

ID = identification number; PS = pavement structure.

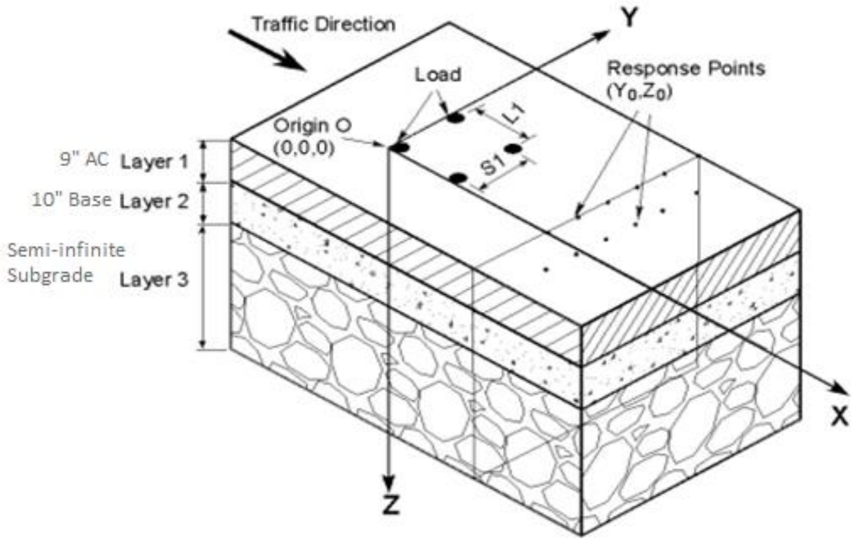

© 2018 UNR.

Figure 24. Picture. 3D schematic of the pavement structure in 3D-Move Analysis.[12]

The viscoelastic properties of the AC layer were characterized using the dynamic modulus (*E**) laboratory data and asphalt-binder properties as a function of temperature and frequency. The 3D-Move Analysis software generates master curves at any reference temperature. The AC behavior was considered linear viscoelastic, whereas unbound materials (CAB and SG) were assumed to behave as linear elastic. Table 13 lists the material properties of each layer, and table 14 and table 15 show the selected viscoelastic properties of the AC material, *E**, and phase angle, respectively. *E** data are for a typical dense-grade hot-mix asphalt (HMA) with a PG64-22 unmodified asphalt binder.[14]

Table 13. Material properties of PS 2.

Layer No.	Layer Type	Material	Thickness (Inches)	Unit Weight (pci)	Poisson's Ratio	Resilient Modulus (psi)
1	AC	Linear viscoelastic	9	0.08	0.40	Variable
2	CAB	Linear elastic	10	0.06	0.40	30,000
3	SG	Linear elastic	240	0.06	0.45	5,000

Table 14. *E values for a typical dense-grade HMA with PG64-22.**

Temperature (°F)	*E** (psi) at 0.1 Hz	*E** (psi) at 0.5 Hz	*E** (psi) at 1 Hz	*E** (psi) at 5 Hz	*E** (psi) at 10 Hz	*E** (psi) at 25 Hz
40	693,889	1,012,294	1,163,463	1,530,813	1,690,524	1,898,005
70	141,296	262,736	334,941	554,052	670,382	842,418
100	21,439	45,076	61,705	123,984	164,420	233,925
130	4,025	7,934	10,801	22,592	31,147	47,465

Table 15. Phase angle values for a typical dense-grade HMA with PG64-22.

Temperature (°F)	Phase Angle (Degrees) at 0.1 Hz	Phase Angle (Degrees) at 0.5 Hz	Phase Angle (Degrees) at 1 Hz	Phase Angle (Degrees) at 5 Hz	Phase Angle (Degrees) at 10 Hz	Phase Angle (Degrees) at 25 Hz
40	22.1	19.0	17.3	15.5	15.9	18.1
70	31.2	29.8	30.1	27.8	27.4	26.3
100	28.5	29.9	31.3	35.0	35.5	36.8
130	23.2	26.8	27.0	33.9	34.1	40.1

2.2.3. 3D-Move Analysis—Outputs

3D-Move Analysis computes stress and strain responses at any point within the pavement structure.(12) However, the focus was given to σ_v distribution that was used in the determination of the nucleus of axle configuration that can be considered representative of the entire SHL configuration. In the following sections, selected key responses and the methodology followed to analyze these responses are discussed.

2.2.4. Overlap of σ_v

The analysis output presented in this section focused on σ_v distribution at various depths within the pavement structure from three individual tires moving in a line to illustrate the effect of overlapping stress distributions.

On the surface, the maximum σ_v ($\sigma_{v\,max}$) was equal to the tire pressure (120 psi), and the stress distribution was limited to the contact area of the tire (represented by a circular area with a radius of 6.586 inches). The σ_v distribution was computed along the center of the tires (A-A in figure 23). As expected, the stresses at the surface from the individual tires did not overlap (figure 25).

However, σ_v distribution at interior pavement locations, points where the depth is greater than 0 inch, show lower amplitudes and considerable overlap. For example, on top of CAB (depth of 9 inches), the $\sigma_{v\,max}$ value was reduced to 39 psi, and the overlap of stresses from the tires was apparent (figure 26). Notably, the stress distribution shows peaks and valleys, reflecting the influence of individual tires. The stress distribution under a given tire gets wider with increased depth.

Figure 26 through figure 29 show the σ_v distribution under the centerline of the tires at various depths within the pavement. As the depth increases, the overlapping of stresses becomes more evident. Below 72 inches of the SG layer surface (z = 91 inches from the top of the asphalt pavement, where z is the depth from the pavement surface), the σ_v distribution (figure 29) was continuous without peaks and valleys. Figure 30 is a composite figure that shows the σ_v distribution at all the depths considered.

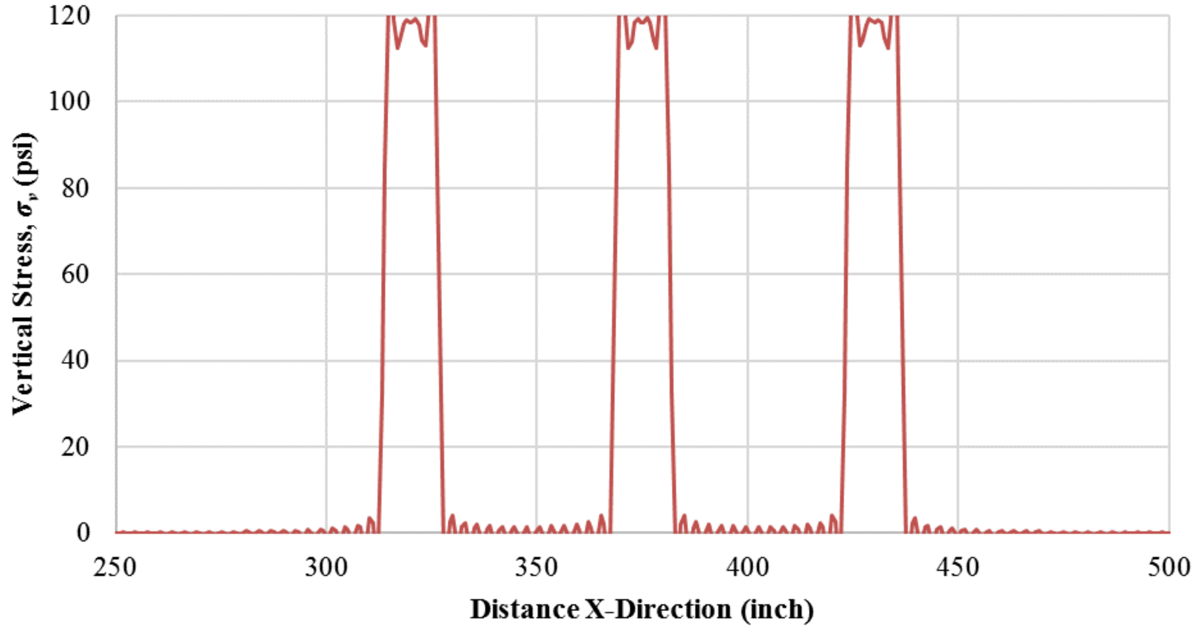

Figure 25. Chart. σ_v distribution on top of AC (z = 0 inch), three tires (SHL case No. 2: LA-8T-14, 100 °F, PS 2).

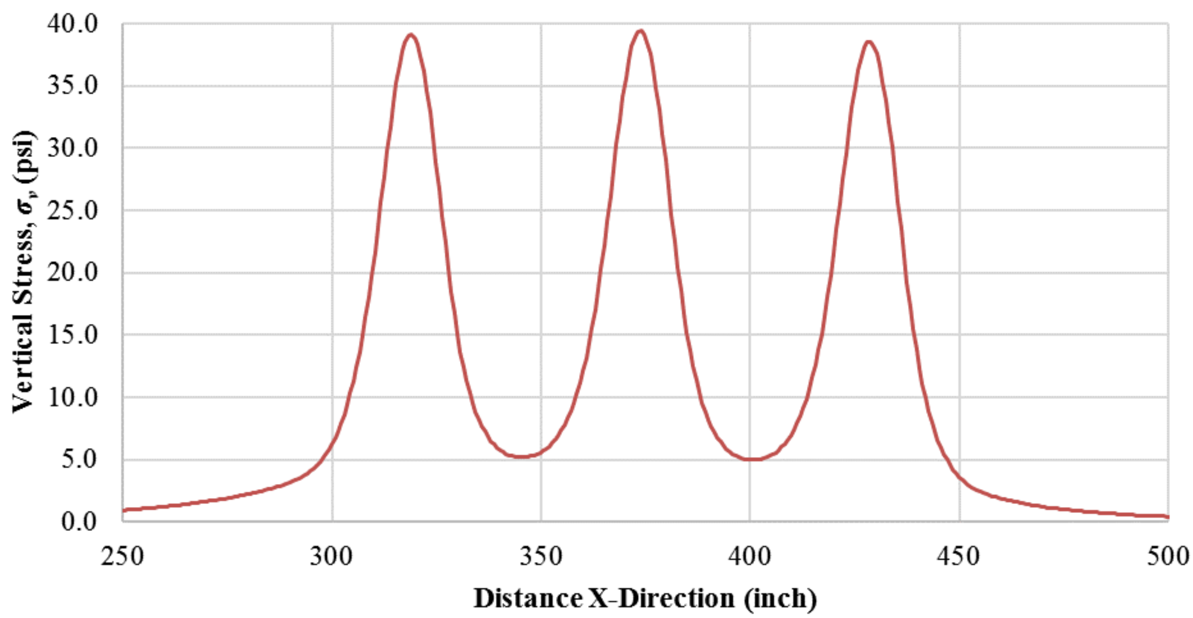

Figure 26. Chart. σ_v distribution on top of CAB (z = 9 inches), three tires (SHL case No. 2: LA-8T-14, 100 °F, PS 2).

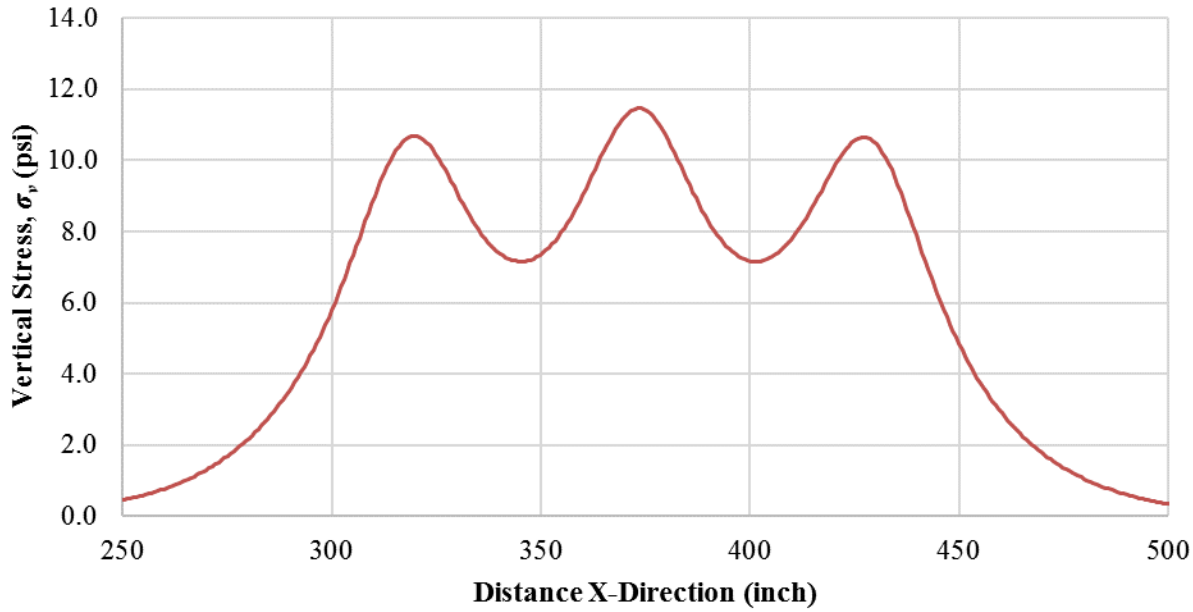

Figure 27. Chart. σ_v distribution on top of SG (z = 19 inches), three tires (SHL case No. 2: LA-8T-14, 100 °F, PS 2).

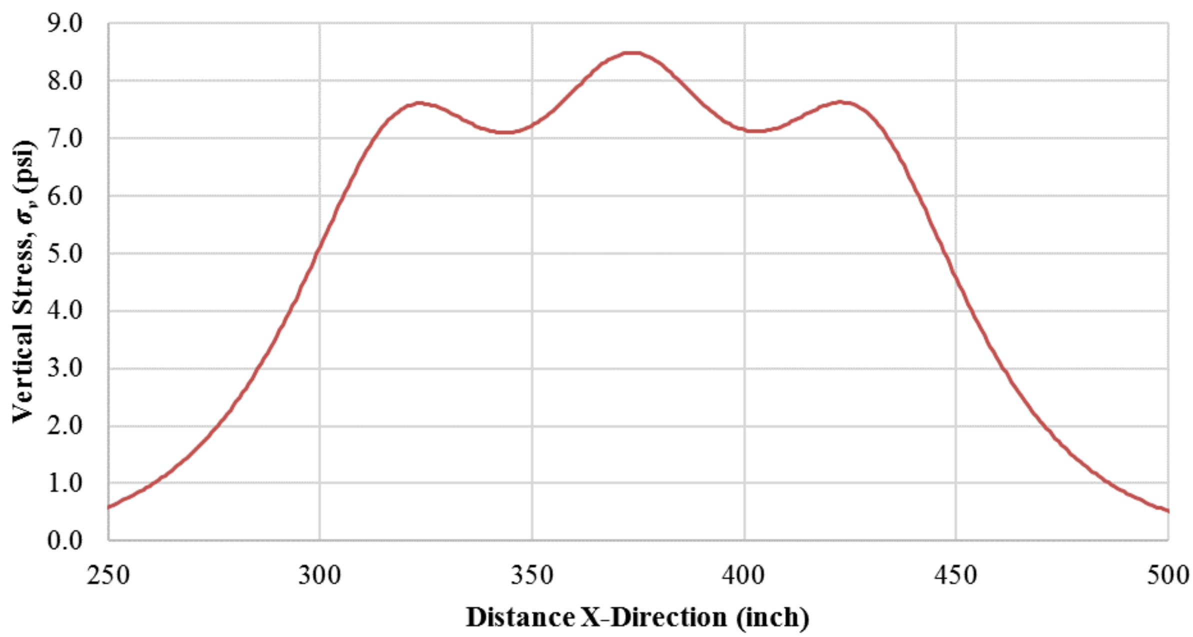

Figure 28. Chart. σ_v distribution at 12 inches below SG (z = 31 inches), three tires (SHL case No. 2: LA-8T-14, 100 °F, PS 2).

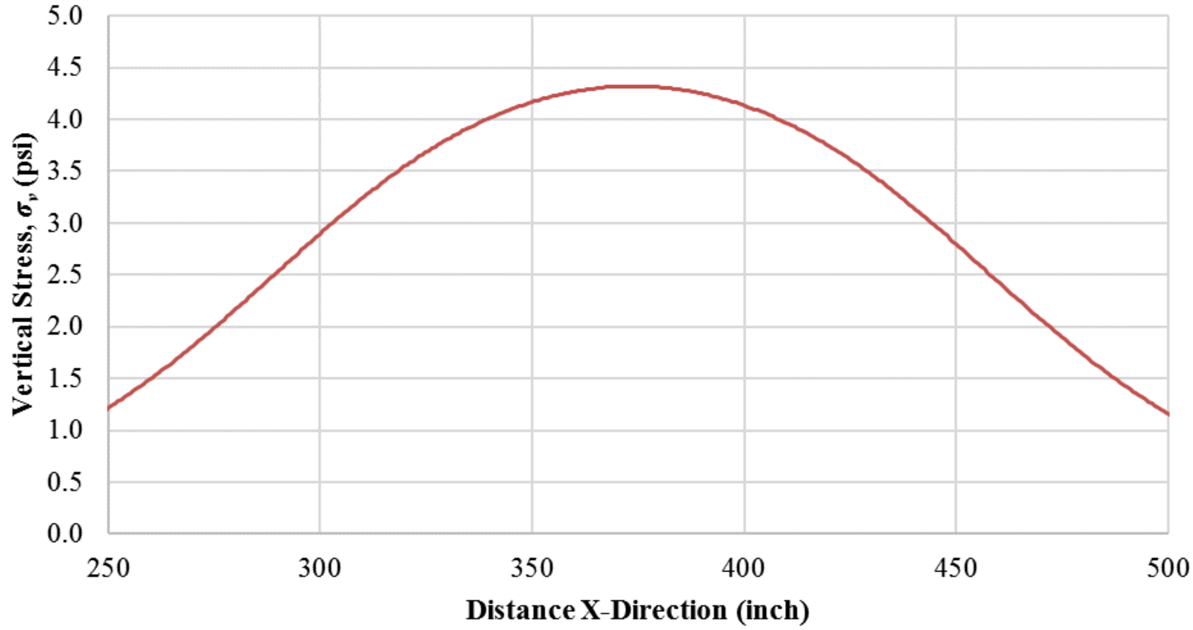

Figure 29. Chart. σ_v distribution at 72 inches below SG (z = 91 inches), three tires (SHL case No. 2: LA-8T-14, 100 °F, PS 2).

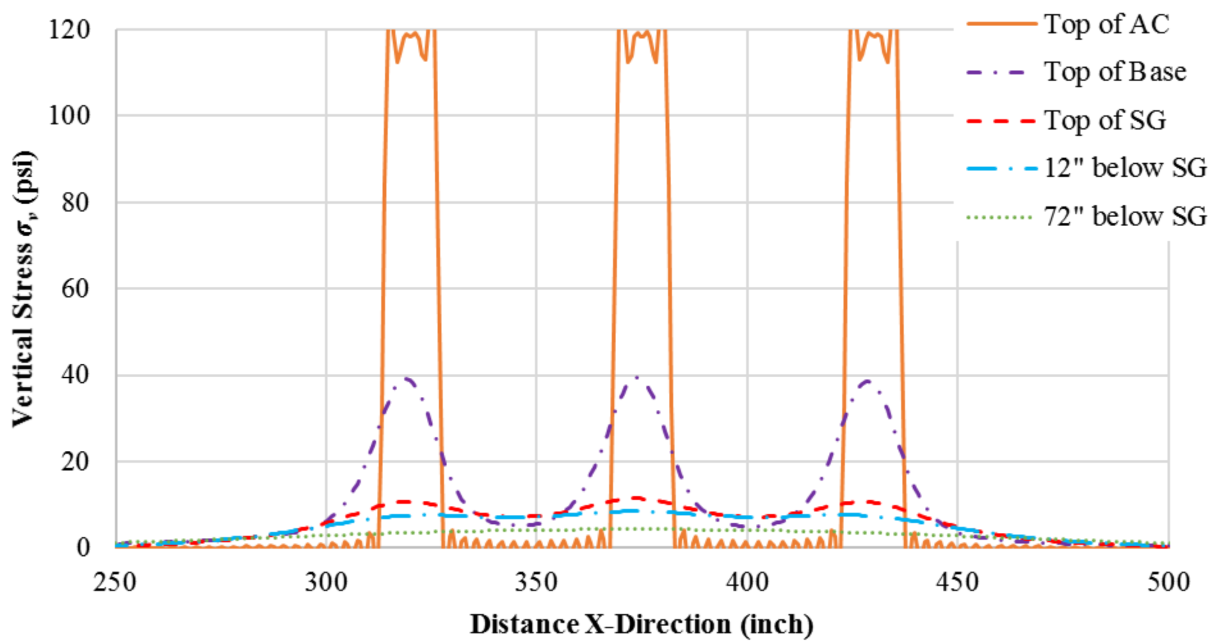

Figure 30. Chart. σ_v distribution at various depths below pavement surface, three tires (SHL case No. 2: LA-8T-14, 100 °F, PS 2).

2.2.5. Variation of σ_v Distributions in *x*-Direction

To observe the role of overlapping as a result of multiple tires, σ_v distribution at the point of interest (in this case, on top of SG and at the center point of the first tire) was computed for a single tire initially. This response was considered the baseline to quantify the influence of additional tires. Then, an additional tire load was added while σ_v distribution at the same point of interest was observed. The change in response value, beyond the baseline value, was due to the additional tire load. The tires were then added in the *x*-direction (vehicle direction) one at a time until a point was reached when the additional tire load had no or negligible influence on the point of interest. Figure 31 shows σ_v distribution at the point of interest on top of SG with three combinations of tires: one, three, and five tires. Additional tires were considered part of the nucleus until the new added tire had minimal influence on the σ_v distribution at the point of interest compared to the baseline σ_v distribution (due to a single tire).

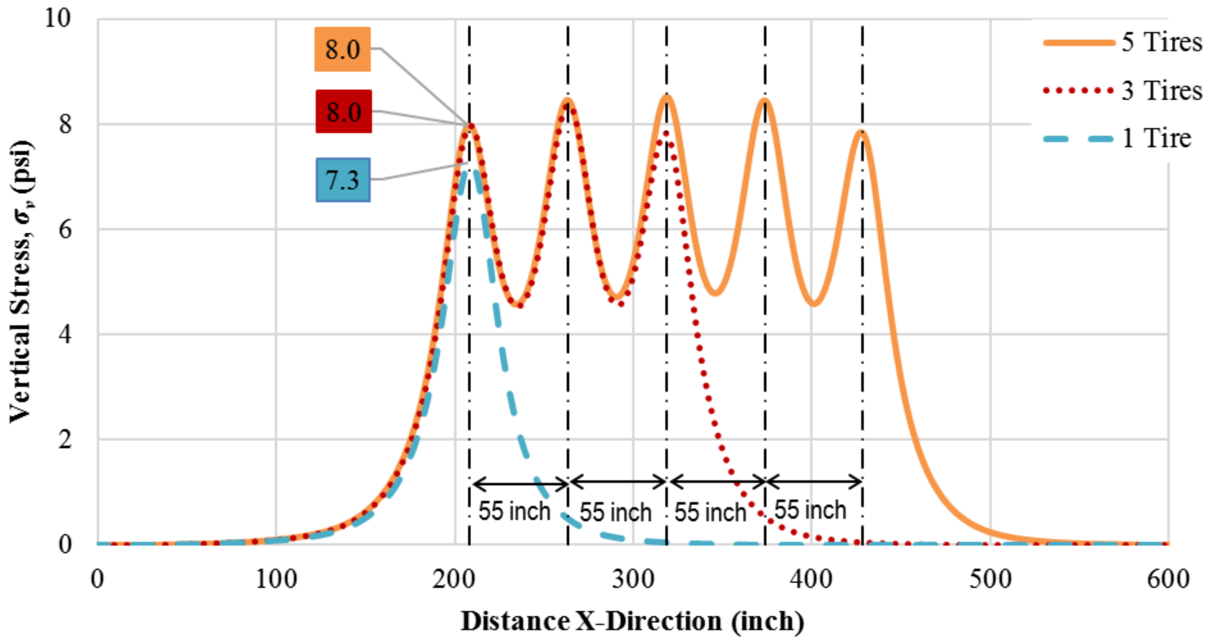

Figure 31. Chart. σ_v distribution on top of SG, adding tires in *x*-direction (SHL case No. 2: LA-8T-14, 100 °F, PS2).

2.2.6. Variation of σ_v Distributions in *y*-Direction

In a similar fashion, additional tire loads were added to the single tire (one tire at a time) in the *y*-direction (transverse direction). The computed σ_v distribution at the point of interest on top of SG is shown in figure 32. This process allows for clear interpretation of the role of additional tires on the σ_v distribution at the point of interest. It is seen from data in figure 32 that the $\sigma_{v\,max}$ under the first tire was unaffected beyond three tires. It should be noted that the influence of adding more tires was affected by various factors, such as the pavement configuration and layer properties.

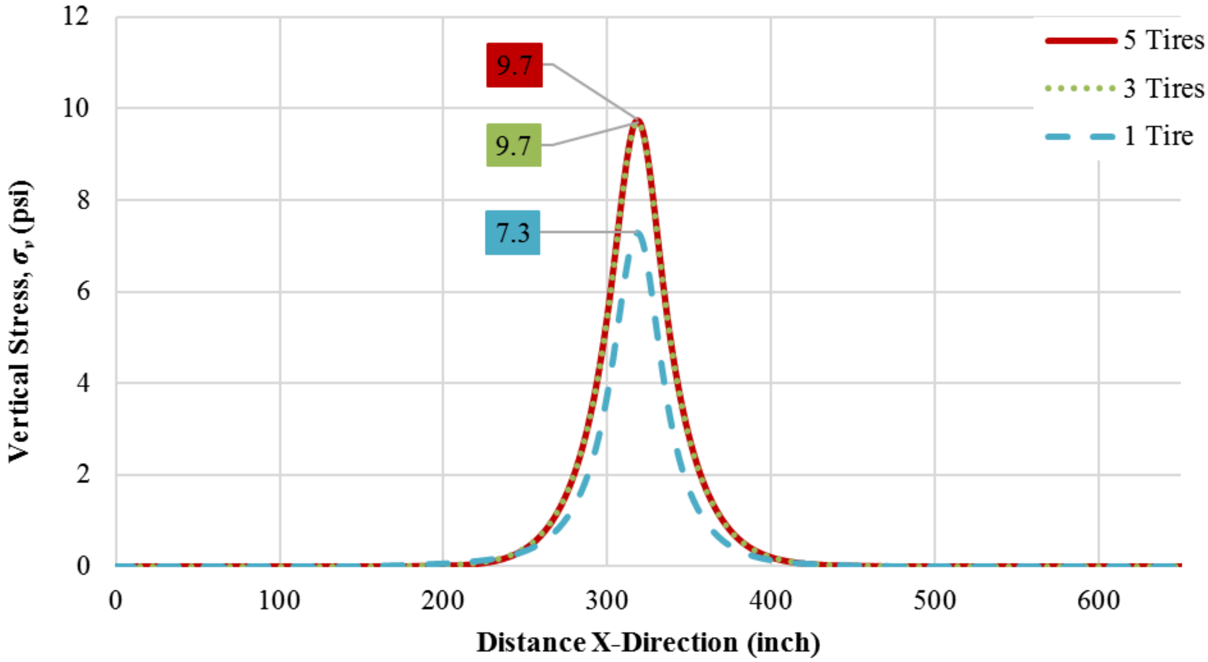

Figure 32. Chart. σ_v distribution on top of SG (z = 19 inches), adding tires in *y*-direction (SHL case No. 2: LA-8T-14, 100 °F, PS 2).

Figure 33 shows the change in $\sigma_{v\ max}$ as more and more tires are considered. These results have been normalized with respect to the $\sigma_{v\ max}$ computed under a single tire, and the findings are shown in figure 34 and figure 35. It is clear from these figures that, beyond a set of three tires, the influence of adding more tires is minimal for both the *x*- and *y*-directions. The number of additional tires in the *x*-direction that influence the point of interest (Nx) is two tires. Similarly, in the *y*-direction, the number of additional tires that influence the point of interest (Ny) is two tires.

A representative nucleus for axle configuration can then be determined based on σ_v distributions that considered the role of adding the tires in both directions. For the axle configuration considered here, two additional tires in each direction were influential (Nx = 2 and Ny = 2), and therefore, to generate $\sigma_{v\ max}$ under a single tire, the representative nucleus becomes a group of five by five tires (figure 36). In other words, when the $\sigma_{v\ max}$ under a given tire is to be considered, two tires should be added in each direction of the tire under consideration.

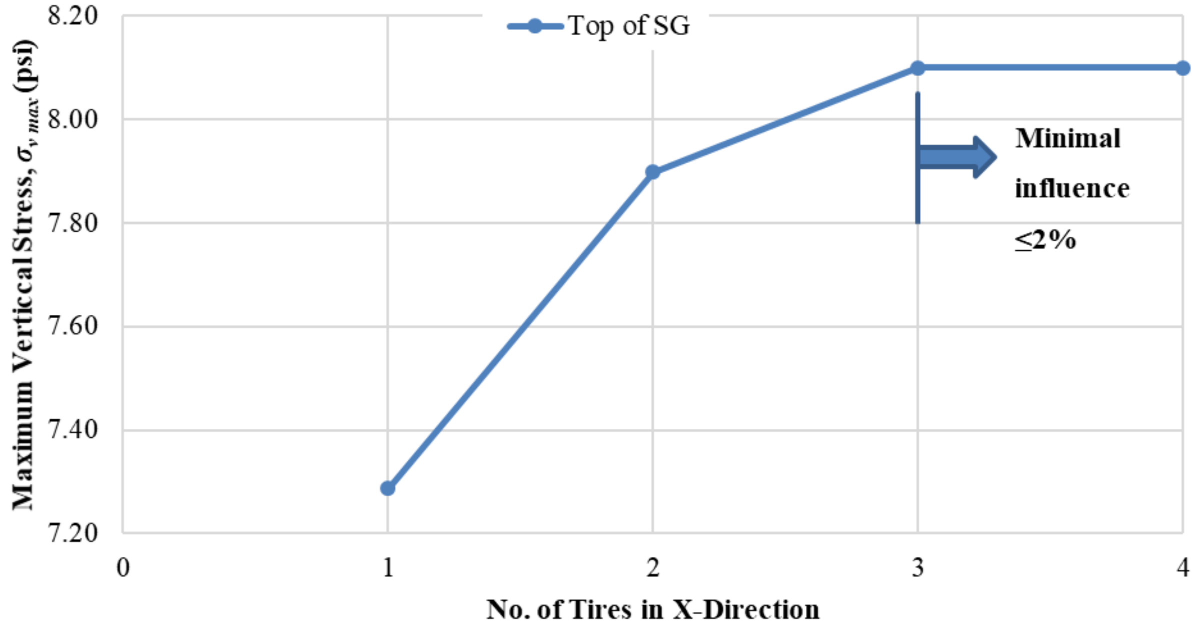

Figure 33. Chart. Change in $\sigma_{v\,max}$ with multiple tires in *x*-direction (SHL case No. 2: LA-8T-14, 100 °F, PS 2).

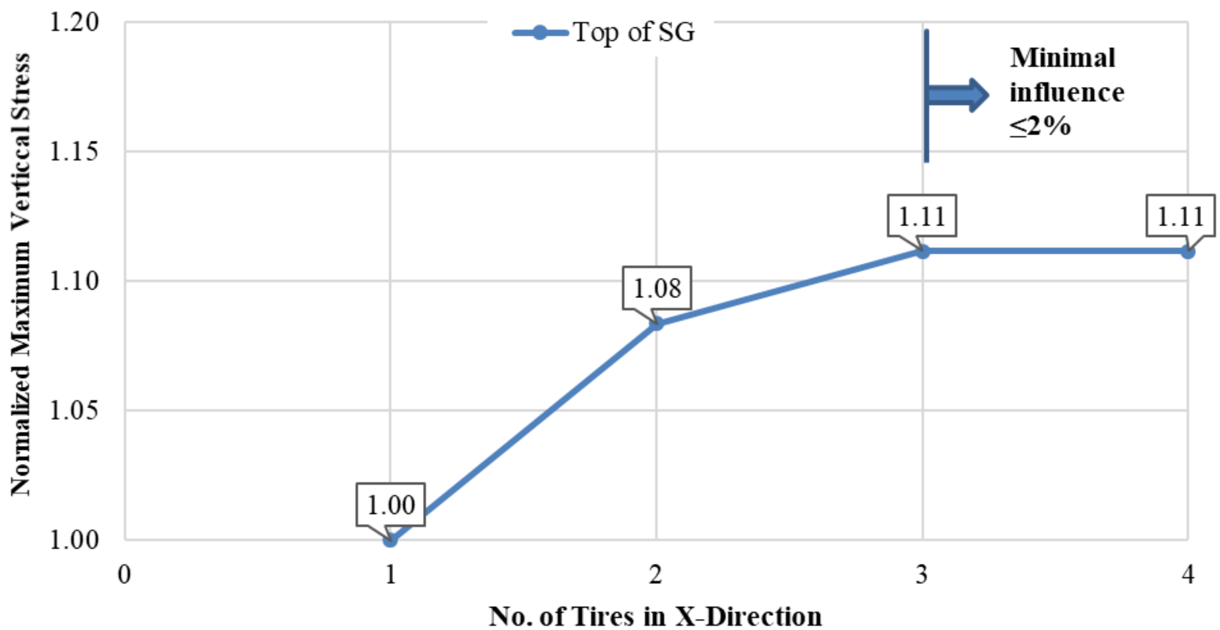

Figure 34. Chart. Normalized $\sigma_{v\,max}$ as a function of number of tires in *x*-direction (SHL case No. 2: LA-8T-14, 100 °F, PS 2).

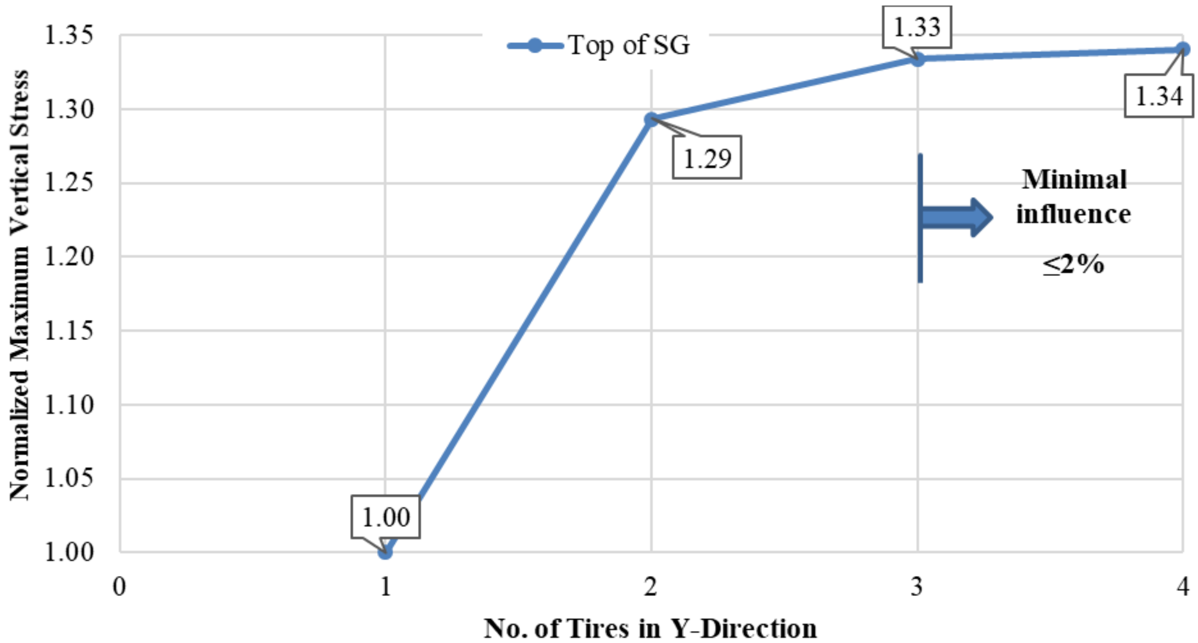

Figure 35. Chart. Normalized $\sigma_{v\ max}$ as a function of number of tires in *y*-direction (SHL case No. 2: LA-8T-14, 100 °F, PS2).

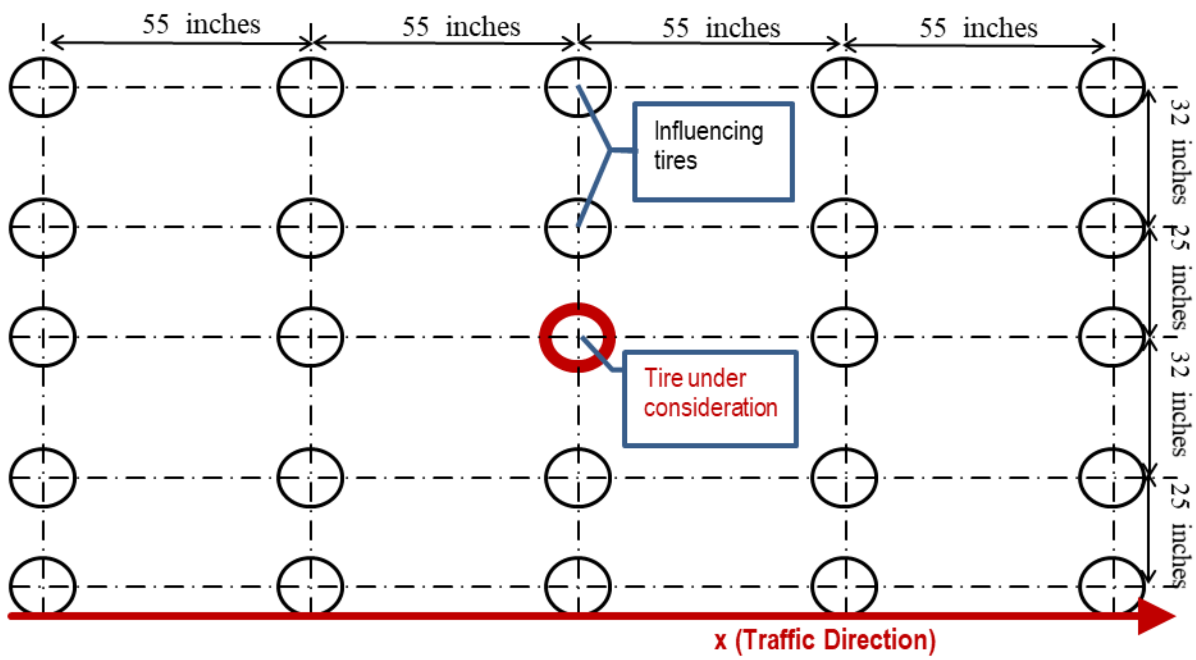

Figure 36. Chart. Representative nucleus (SHL case No. 2: LA-8T-14, 100 °F, PS 2).

2.3. MAXIMUM AVERAGE STRESS USING NUCLEUS OF AXLE CONFIGURATION

The pavement structure considered (PS 2) was 9 inches of AC, 10 inches of CAB, and semi-infinite SG. σ_v distribution resulting from the nucleus shown in figure 36 can be considered representative of the entire SHL vehicle LA-8T-14.

The resulting σ_v distribution on top of SG due to the SHL axle configuration LA-8T-14 with the nucleus, five axles with six tires per axle, is shown in figure 37 (3D view) and figure 38 (top view). These figures reveal that the peak amplitude, which occurs under the middle two tires (figure 38), was approximately 13.5 psi, whereas the amplitude at the adjacent valley was approximately 9.2 psi. In other words, the stress at the valley was approximately 68 percent of the peak.

The average uniform σ_v (q_{ave}) induced by the SHL at the depth of interest was then evaluated by considering the volume of the σ_v distribution within an imaginary rectangular area around the middle dual tires (figure 38 and figure 39). The average pressure value was 10.5 psi, calculated by dividing the integrated volume within this rectangle of 32,964 lb (figure 39) by the area of the rectangle 3,135 inches^2 (indicated by the black dashed line in figure 38).

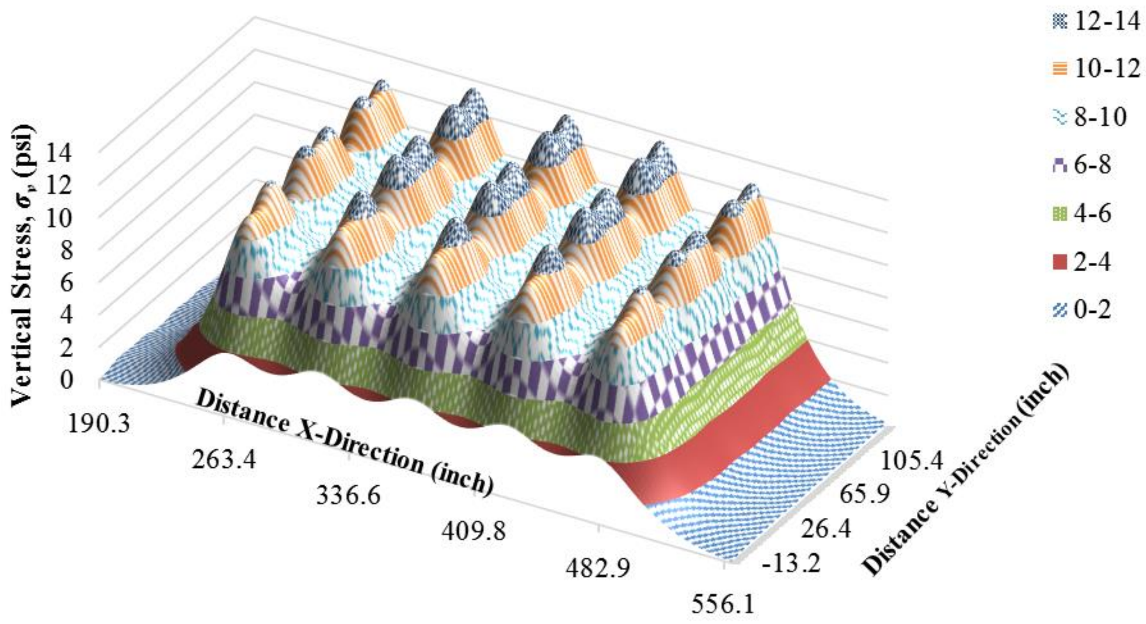

Figure 37. Chart. σ_v distribution on top of SG five by six tires (SHL case No. 2: LA-8T-14, 100 °F, PS 2)—3D view.

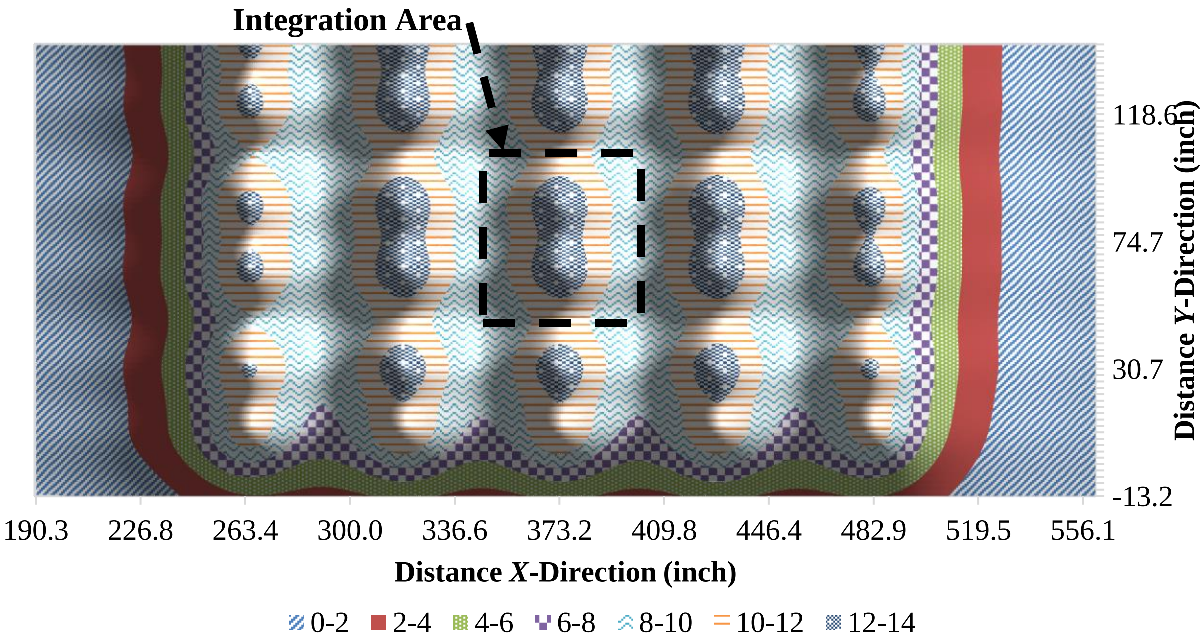

Figure 38. Chart. σ_v distribution on top of SG five by six tires (SHL case No. 2: LA-8T-14, 100 °F, PS 2)—top view.

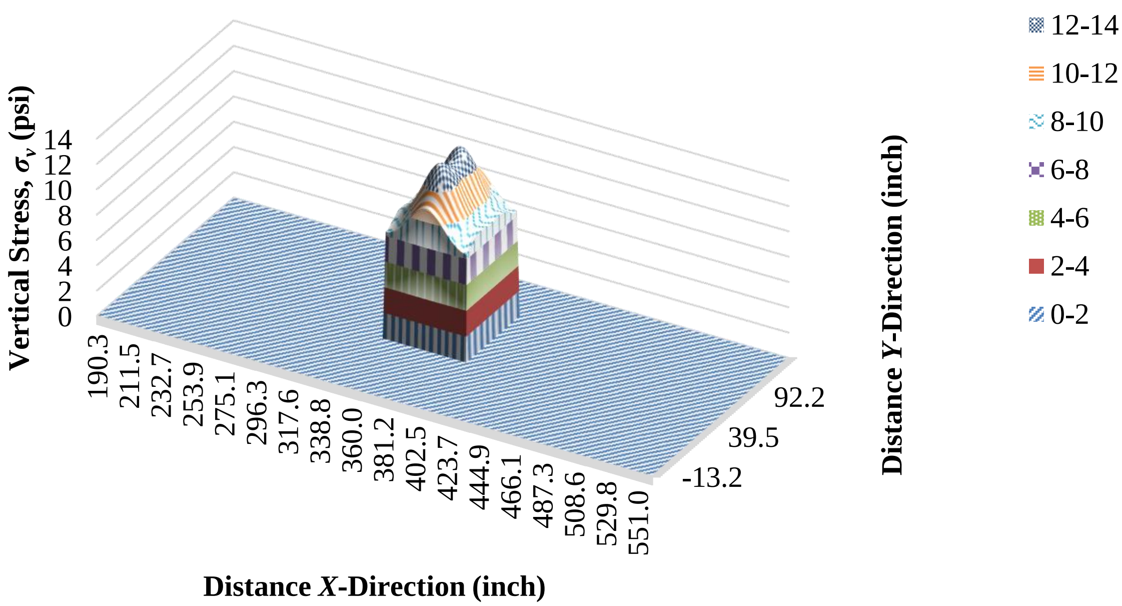

Figure 39. Chart. σ_v distribution at middle dual tires on top of SG (SHL case No. 2: LA-8T-14, 100 °F, PS 2)—3D view.

The q_{ave} found using the nucleus of the SHL vehicle could be used in various applications. The required maximum pressure on top of buried utilities due to SHL, which is needed in the analysis, is a good example. Another application is when investigating the bearing capacity failure under SHL, where a certain fixed shape (circle or rectangle) with a uniform stress distribution is required.

For a bearing capacity investigation, the computed σ_v distribution needs to be associated with a fixed shape and a uniform stress distribution. The entire SHL axle configuration of LA-8T-14 is rectangular in shape (figure 23) with a set of dual tires equally distributed along axles, and the axles are equally distributed across the entire vehicle. This means that, as a conservative measure, q_{ave} of 10.5 psi should be assumed to cover the entire rectangular area of the vehicle. This stress distribution can be considered the worst-case scenario that could be generated under an SHL with this load configuration under consideration. With that, bearing capacity analysis can be carried out to check for failure in the SG using conventional bearing capacity equations. Volume VI: Appendix E presents a case of bearing capacity investigation using the Meyerhof general bearing capacity equation.(5)

As a representative case, the SHL axle configuration of LA-8T-14 (figure 40) was used to illustrate the methodology to establish the σ_v distribution on the SG. In the next chapter, the procedure to identify a representative nucleus of any axle configuration for the analysis of SHL moves is examined using multiple load cases and pavement structures.

As noted, the nucleus can be considered representative of the entire SHL configuration considered here relative to the σ_v distribution within the pavement structure. This nucleus can then be used to calculate the q_{ave}, which can be subsequently used in the bearing capacity analysis. The identification of the nucleus eliminates the need to compute the σ_v distribution under the entire SHL vehicle with consideration given to specifics of the loaded areas. For example, in the case of the SHL axle configuration of LA-8T-14 with 224 tires, the representative nucleus only needs to be modeled for pavement response analysis, eliminating the need to model all of the SHL tires.

CHAPTER 3. SENSITIVITY ANALYSIS

A full factorial experiment was conducted to further illustrate the proposed nucleus concept by implementing the methodology outlined in the previous chapter. The influence of various pavement-structure load configurations and pavement analysis temperatures were considered in this analysis. An emphasis was to develop the nucleus for the tire load configuration. Table 16 presents the full factorial experiment; the nucleus was identified for all the cases marked “Y.” However, for select cases, q_{ave} was also calculated, aiming to compare the results for different load cases. SHL axles and tire configurations considered in this full factorial study are from three permit requests for SHL movements received by LaDOTD (table 17 and figure 5, figure 40, and figure 41). The results of this analysis are presented in the following sections.

Table 16. Nucleus full factorial experiment.

SHL-Vehicle Speed (mph)	SHL Configuration Load Case	Analysis Temperature (°F)	Pavement Structure
10	No. 1: LA-4T-01	100	PS 1: 6-inch AC and 8-inch CAB
10	No. 1: LA-4T-01	100	PS 2: 9-inch AC and 10-inch CAB
10	No. 1: LA-4T-01	100	PS 3: 12-inch AC and 12-inch CAB
10	No. 1: LA-4T-01	70	PS 1: 6-inch AC and 8-inch CAB
10	No. 1: LA-4T-01	70	PS 2: 9-inch AC and 10-inch CAB
10	No. 1: LA-4T-01	70	PS 3: 12-inch AC and 12-inch CAB
10	No. 1: LA-4T-01	40	PS 1: 6-inch AC and 8-inch CAB
10	No. 1: LA-4T-01	40	PS 2: 9-inch AC and 10-inch CAB
10	No. 1: LA-4T-01	40	PS 3: 12-inch AC and 12-inch CAB
10	No. 2: LA-8T-14	100	PS 1: 6-inch AC and 8-inch CAB
10	No. 2: LA-8T-14	100	PS 2: 9-inch AC and 10-inch CAB
10	No. 2: LA-8T-14	100	PS 3: 12-inch AC and 12-inch CAB
10	No. 2: LA-8T-14	70	PS 1: 6-inch AC and 8-inch CAB
10	No. 2: LA-8T-14	70	PS 2: 9-inch AC and 10-inch CAB
10	No. 2: LA-8T-14	70	PS 3: 12-inch AC and 12-inch CAB
10	No. 2: LA-8T-14	40	PS 1: 6-inch AC and 8-inch CAB
10	No. 2: LA-8T-14	40	PS 2: 9-inch AC and 10-inch CAB
10	No. 2: LA-8T-14	40	PS 3: 12-inch AC and 12-inch CAB
10	No. 3: LA-12T-16	100	PS 1: 6-inch AC and 8-inch CAB
10	No. 3: LA-12T-16	100	PS 2: 9-inch AC and 10-inch CAB
10	No. 3: LA-12T-16	100	PS 3: 12-inch AC and 12-inch CAB
10	No. 3: LA-12T-16	70	PS 1: 6-inch AC and 8-inch CAB
10	No. 3: LA-12T-16	70	PS 2: 9-inch AC and 10-inch CAB
10	No. 3: LA-12T-16	70	PS 3: 12-inch AC and 12-inch CAB
10	No. 3: LA-12T-16	40	PS 1: 6-inch AC and 8-inch CAB
10	No. 3: LA-12T-16	40	PS 2: 9-inch AC and 10-inch CAB
10	No. 3: LA-12T-16	40	PS 3: 12-inch AC and 12-inch CAB

Table 17. SHL cases considered in the full factorial study.

SHL Case No.	GVW (lb)	Axle Weight (lb)	No. of Axles	No. of Tires per Axle	Axle Width[a]	Center-to-Center Distance[b]	Tire Load (lb)	Tire Width
1	672,624	37,368	18	4	7 ft 11.6875 inches	4 ft 7 inches	9,342	1 ft 1.5625 inches
2	3,660,552	130,734	28	8	17 ft 5.8125 inches	4 ft 7 inches	16,342	1ft 1.5625 inches
3	1,754,220	73,971 and 72,214	24	12	17 ft 5.8125 inches	4 ft 7 inches	6,164 and 6,018	1 ft 2 inches

[a]Measured out-to-out edges of the outside tires.
[b]Between adjacent axles.

3.1. INFLUENCE OF PAVEMENT STRUCTURE

The pavement structures selected for consideration in the factorial experiment represent thin, intermediate, and thick AC pavements (table 12). The work presented thus far considered the σ_v distribution on top of SG resulting from the SHL axle configuration of LA-8T-14 (SHL case No. 2) and used PS 2 (9 inches of AC, 10 inches of CAB, and a semi-infinite SG layer).

3.1.1. PS 1 (6-Inch AC and 8-Inch CAB)

A similar analysis was undertaken for other pavement structures identified in table 12. The case considered for demonstration in this section is the thinner pavement structure (PS 1) with 6 inches of AC, 8 inches of CAB, and a semi-infinite SG layer. It should be noted that all other 3D-Move Analysis inputs remained the same as the analysis presented earlier for PS 2.[(12)]

Variation of σ_v *Distributions in* x*-Direction*

To observe the role of overlapping as a result of multiple tires, the σ_v distributions were computed initially for a single tire, followed by including additional tires in the *x*-direction (vehicle direction) with one additional tire at a time. Figure 42 shows the $\sigma_{v\ max}$ distribution on top of SG with different combinations of tires, and figure 43 shows the $\sigma_{v\ max}$ normalized with respect to the initial single-tire case.

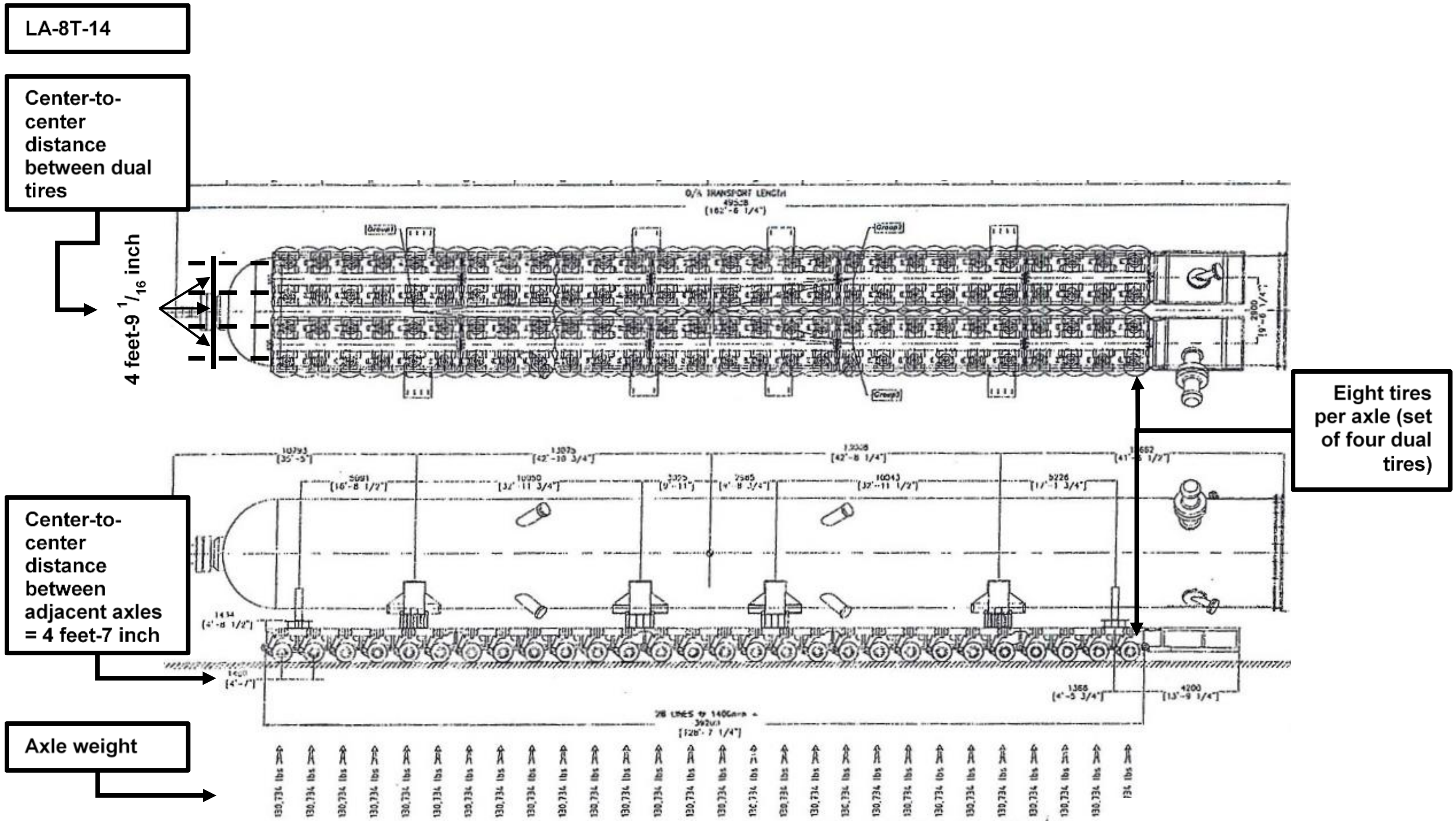

Modified from © 2016 LaDOTD.[11]

Figure 40. Picture. SHL-vehicle case analysis (reactors transport)—case No. 2: LA-8T-14.

[11]Unpublished source obtained through personal communication August 2018.

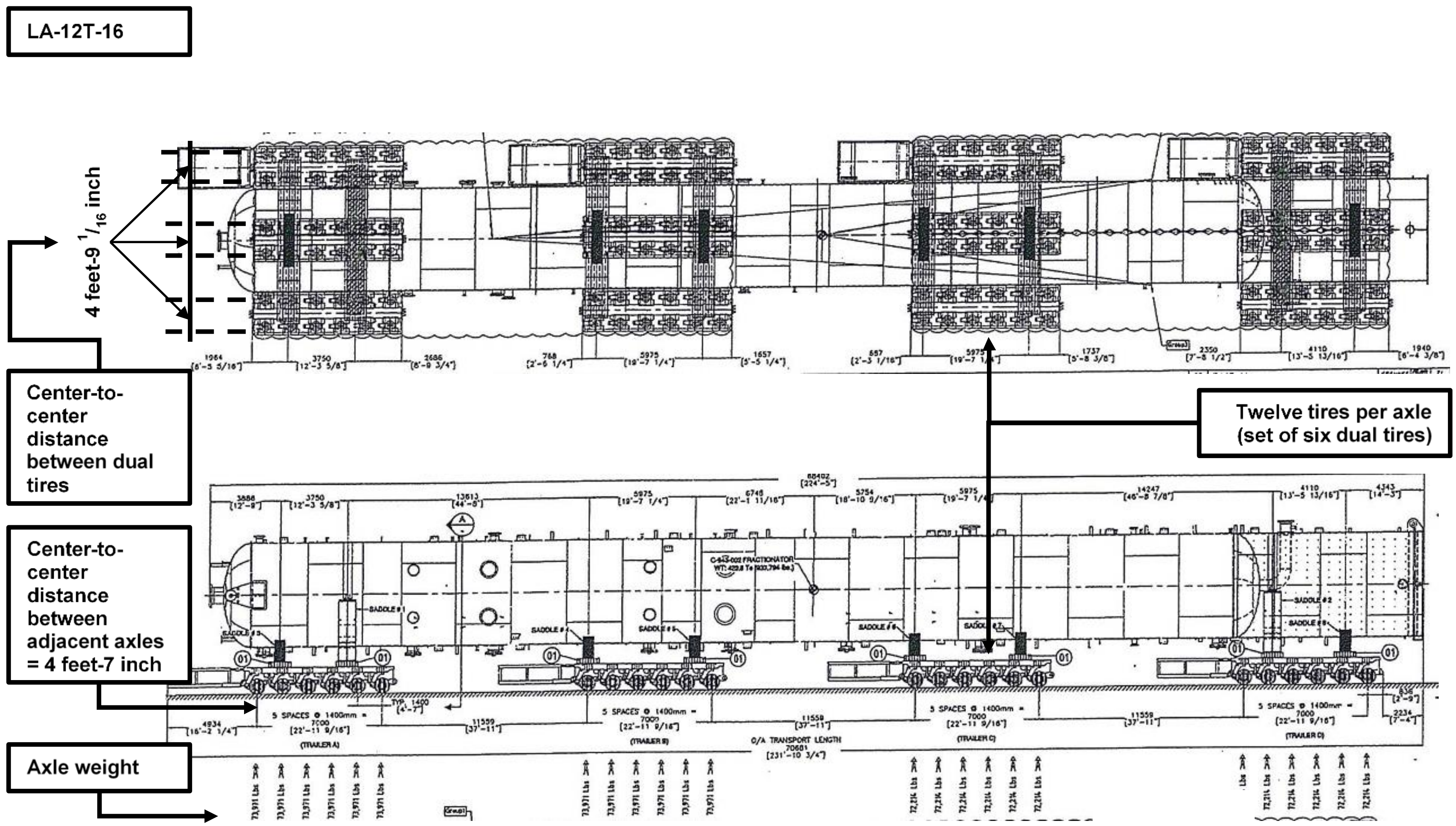

Modified from © 2016 LaDOTD.[12]

Figure 41. Picture. SHL-vehicle case analysis (C-943-002 fractionator)—case No. 3: LA-12T-16.

[12] Unpublished source obtained through personal communication August 2018.

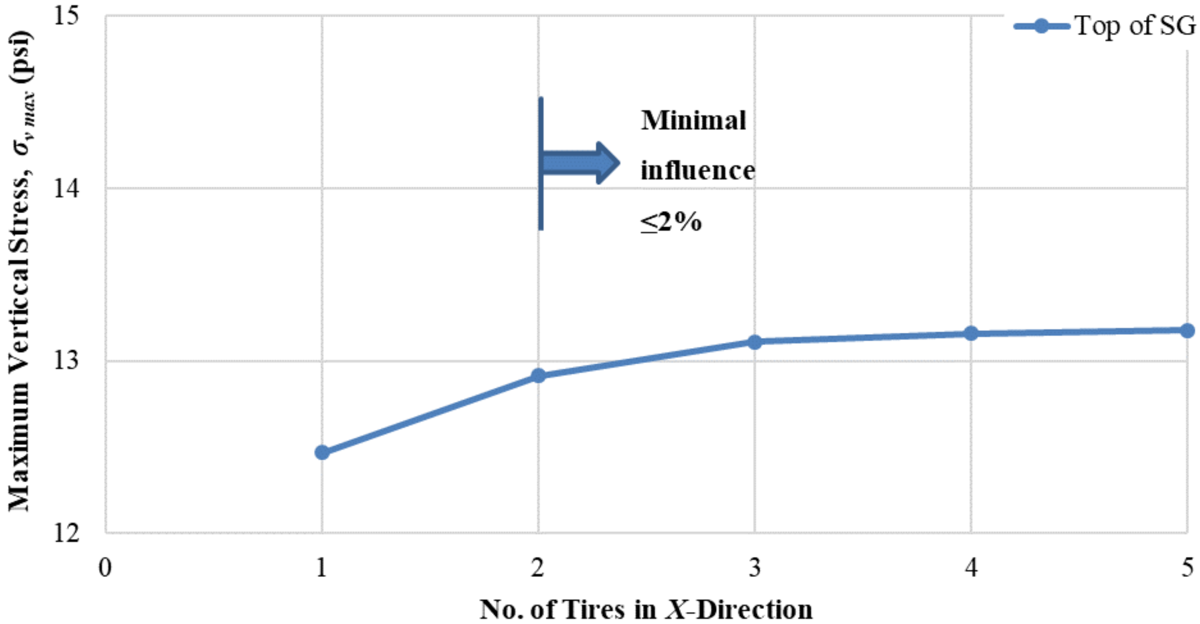

Figure 42. Chart. Change in $\sigma_{v\,max}$ with added tires in *x*-direction (SHL case No. 2: LA-8T-14, 100 °F, PS 1).

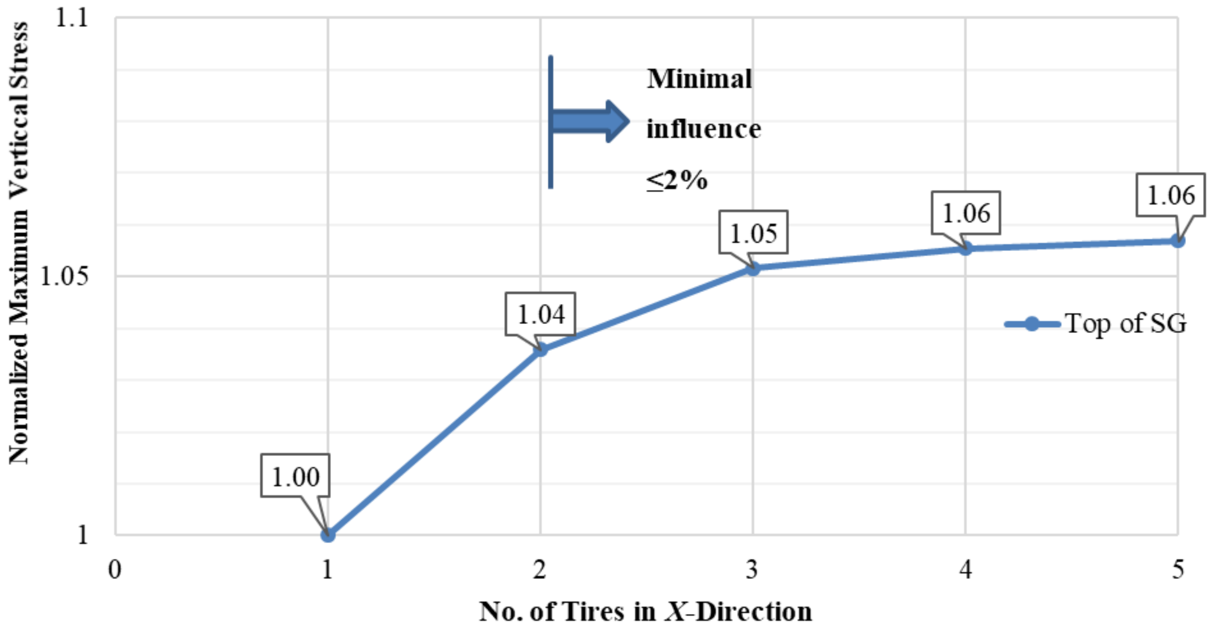

Figure 43. Chart. Change in normalized $\sigma_{v\,max}$ with added tires in *x*-direction (SHL case No. 2: LA-8T-14, 100 °F, PS 1).

Variation of σ_v Distributions in y-Direction

Similarly, the values of $\sigma_{v\ max}$ and the normalized values of $\sigma_{v\ max}$ on top of SG with different combinations of tires are shown in figure 44 and figure 45.

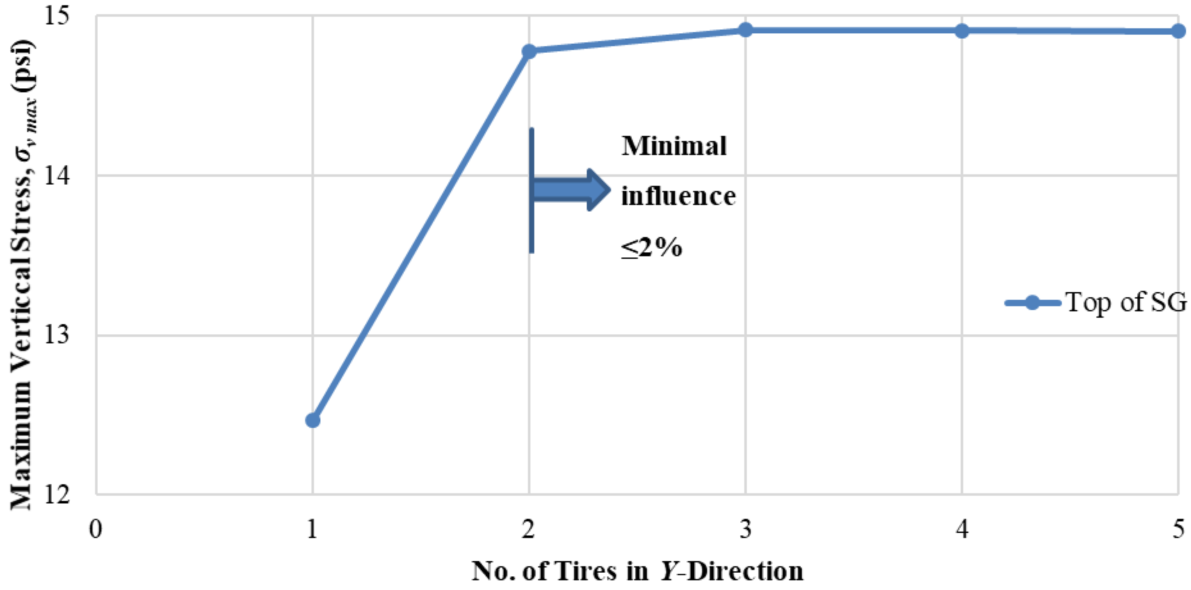

Figure 44. Chart. Change in $\sigma_{v\ max}$ with added tires in *y*-direction (SHL case No. 2: LA-8T-14, 100 °F, PS 1).

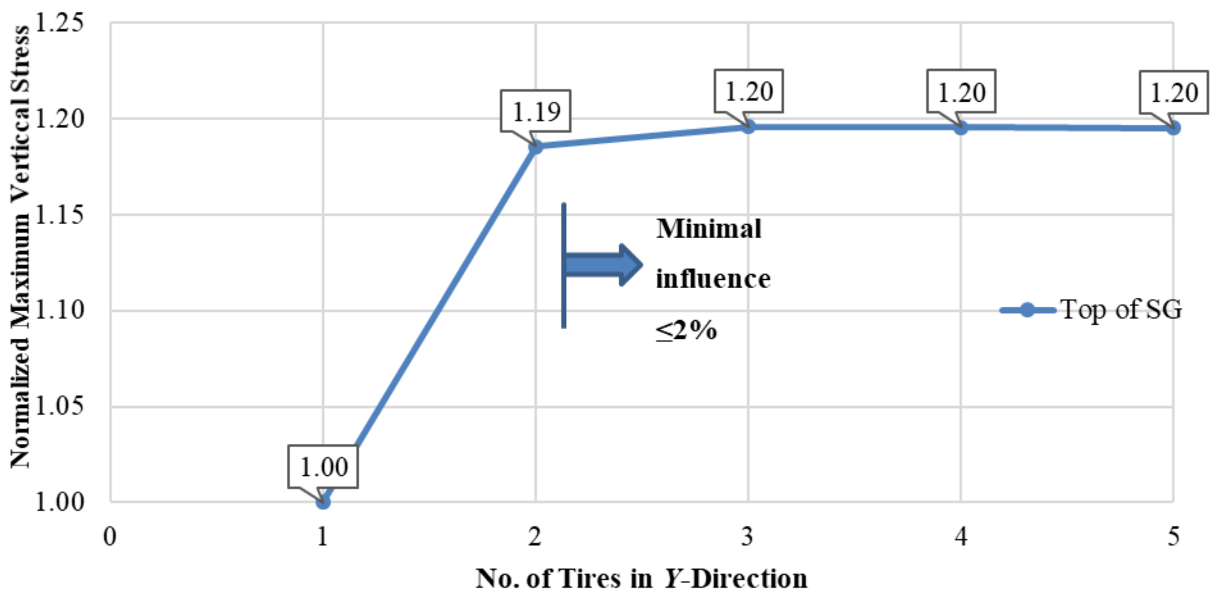

Figure 45. Chart. Change in normalized $\sigma_{v\ max}$ with added tires in *y*-direction (SHL case No. 2: LA-8T-14, 100 °F, PS 1).

In both directions, additional tires were considered until the increment in $\sigma_{v\ max}$ from new added tires was less than 2 percent of $\sigma_{v\ max}$ from the single tire (initial load). The nucleus for this case (SHL case No. 2: LA-8T-14, PS 1) consists of one additional tire in each direction (*x* and *y*). The representative nucleus of SHL axle configuration is shown in figure 46.

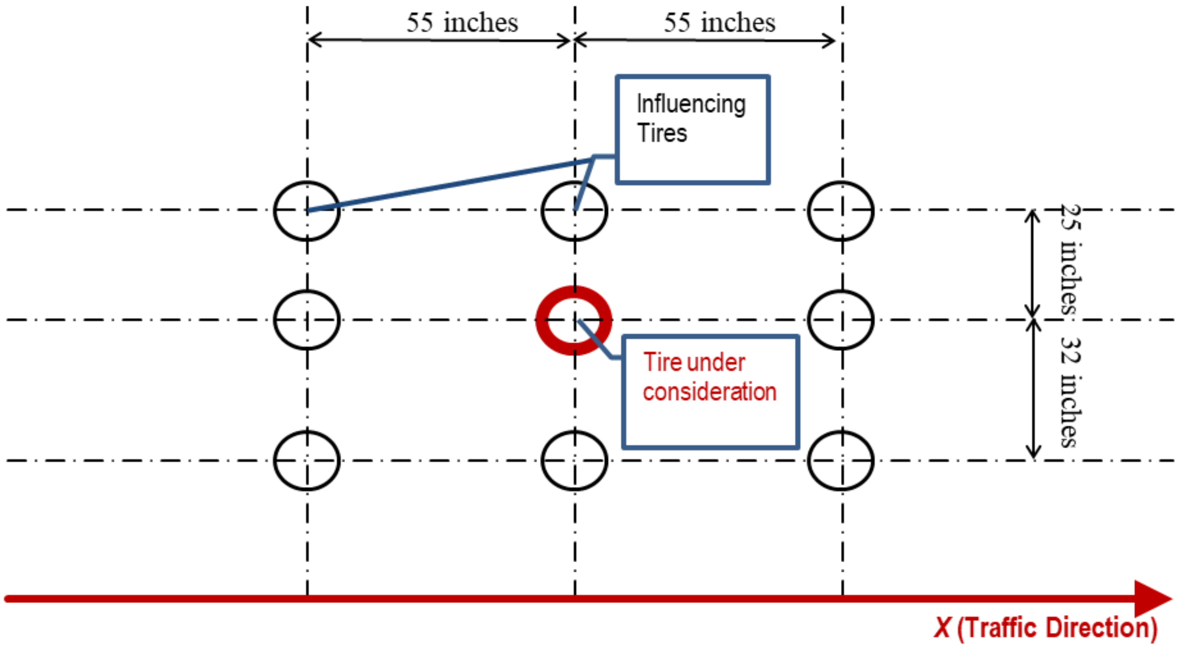

Figure 46. Chart. Representative nucleus (SHL case No. 2: LA-8T-14, 100 °F, PS 1).

Maximum Average Stress Using 3D-Move Analysis

σ_v on top of SG due to the nucleus representing the SHL axle configuration of SHL case No. 2 (LA-8T-14) is shown in figure 47 (3D view) and figure 48 (top view). These figures reveal that the peak amplitude, which occurs between the two tires (figure 47), was approximately 7.2 psi, whereas the amplitude at the adjacent valley was approximately 10.2 psi. In other words, the stress at the valley was approximately 59 percent of the peak.

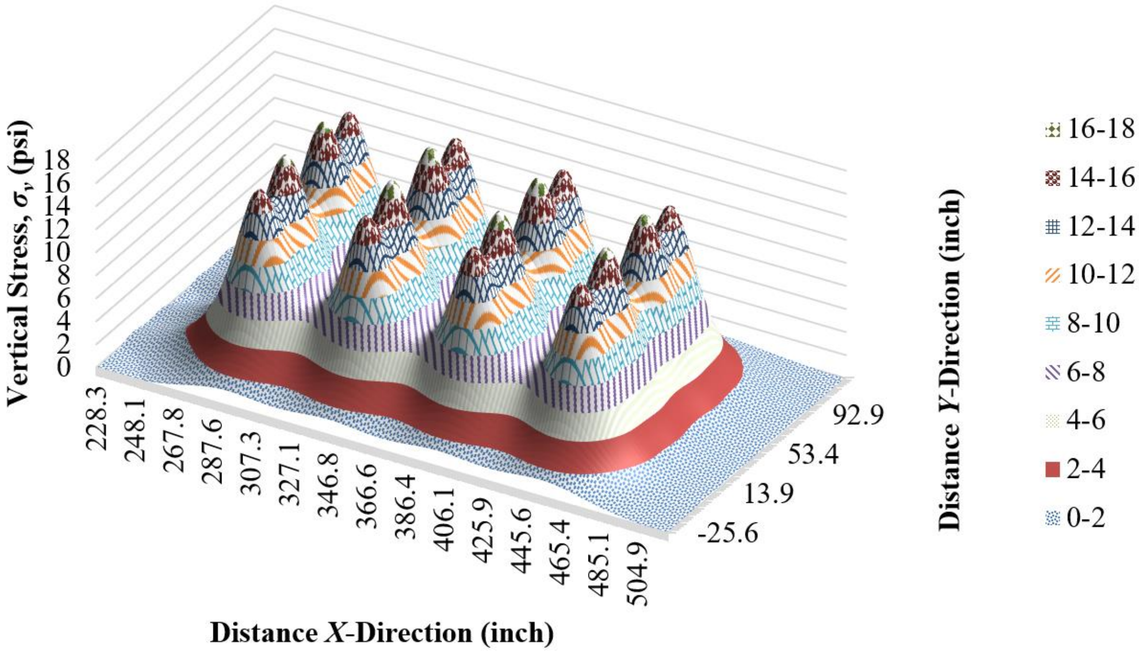

Figure 47. Chart. σ_v distribution on top of SG four by four tires (SHL case No. 2: LA-8T-14, 100 °F, PS 1)—3D view.

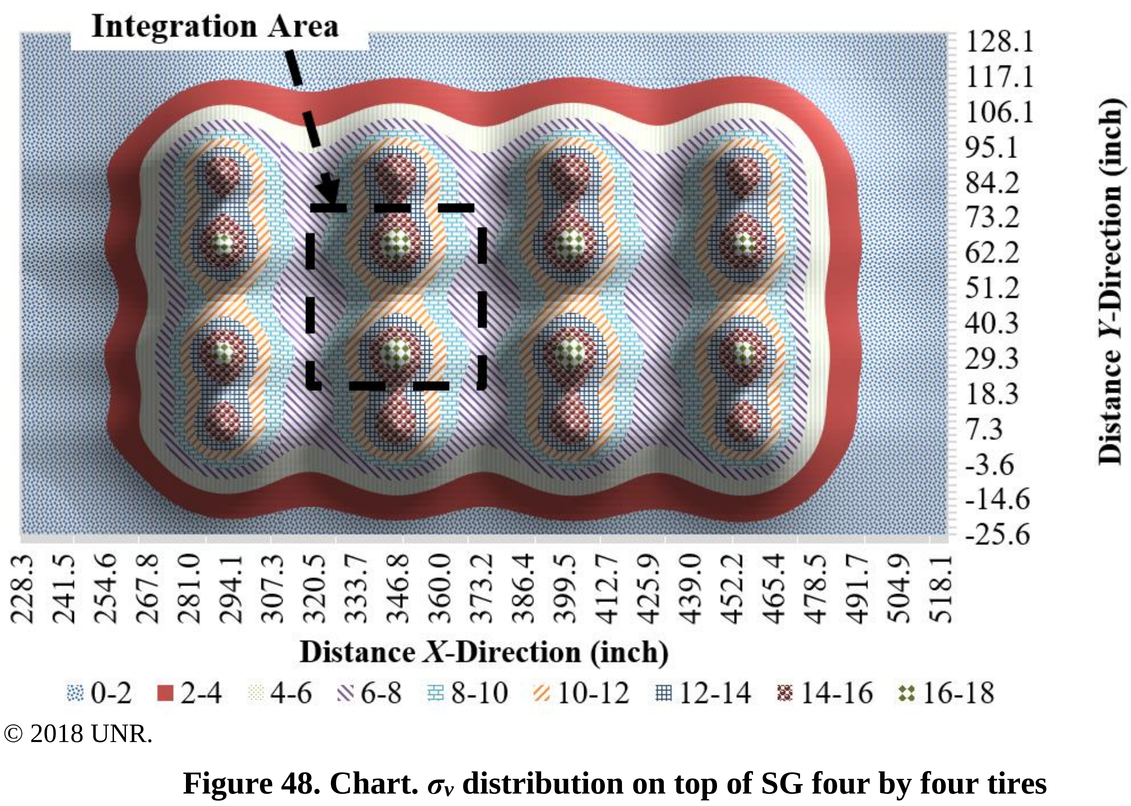

Figure 48. Chart. σ_v distribution on top of SG four by four tires (SHL case No. 2: LA-8T-14, 100 °F, PS 1)—top view.

q_{ave} induced by the SHL was then evaluated by considering the volume of the σ_v distribution within a rectangular area around the middle dual tires (figure 48 and figure 49). A q_{ave} of 11.0 psi was calculated by dividing the integrated volume within this rectangle, 34.395 kips (figure 49), by the area of the rectangle, 3,135 inches^2 (indicated by the black dashed line in figure 48).

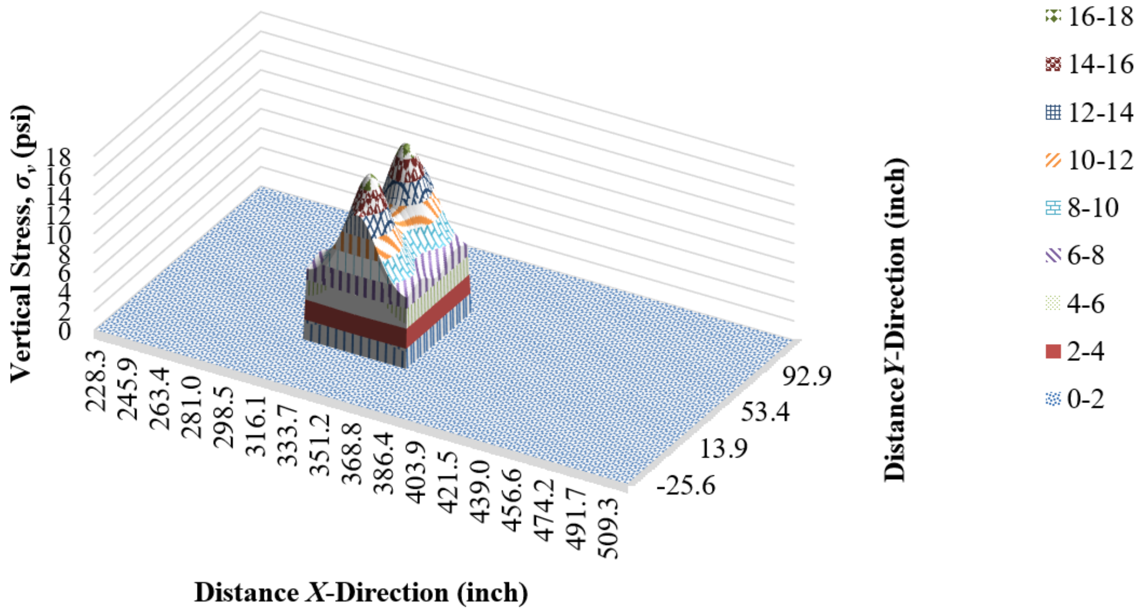

Figure 49. Chart. σ_v distribution at middle dual tires on top of SG (SHL case No. 2: LA-8T-14, 100 °F, PS 1)—3D view.

3.1.2. PS 3 (12-Inch AC and 12-Inch CAB)

In this section, a similar analysis is illustrated for the thickest AC PS 3 with the LA-8T-14 SHL configuration. In all cases, other than the loading, the 3D-Move Analysis inputs remained the same.(12)

Variation of σ_v *Distributions in* x*-Direction*

To observe the role of overlapping as a result of multiple tires, the σ_v distributions were computed initially for a single tire, followed by including additional tires in the *x*-direction (vehicle direction) by adding one tire at a time. Figure 50 shows the $\sigma_{v\ max}$ distribution on top of SG for the PS 3 with different combinations of tires, and figure 51 shows the $\sigma_{v\ max}$ normalized with respect to the initial single-tire case.

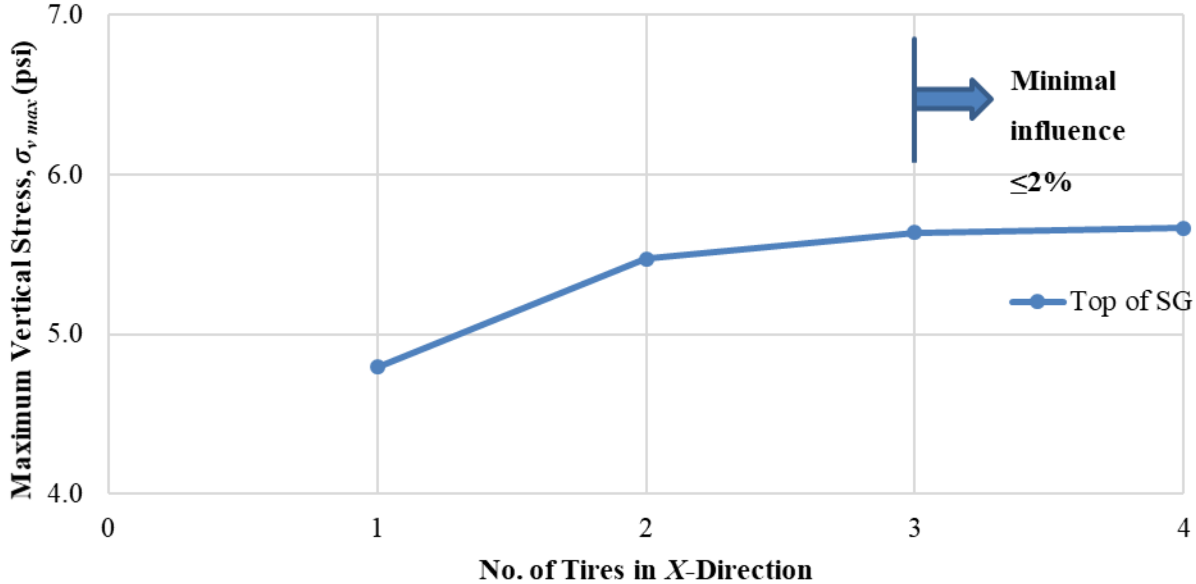

Figure 50. Chart. Change in $\sigma_{v\ max}$ with added tires in *x*-direction (SHL case No. 2: LA-8T-14, 100 °F, PS 3).

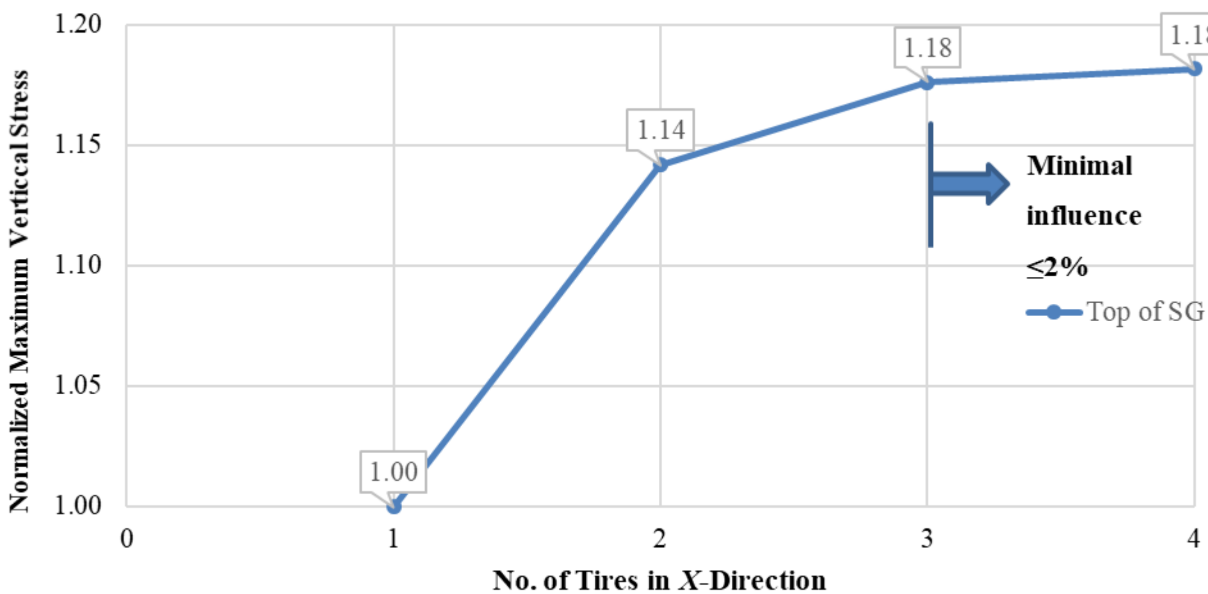

Figure 51. Chart. Change in normalized $\sigma_{v\ max}$ with added tires in *x*-direction (SHL case No. 2: LA-8T-14, 100 °F, PS 3).

Variation of σ_v *Distributions in* y*-Direction*

The σ_v distribution on top of SG with different combinations of tires is shown in figure 52. In both directions, additional tires were considered until the new added tire had minimal influence on the σ_v distribution computed under the first tire (lower than 2 percent). The nucleus for this case (SHL case No. 2: LA-8T-14, PS 3) consists of one additional tire in each direction (*x* and *y*). The corresponding representative load nucleus is shown in figure 54.

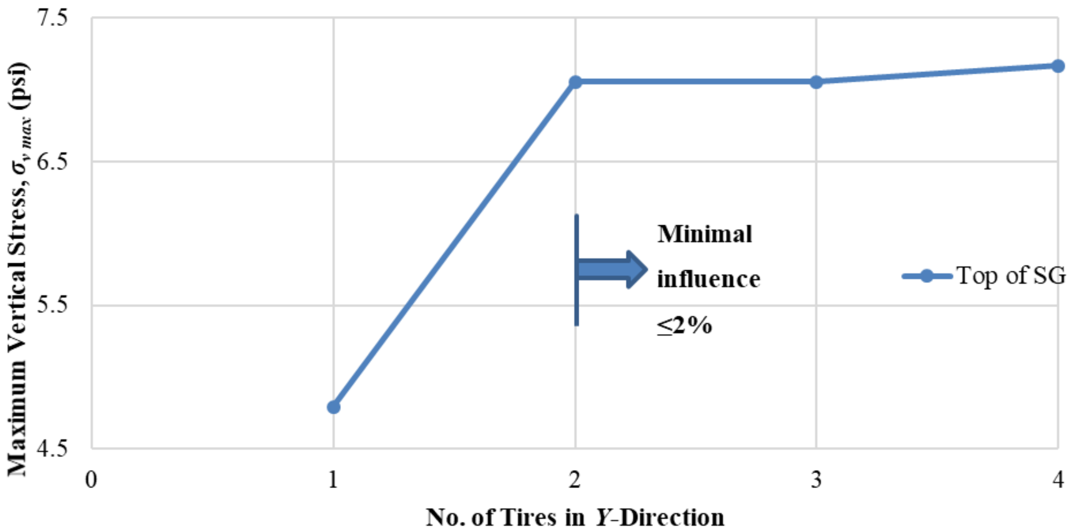

Figure 52. Chart. Change in $\sigma_{v\,max}$ with added tires in *y*-direction (SHL case No. 2: LA-8T-14, 100 °F, PS 3).

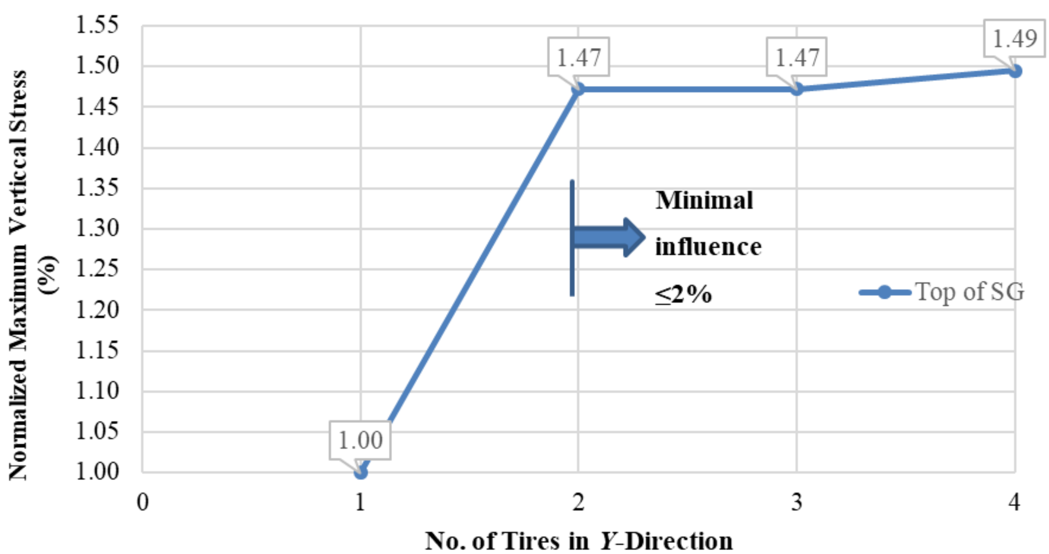

Figure 53. Chart. Change in normalized $\sigma_{v\,max}$ with added tires in *y*-direction (SHL case No. 2: LA-8T-14, 100 °F, PS 3).

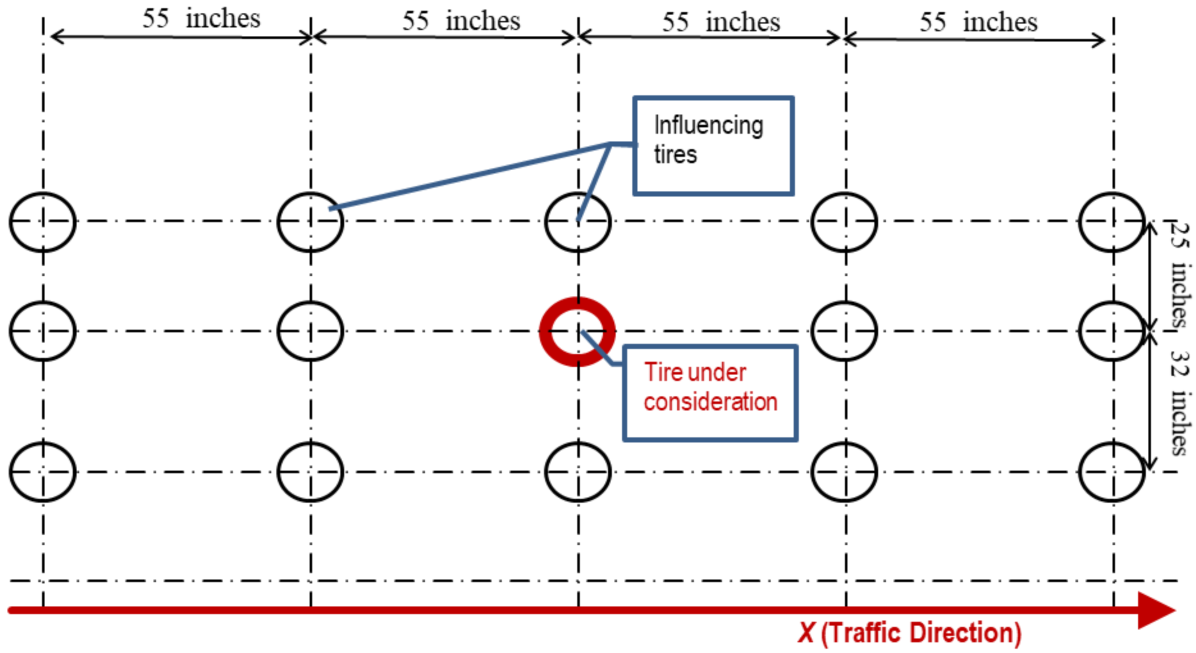

Figure 54. Chart. Representative nucleus (SHL case No. 2: LA-8T-14, 100 °F, PS 3).

3.1.3. Summary of Influence of Pavement Structure

Figure 55 and figure 56 show the change in $\sigma_{v\ max}$ with added tires in the *x*-direction and *y*-direction, respectively, for all evaluated pavement structures under SHL case No. 2 (LA-8T-14) and AC analysis temperature of 100 °F. The results are summarized in table 18. As expected, the $\sigma_{v\ max}$ on top of SG decreased with the increase in pavement structure thicknesses.

Table 18. Summary of influence of pavement structure for SHL case No. 2: LA-8T-14.

SHL-Vehicle Speed (mph)	Analysis Temperature (°F)	Pavement Structure	*Nx*	*Ny*	$\sigma_{v\ max}$ (psi)
10	100	PS 1: 6-inch AC and 8-inch CAB	1	1	14.9
10	100	PS 2: 9-inch AC and 10-inch CAB	2	2	9.8
10	100	PS 3: 12-inch AC and 12-inch CAB	2	1	7.1

PS = pavement structure.

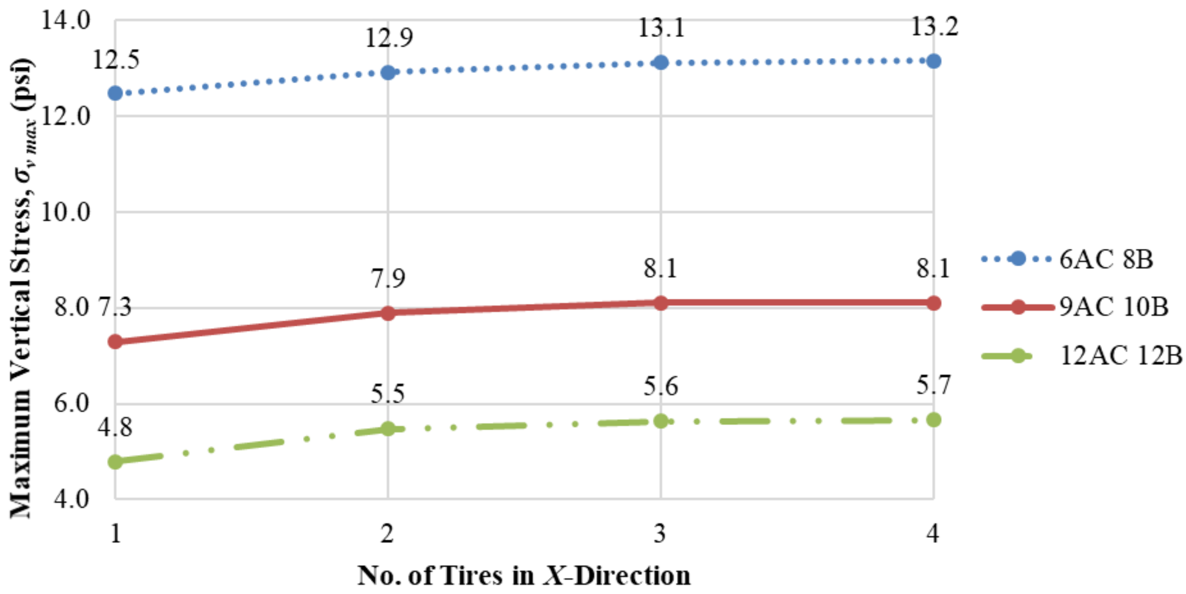

Figure 55. Chart. Change in $\sigma_{v\,max}$ with added tires in *x*-direction (SHL case No. 2: LA-8T-14, 100 °F, all PSs).

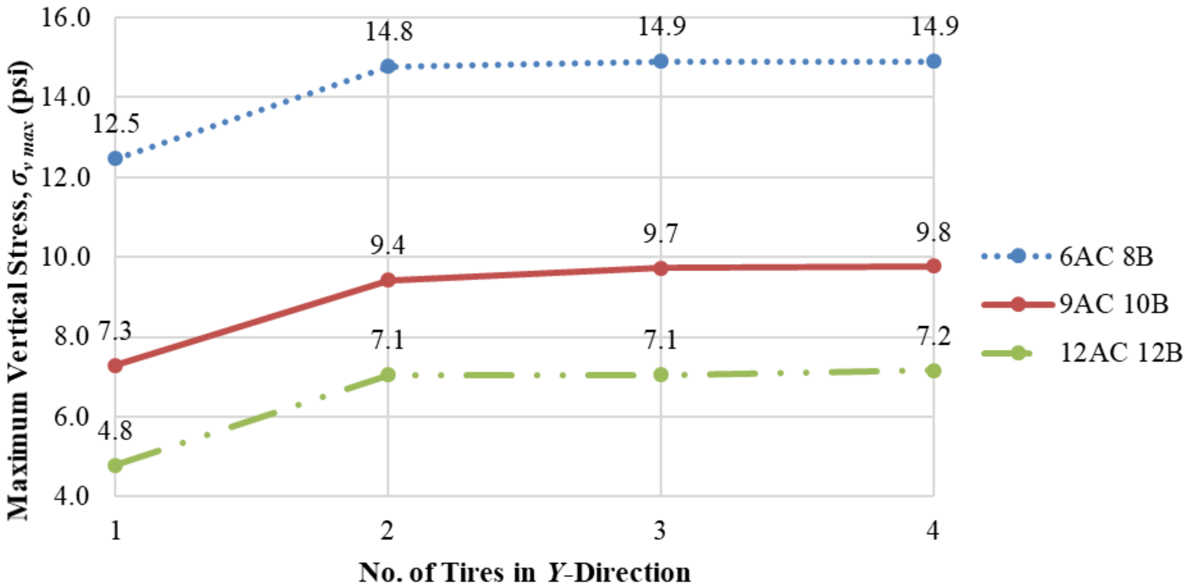

Figure 56. Chart. Change in $\sigma_{v\,max}$ with added tires in *y*-direction (SHL case No. 2: LA-8T-14, 100 °F, all PSs).

3.2. INFLUENCE OF DIFFERENT SHL CONFIGURATIONS

The work presented in the previous sections considered the σ_v distribution on top of SG resulting from the SHL axle configuration of SHL case No. 2 (LA-8T-14). Similar analyses were undertaken for SHL case No. 1 (LA-4T-1) and case No. 3 (LA-12T-16) and are summarized in section 3.2.1 and section 3.2.2, respectively.

3.2.1. SHL Case No. 1 (LA-4T-1)

The load case selected for this part of the effort is SHL case No. 1 (LA-4T-1), which consists of 4 tires in each of its 18 axles, a GVW of 672,624 lb, an axle weight of approximately 37,368 lb, and a tire load of approximately 9,342 lb per tire, as shown in figure 5. The pavement structure considered is PS 1 (6-inch AC, 8-inch CAB, and a semi-infinite SG layer), and the AC analysis temperature was 100 °F.

Variation of σ_v *Distribution in* x*-Direction*

To observe the role of overlapping as a result of multiple tires, σ_v distributions were computed initially for a single tire, followed by the consideration of additional tires in the *x*-direction (vehicle direction). Figure 57 shows σ_v distribution on top of SG with different combinations of tires. In this case, the values of the $\sigma_{v\,max}$ are relatively small, and as a result, the normalized values of σ_v might indicate a false representation of notable increase from tire to tire, whereas the actual change is less than 0.2 psi.

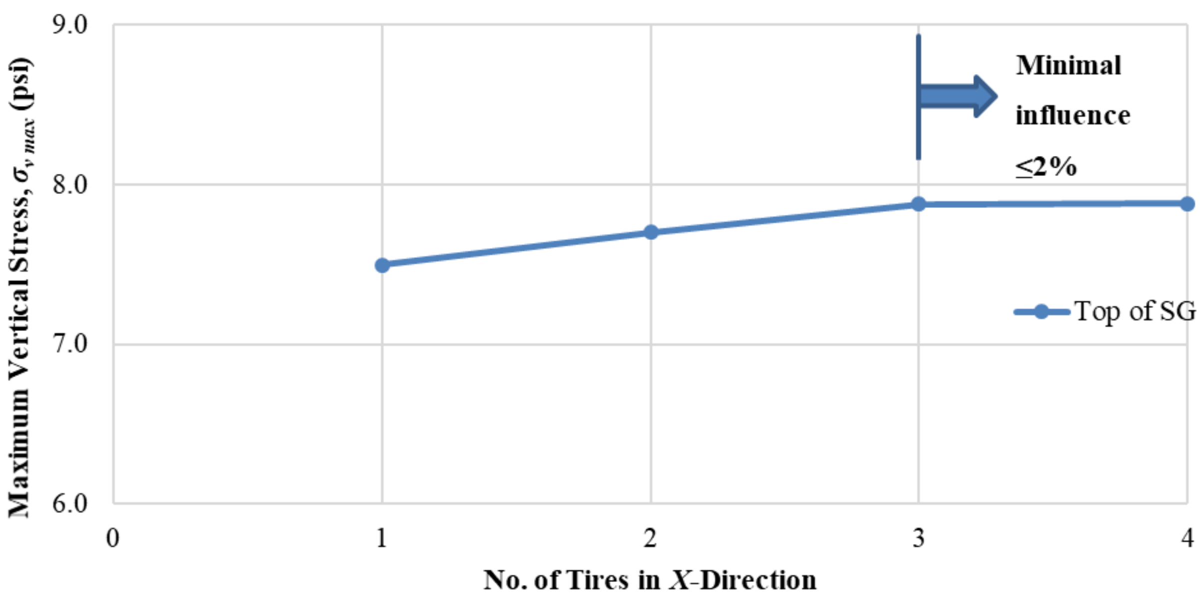

Figure 57. Chart. Change in $\sigma_{v\,max}$ with added tires in *x*-direction (SHL case No. 1: LA-4T-1, 100 °F, PS 1).

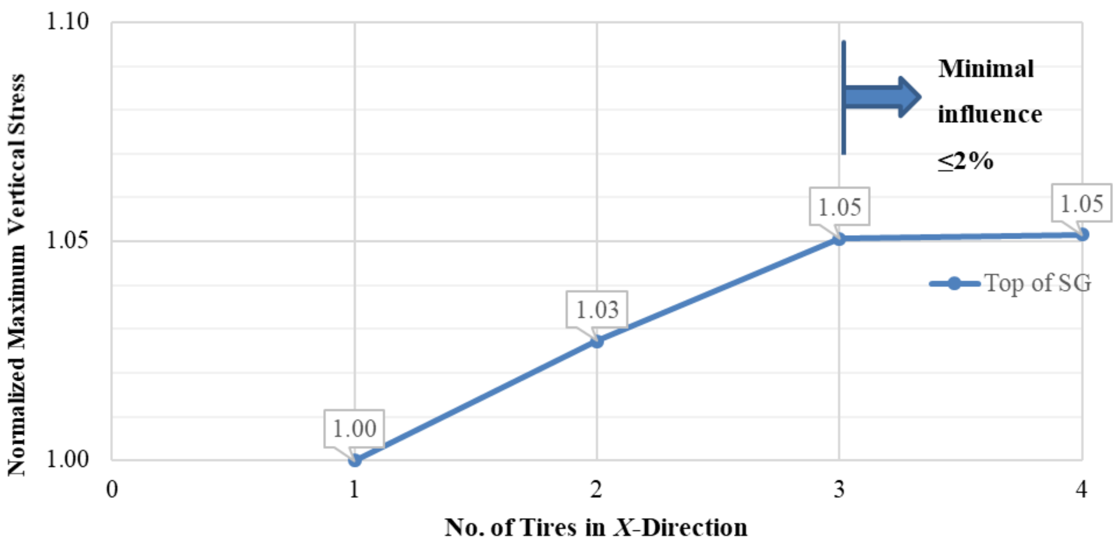

Figure 58. Chart. Change in normalized $\sigma_{v\ max}$ with added tires in *x*-direction (SHL case No. 1: LA-4T-1, 100 °F, PS 1).

Variation of σ_v *Distributions in* y*-Direction*

Similarly, the values of $\sigma_{v\ max}$ and the normalized values of σ_v on top of SG with different combinations of tires are shown in figure 59. In both directions, additional tires were considered until the new added tire had minimal influence on the σ_v distribution computed under the first tire (lower than 2 percent). The nucleus for this case (PS 2, LA-4T-1) consists of one additional tire in each direction. The corresponding representative nucleus of the SHL axle configuration is shown in figure 61.

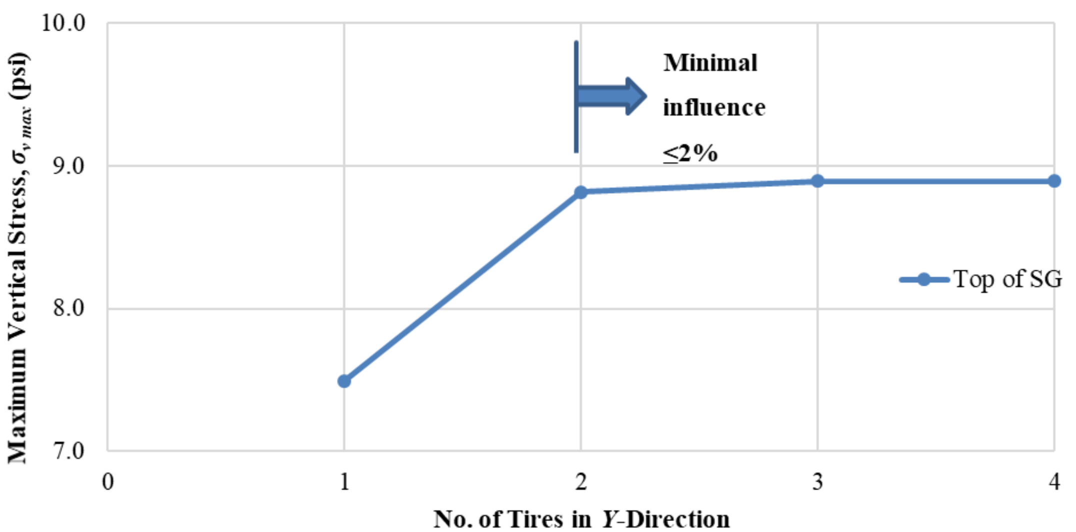

Figure 59. Chart. Change in $\sigma_{v\ max}$ with added tires in *y*-direction (SHL case No. 1: LA-4T-1, 100 °F, PS 1).

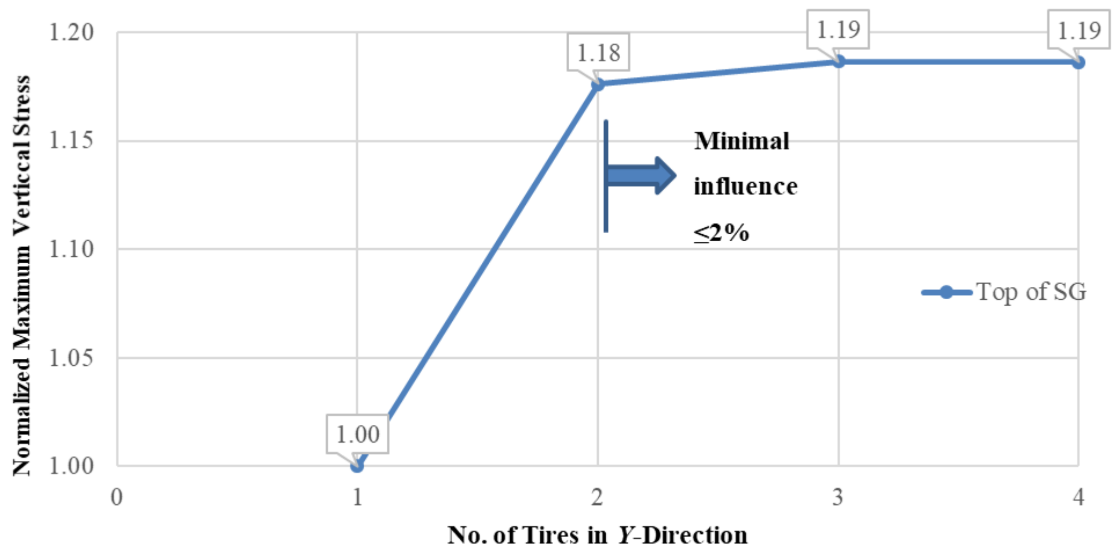

Figure 60. Chart. Change in normalized $\sigma_{v\,max}$ with added tires in *y*-direction (SHL case No. 1: LA-4T-1, 100 °F, PS 1).

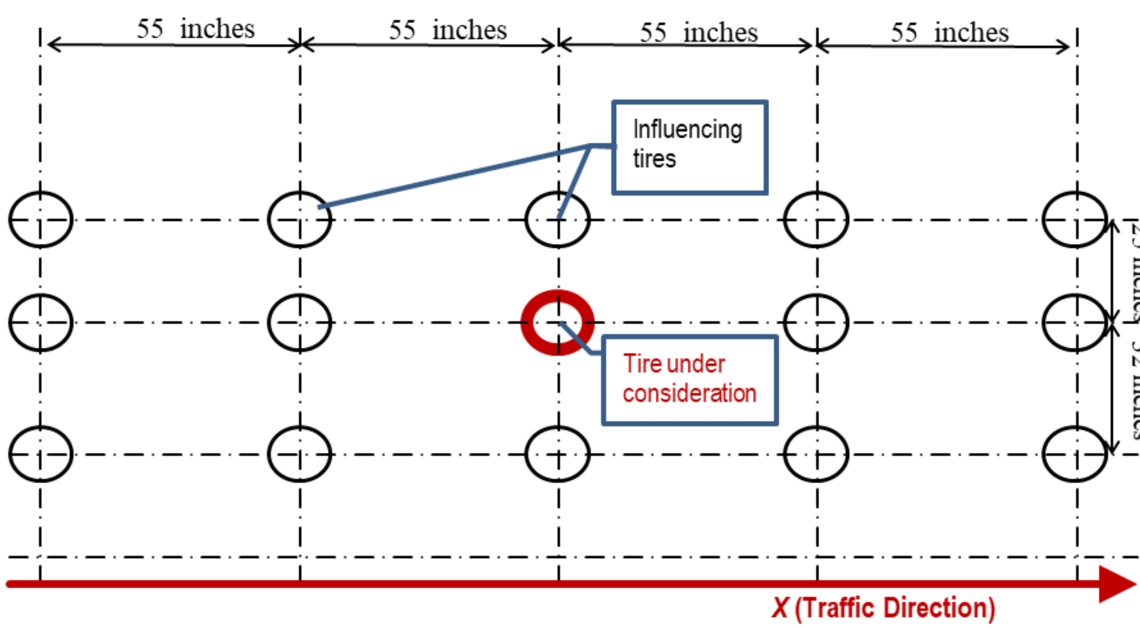

Figure 61. Chart. Representative nucleus (SHL case No. 1: LA-4T-1, 100 °F, PS 1).

3.2.2. SHL Case No. 3 (LA-12T-16)

The work presented so far considered the σ_v distribution on top of SG resulting from two SHL axle configurations (case No. 1: LA-12T-16 and case No. 2: LA-8T-14). The load case presented in this part is case No. 3: LA-12T-16, which consists of 12 tires in each of its 24 axles, a GVW of 1,754,220 lb, an axle weight of approximately 74,000 lb, and a tire load of approximately

6,200 lb per tire, as shown in figure 41. The pavement structure considered for illustration was PS 1 (6-inch AC, 8-inch CAB, and a semi-infinite SG layer), and the AC analysis temperature was 100 °F.

Variation of σ_v *Distribution in* x*-Direction*

To observe the role of overlapping as a result of multiple tires, the σ_v distributions were computed initially for a single tire, followed by the consideration of additional tires in the *x*-direction (vehicle direction). Figure 62 shows the $\sigma_{v\ max}$ distribution on top of SG with different combinations of tires, and figure 63 shows $\sigma_{v\ max}$ normalized with respect to the single-tire case.

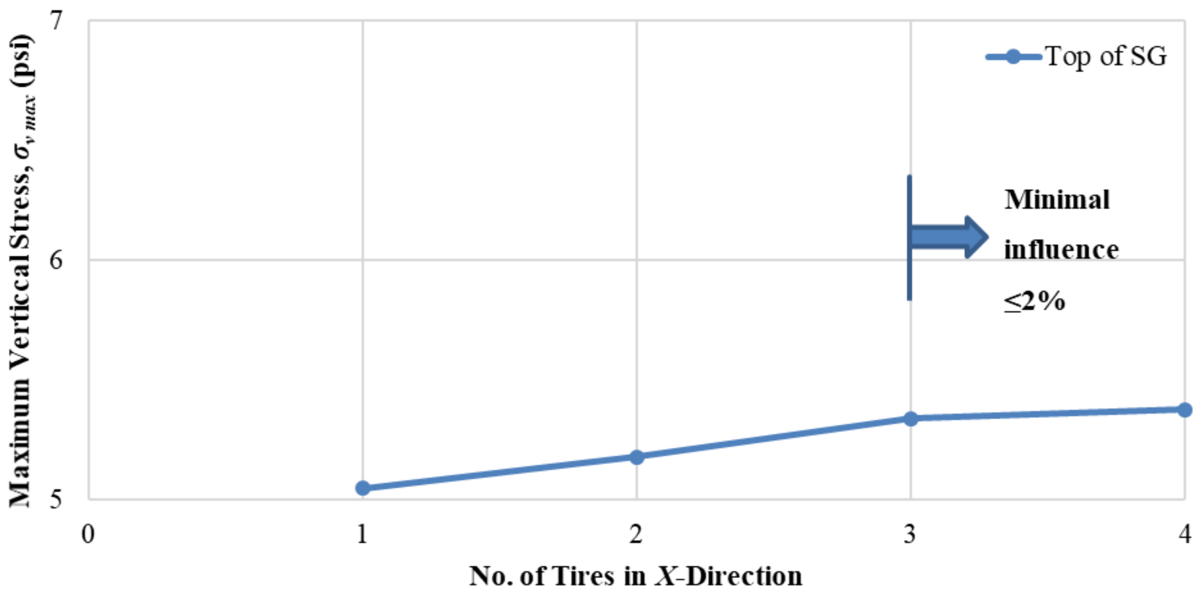

Figure 62. Chart. Change in $\sigma_{v\ max}$ with added tires in *x*-direction (SHL case No. 3: LA-12T-16, 100 °F, PS 1).

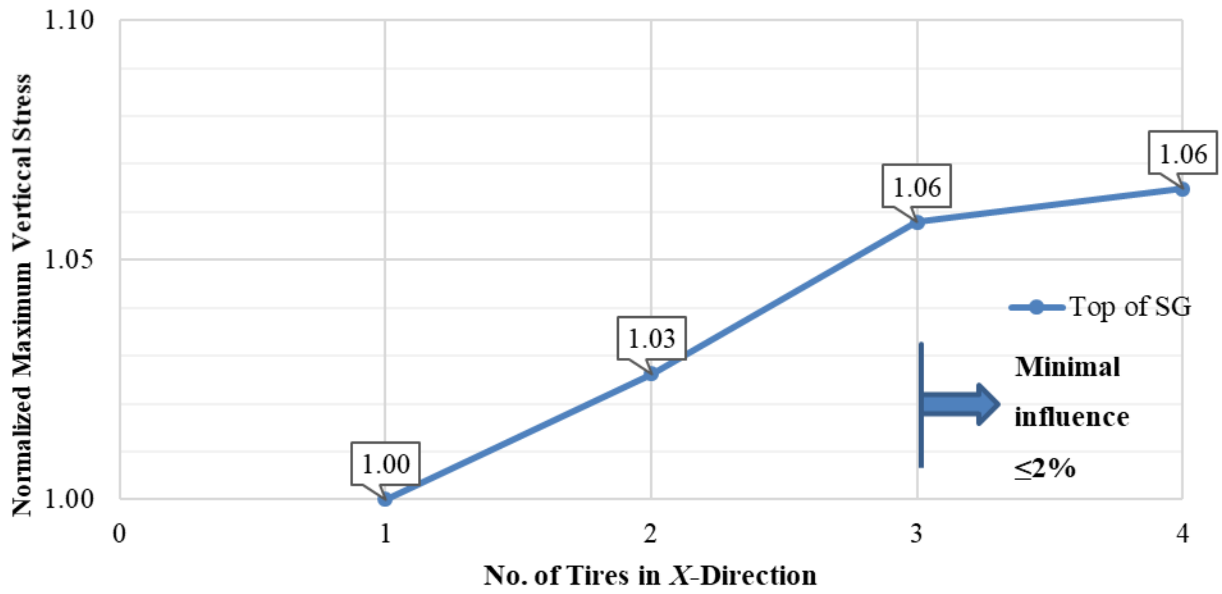

Figure 63. Chart. Change in normalized $\sigma_{v\,max}$ with added tires in *x*-direction (SHL case No. 3: LA-12T-16, 100 °F, PS 1).

Variation of σ_v *Distributions in* y-*Direction*

The values of $\sigma_{v\,max}$ and the normalized values of $\sigma_{v\,max}$ on top of SG with different combinations of tires are shown in figure 64 and figure 65.

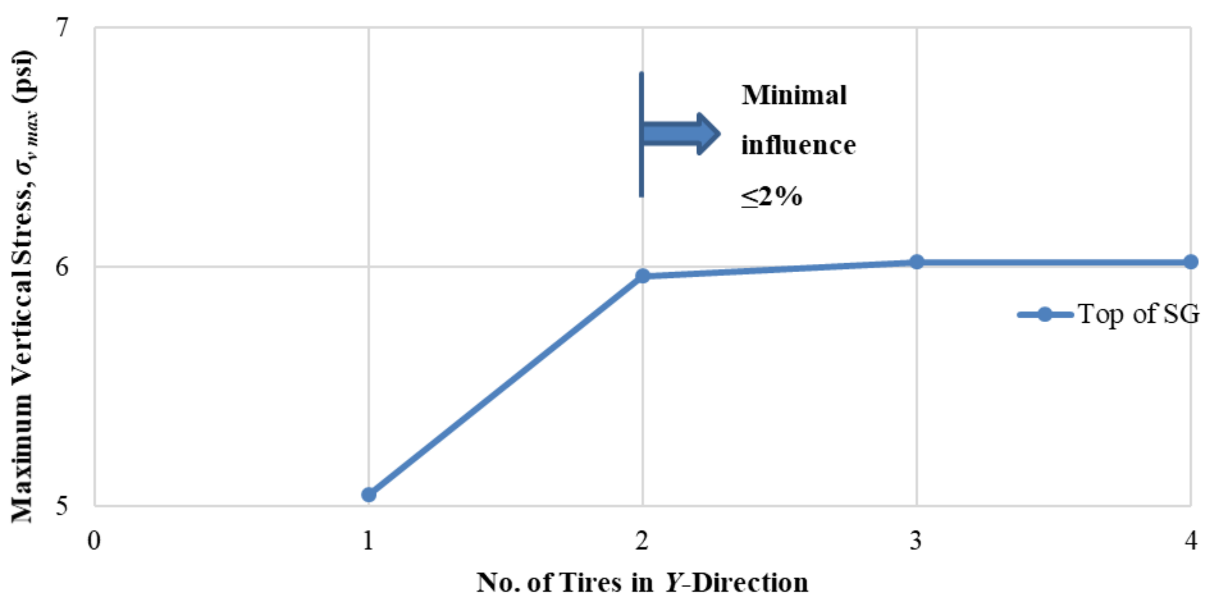

Figure 64. Chart. Change in $\sigma_{v\,max}$ with added tires in *y*-direction (SHL case No. 3: LA-12T-16, 100 °F, PS 1).

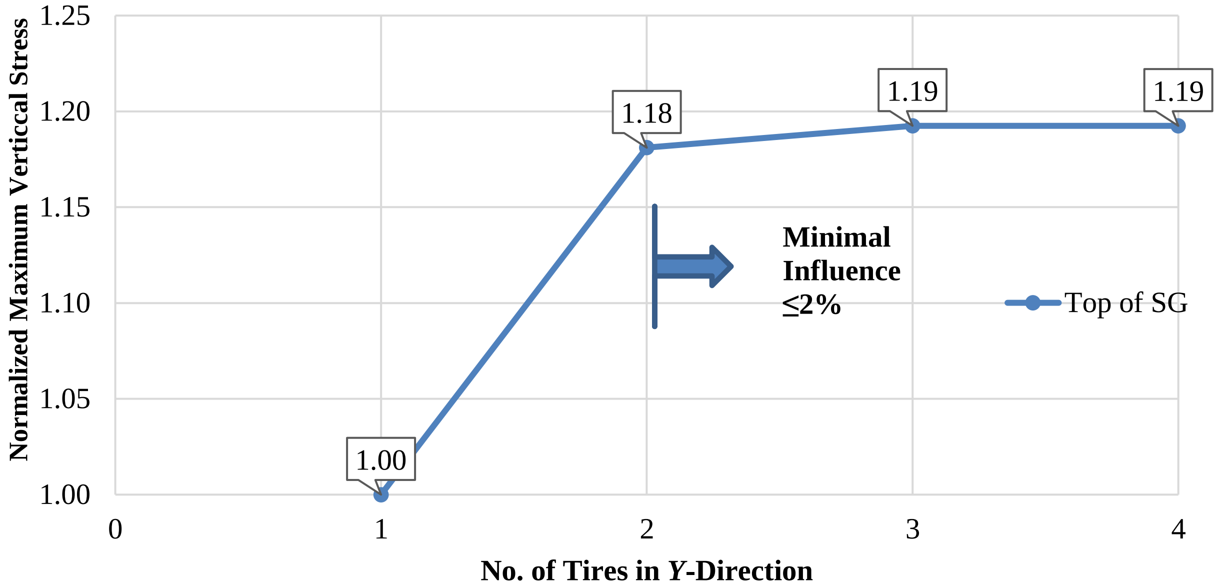

Figure 65. Chart. Change in normalized $\sigma_{v\,max}$ with added tires in *y*-direction (SHL case No. 3: LA-12T-16, 100 °F, PS 1).

In both directions, additional tires were considered until the new added tire had minimal influence on σ_v distribution computed with the first tire (lower than 2 percent). The nucleus for this case (SHL case No. 3, PS 1) consists of one additional tire in each direction. The representative nucleus of SHL axle configuration is shown in figure 66.

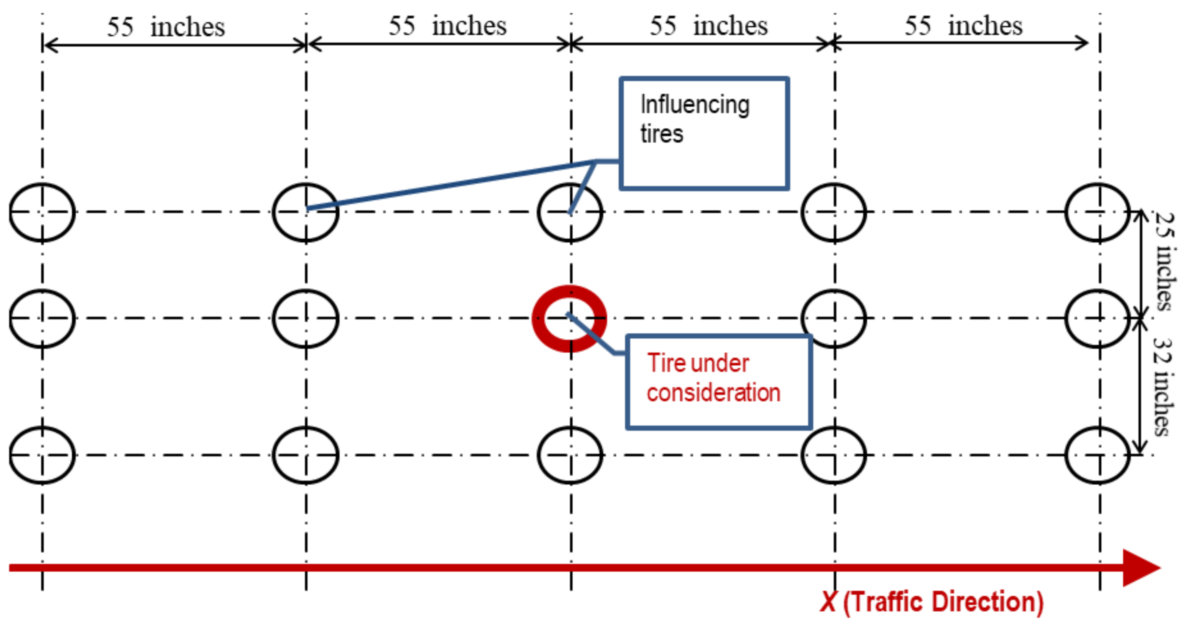

Figure 66. Chart. Representative nucleus (SHL case No. 3: LA-12T-16, 100 °F, PS 1).

Maximum Average Stress Using 3D-Move Analysis

σ_v distribution on top of SG due to the SHL axle configuration LA-12T-16 with the nucleus is shown in figure 67 (3D view) and figure 68 (top view).

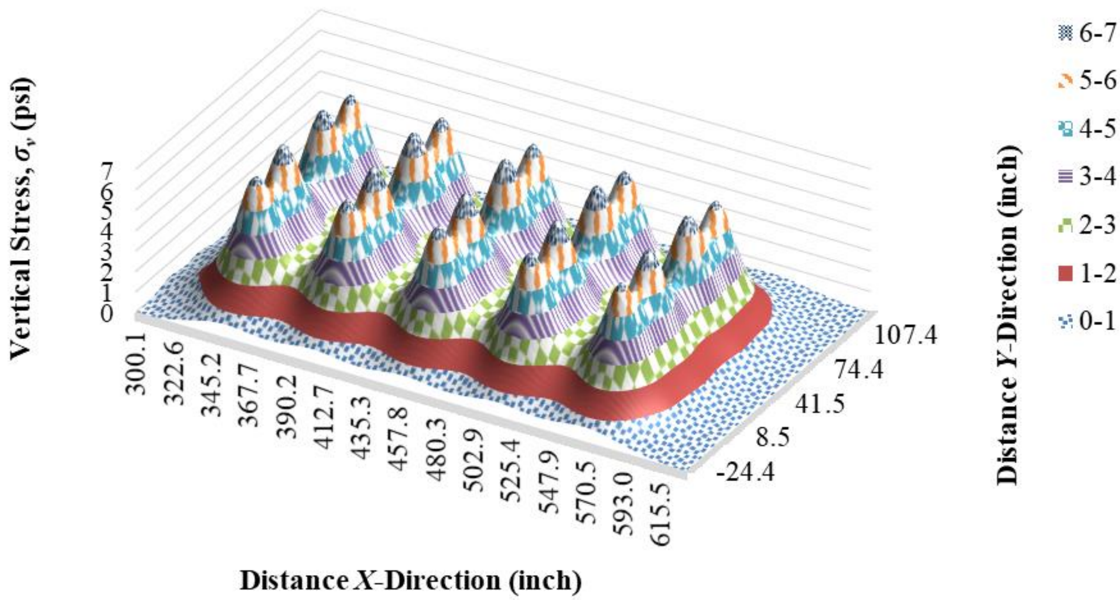

Figure 67. Chart. σ_v distribution on top of SG four by four tires (SHL case No. 3: LA-12T-16, 100 °F, PS 1)—3D view.

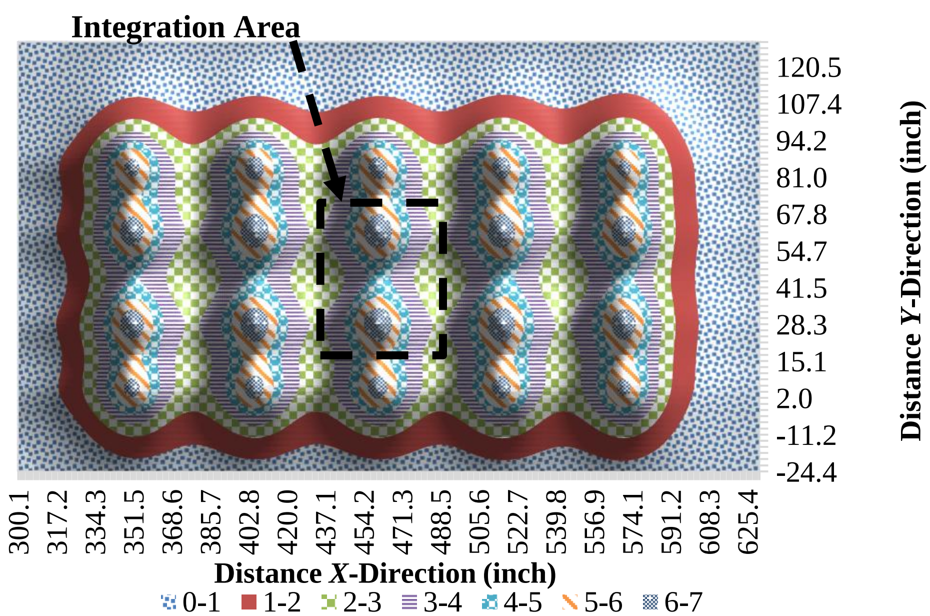

Figure 68. Chart. σ_v distribution on top of SG four by four tires (SHL case No. 3: LA-12T-16, 100 °F, PS 1)—top view.

These figures reveal that the peak amplitude, which occurs between the two tires (figure 67), was approximately 7.0 psi, whereas the amplitude at the adjacent valley was approximately 5.4 psi. In other words, the σ_v at the valley was approximately 77 percent of the peak σ_v.

3.2.3. Summary of Influence of Different SHL Configurations

Figure 69 and figure 70 show the change in $\sigma_{v\ max}$ with added tires in the *x*-direction and *y*-direction, respectively, for the three load cases evaluated. The results are summarized in table 19. The $\sigma_{v\ max}$ on top of SG was observed to increase with the increase of tire load.

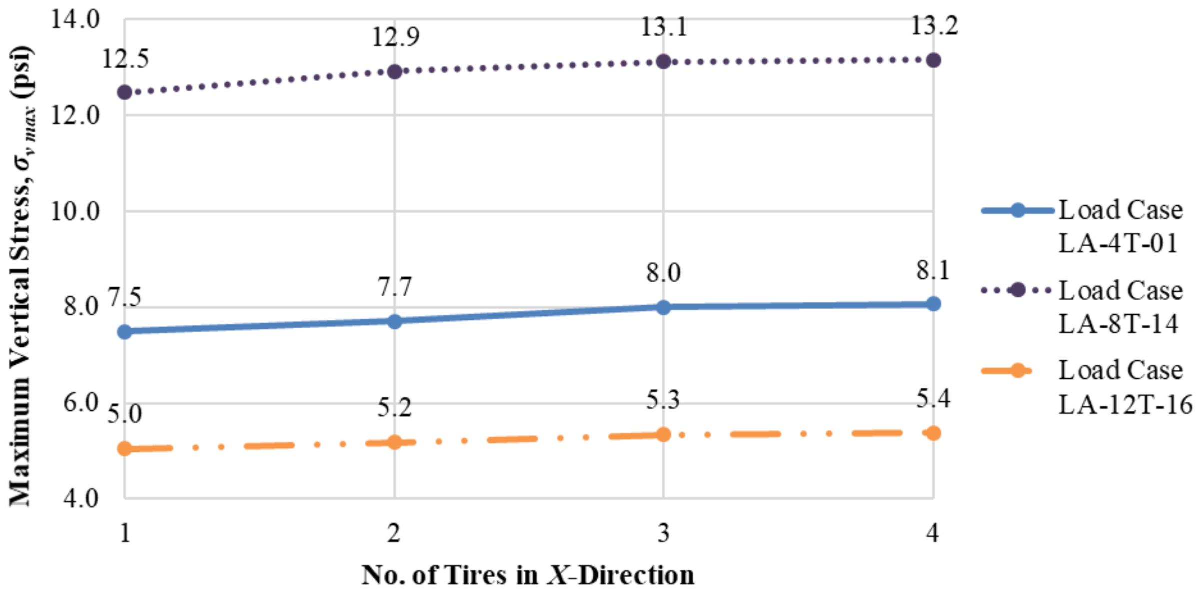

Figure 69. Chart. Change in $\sigma_{v\ max}$ with added tires in *x*-direction (all SHL cases, 100 °F, PS 1).

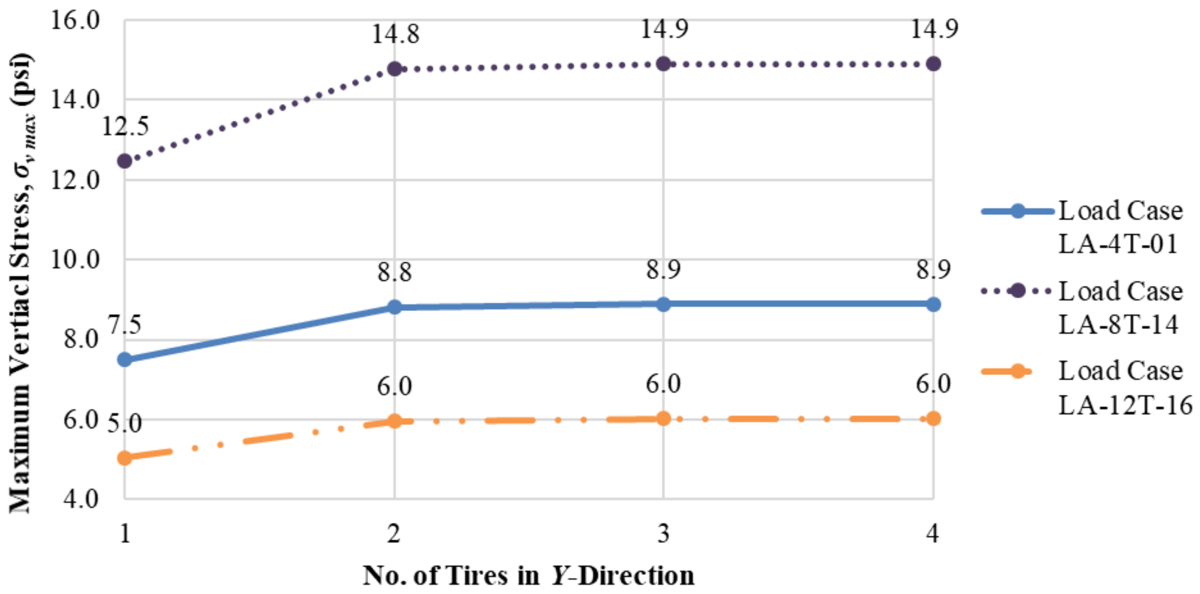

Figure 70. Chart. Change in $\sigma_{v\ max}$ with tires in *y*-direction (all SHL cases, 100 °F, PS 1).

Table 19. Summary of influence of different SHL configurations.

SHL-Vehicle Speed (mph)	SHL Configuration	Analysis Temperature (°F)	Pavement Structure	*Nx*	*Ny*	$\sigma_{v\ max}$ (psi)
10	SHL case No. 1: LA-4T-01	100	PS 1: 6-inch AC and 8-inch CAB	2	1	8.9
10	SHL case No. 2: LA-8T-14	100	PS 1: 6-inch AC and 8-inch CAB	1	1	14.9
10	SHL case No. 3: LA-12T-16	100	PS 1: 6-inch AC and 8-inch CAB	2	1	6.0

PS = pavement structure.

3.3. INFLUENCE OF ANALYSIS TEMPERATURE

The work presented so far considered 100 °F as the analysis temperature, representing the worst-case scenario relative to AC modulus among the three temperatures under consideration. A similar analysis was undertaken for the other two temperatures of 70 and 40 °F. A summary of the results is presented in this section. The SHL case considered for the temperature analyses presented in this section was LA-8T-14, and the pavement structure was PS 1 (6-inch AC, 8-inch CAB, and a semi-infinite SG layer). Figure 71 and figure 72 show the change in $\sigma_{v\ max}$ with added tires in the *x*- and *y*-directions for multiple temperatures. The results are summarized in table 20. The value of the $\sigma_{v\,max}$ on top of SG decreased, as the analysis temperature decreased. This was expected as the AC layer stiffness increases with the drops temperature.

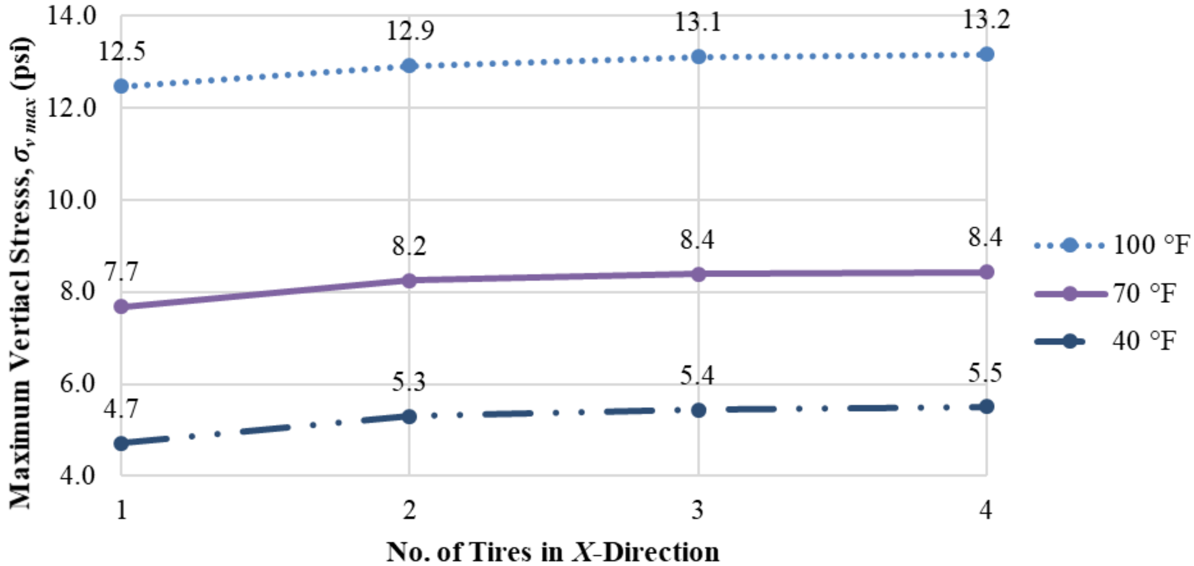

Figure 71. Chart. $\sigma_{v\,max}$ change with tires in *x*-direction for three temperatures.

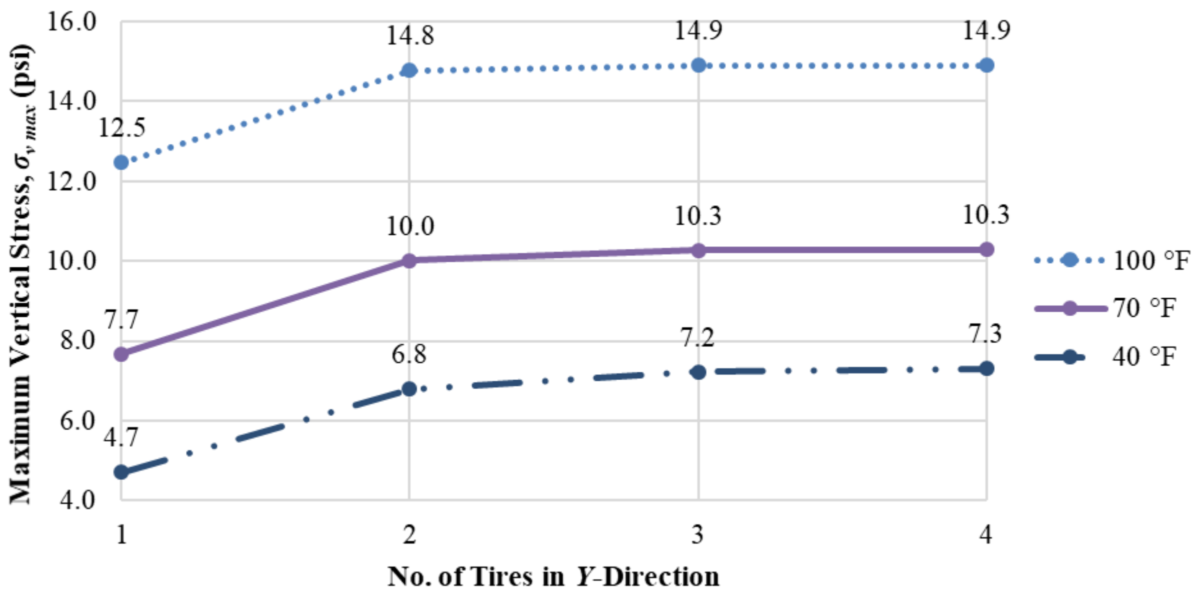

Figure 72. Chart. $\sigma_{v\,max}$ change with tires in *y*-direction for three temperatures.

Table 20. Summary of influence of analysis temperature.

SHL-Vehicle Speed (mph)	SHL-Vehicle Configuration	Analysis Temperature (°F)	Pavement Structure	*Nx*	*Ny*	σ_v *max* (psi)
10	SHL case No. 2: LA-8T-14	100	PS 1: 6-inch AC and 8-inch CAB	1	1	14.9
10	SHL case No. 2: LA-8T-14	70	PS 1: 6-inch AC and 8-inch CAB	1	2	10.3
10	SHL case No. 2: LA-8T-14	40	PS 1: 6-inch AC and 8-inch CAB	2	2	7.3

PS = pavement structure.

In both directions, additional tires were considered until the new added tire had minimal influence on the σ_v distribution computed under the first tire (lower than 2 percent). The nucleus for these two cases (70 and 40 °F) consists of one additional tire in each direction. The corresponding representative nucleus of the SHL axle configuration is shown in figure 73.

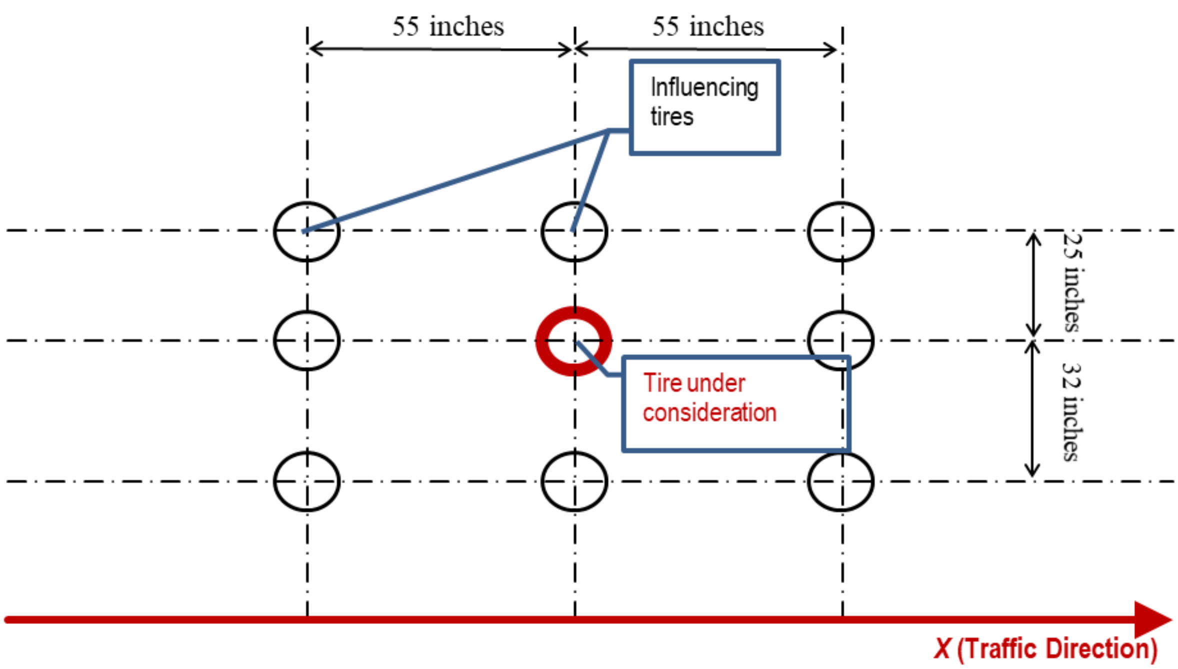

Figure 73. Chart. Representative nucleus of SHL axle configuration (70 °F, 40 °F).

3.4. SUMMARY OF SENSITIVITY ANALYSIS RESULTS

The factorial experiment results are presented in table 21. The influence of various pavement structure, load configurations, and pavement analysis temperatures on $\sigma_{v\ max}$ induced on top of SG and determination of the nucleus that can be used to represent axle group(s) are detailed.

Considering the change in $\sigma_{v\ max}$ with temperature and evaluated SHL cases, figure 74 presents the change in $\sigma_{v\ max}$ with temperature for the three pavement structures considered under SHL case No. 1 (LA-4T-1). The value of $\sigma_{v\ max}$ on top of SG was observed to decrease with the increase in pavement structure thicknesses, at the same time $\sigma_{v\ max}$ increased, as the analysis temperature increased. This corresponds to the increase in AC layer stiffness due to drop in temperature or increase in pavement structure thicknesses. A similar trend is observed in figure 75 under SHL case No. 2 (LA-8T-14) and figure 76 under SHL case No. 3 (LA-12T-16).

The factorial experiment results are presented in table 21 and figure 77. The influence of various pavement structure, load configurations, and pavement analysis temperatures on $\sigma_{v\ max}$ and the SHL nucleus were considered in this experiment.

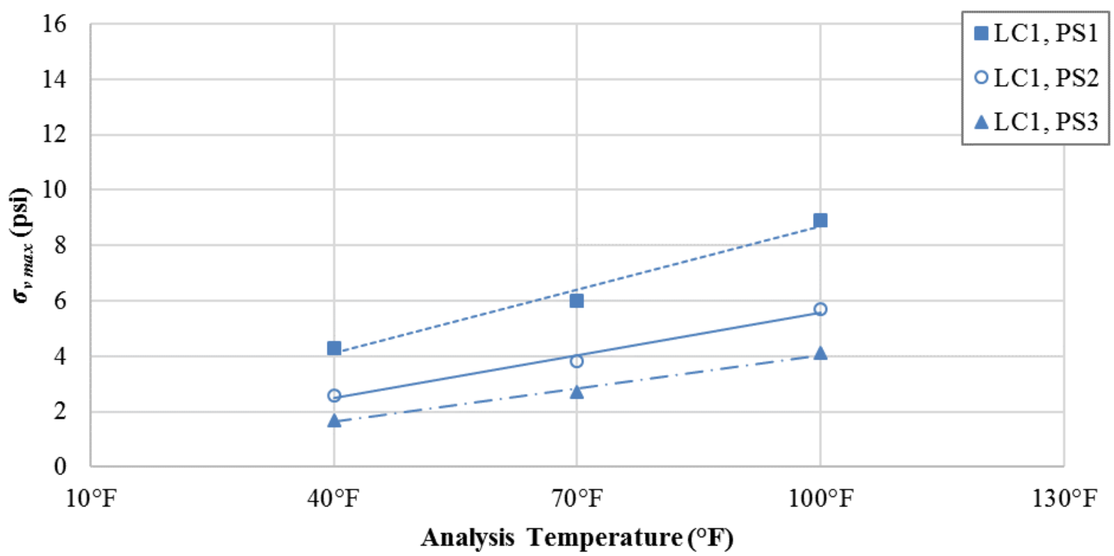

LC = load configuration.

Figure 74. Chart. Change in $\sigma_{v\ max}$ with temperature for various pavement structures (SHL case No. 1: LA-4T-1).

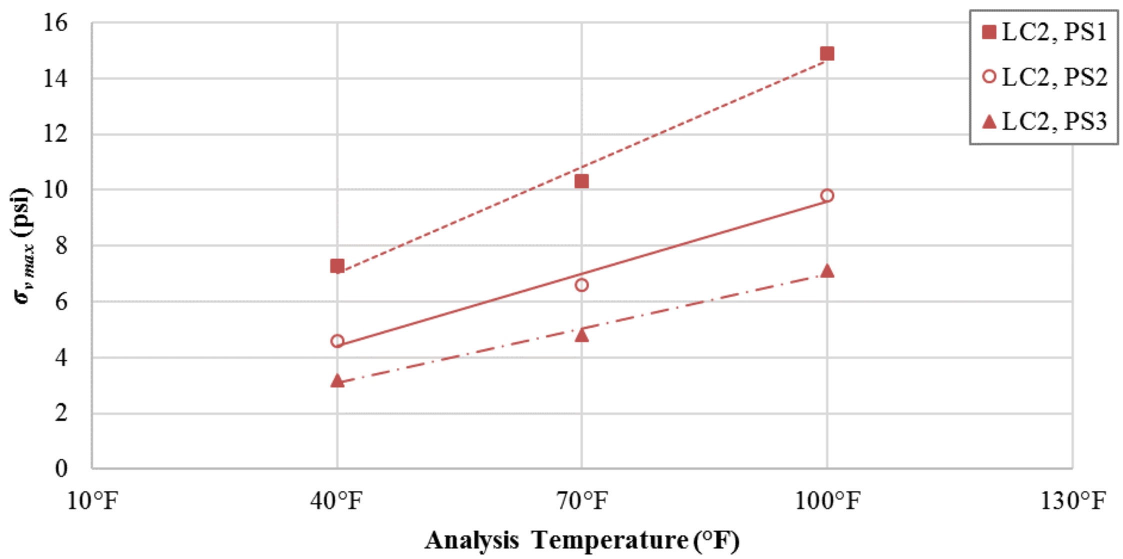

© 2018 UNR.
LC = load configuration.

Figure 75. Chart. Change in $\sigma_{v\ max}$ with temperature for various pavement structures (SHL case No. 2: LA-8T-14).

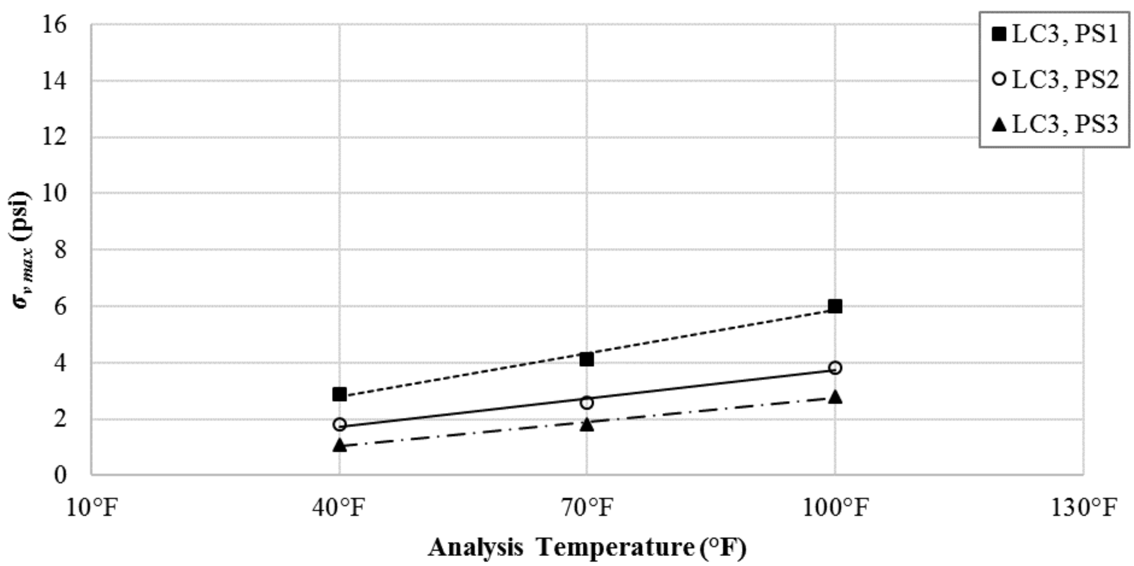

© 2018 UNR.
LC = load configuration.

Figure 76. Chart. Change in $\sigma_{v\ max}$ with temperature for various pavement structures (SHL case No. 3: LA-12T-16).

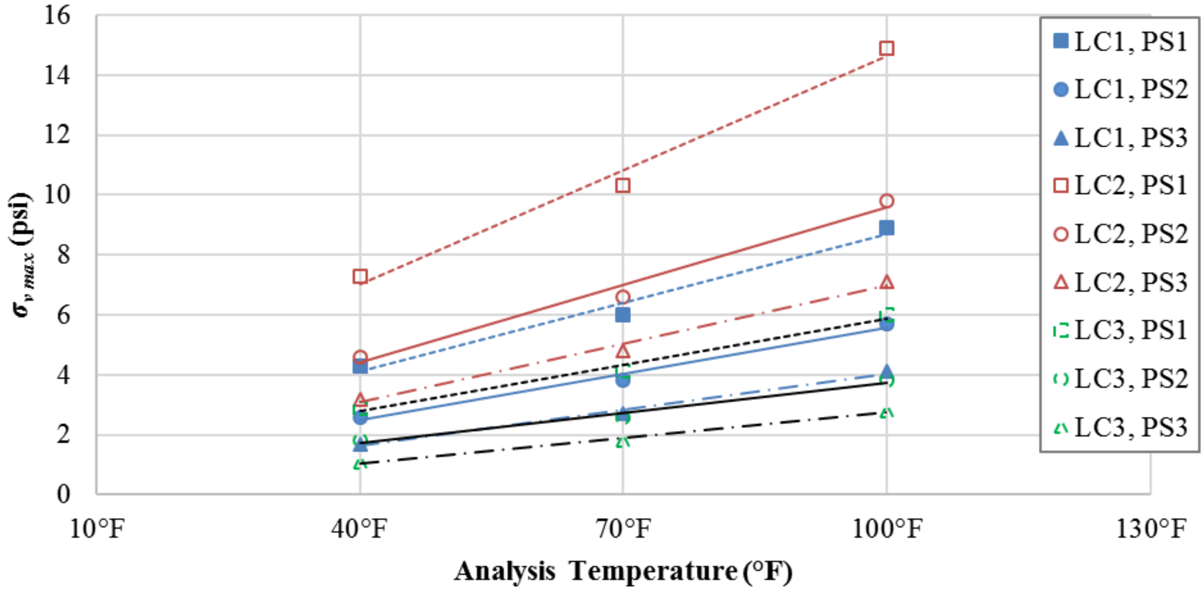

LC = load configuration.

Figure 77. Chart. Change in $\sigma_{v\,max}$ with temperature for various pavement structures and SHL cases.

Table 21. Summary of sensitivity analysis results (nucleus size).

SHL-Vehicle Speed (mph)	SHL Configuration Load Case	Analysis Temperature (°F)	Pavement Structure	*Nx*	*Ny*	q_{ave} (psi)
10	No. 1: LA-4T-01	100	PS 1: 6-inch AC and 8-inch CAB	2	1	8.9
10	No. 1: LA-4T-01	100	PS 2: 9-inch AC and 10-inch CAB	2	2	5.7
10	No. 1: LA-4T-01	100	PS 3: 12-inch AC and 12-inch CAB	2	3	4.1
10	No. 1: LA-4T-01	70	PS 1: 6-inch AC and 8-inch CAB	2	2	6.0
10	No. 1: LA-4T-01	70	PS 2: 9-inch AC and 10-inch CAB	2	3	3.8
10	No. 1: LA-4T-01	70	PS 3: 12-inch AC and 12-inch CAB	2	3	2.7
10	No. 1: LA-4T-01	40	PS 1: 6-inch AC and 8-inch CAB	1	2	4.3
10	No. 1: LA-4T-01	40	PS 2: 9-inch AC and 10-inch CAB	2	2	2.6
10	No. 1: LA-4T-01	40	PS 3: 12-inch AC and 12-inch CAB	4	3	1.7
10	No. 2: LA-8T-14	100	PS 1: 6-inch AC and 8-inch CAB	1	1	14.9
10	No. 2: LA-8T-14	100	PS 2: 9-inch AC and 10-inch CAB	2	2	9.8
10	No. 2: LA-8T-14	100	PS 3: 12-inch AC and 12-inch CAB	2	1	7.1
10	No. 2: LA-8T-14	70	PS 1: 6-inch AC and 8-inch CAB	1	2	10.3
10	No. 2: LA-8T-14	70	PS 2: 9-inch AC and 10-inch CAB	2	3	6.6
10	No. 2: LA-8T-14	70	PS 3: 12-inch AC and 12-inch CAB	2	3	4.8
10	No. 2: LA-8T-14	40	PS 1: 6-inch AC and 8-inch CAB	2	2	7.3
10	No. 2: LA-8T-14	40	PS 2: 9-inch AC and 10-inch CAB	2	4	4.6
10	No. 2: LA-8T-14	40	PS 3: 12-inch AC and 12-inch CAB	4	4	3.2
10	No. 3: LA-12T-16	100	PS 1: 6-inch AC and 8-inch CAB	2	1	6.0
10	No. 3: LA-12T-16	100	PS 2: 9-inch AC and 10-inch CAB	2	2	3.8
10	No. 3: LA-12T-16	100	PS 3: 12-inch AC and 12-inch CAB	3	4	2.8
10	No. 3: LA-12T-16	70	PS 1: 6-inch AC and 8-inch CAB	2	2	4.1
10	No. 3: LA-12T-16	70	PS 2: 9-inch AC and 10-inch CAB	3	4	2.6
10	No. 3: LA-12T-16	70	PS 3: 12-inch AC and 12-inch CAB	3	4	1.8
10	No. 3: LA-12T-16	40	PS 1: 6-inch AC and 8-inch CAB	3	4	2.9
10	No. 3: LA-12T-16	40	PS 2: 9-inch AC and 10-inch CAB	3	4	1.8
10	No. 3: LA-12T-16	40	PS 3: 12-inch AC and 12-inch CAB	4	4	1.1

PS = pavement structure.

CHAPTER 4. AXLE GROUPING FOR AN SHL VEHICLE

The nucleus of an SHL analysis vehicle is a segment (or element) of the axle-load configuration that can be regarded as representative of the entire SHL truck. Subsequently, σ_v distribution (or any other pavement response) under the entire SHL configuration can be estimated by superimposing the stresses calculated under the nucleus, eliminating the need to model the entire SHL. However, SHL vehicles vary in terms of axle configuration (i.e., number of axles, spacing between the axles, number of tires per axle, spacing between the tires, tire load, etc.).

In general, SHL vehicles fall under three categories. In the first category, similar axles (i.e., similar number of tires per axle, spacing between the tires, and tire load) are evenly distributed along the entire length of the SHL unit. In this category, the spacing between the axles is close enough that the stress distributions from the tires on two adjacent axles clearly overlap beyond a specific depth (e.g., top of SG). For instance, in the LA-8T-14 permit (figure 40 and figure 78), similar axles were evenly distributed with the spacing of 4.6 ft along the entire length of the SHL unit. In this case, all the axles can be treated as belonging to one group, and the identification of the nucleus can be initiated for this single group.

In the second category, the SHL unit consists of two or more separate dollies, which have a large gap between them relative to the spacing between the axles present within the dollies. As shown in figure 79 (permit shown in figure 41), the SHL unit in the LA-12T-16 permit consisted of 4 individual dollies, and each dolly had 6 axles and 12 tires per axle. The spacing between the dollies was as much as 38 ft. In such a case, each dolly should be considered as one group (i.e., a total of four groups). The nucleus for each group should be subsequently determined.

The third category covers general cases with any axle configuration. Figure 80 shows a schematic of an SHL-vehicle configuration retrieved from an NDOT permit. It can be seen that different axles (single, tandem, and tridem) with different spacings were used in this SHL vehicle. In this case, there are many axle groups, and each group can have separate nucleus.

In order to accommodate all three categories outlined above, two or more axles that are able to meet the following criteria are defined as one group. In other words, they belong to a single group of axles:

- Similar number of tires per axle.
- Similar spacing between tires.
- Similar tire load.
- Spacing between the axles less than 60 inches.

Previous studies revealed that, when the spacing between two adjacent axles is greater than 60 inches, there is no significant interaction between the tires.[15,16] It should be mentioned that, when the pavement responses from a standard truck are evaluated, the tire group present on only one side of the truck is considered, which means that the influence of the tire group in the transverse direction is not included.

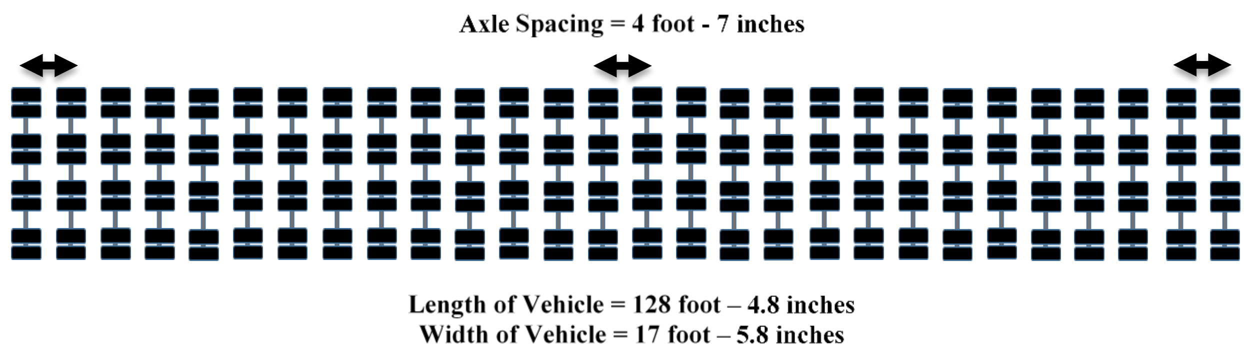

Figure 78. Illustration. Example configuration of a permitted SHL vehicle (LA-8T-14).

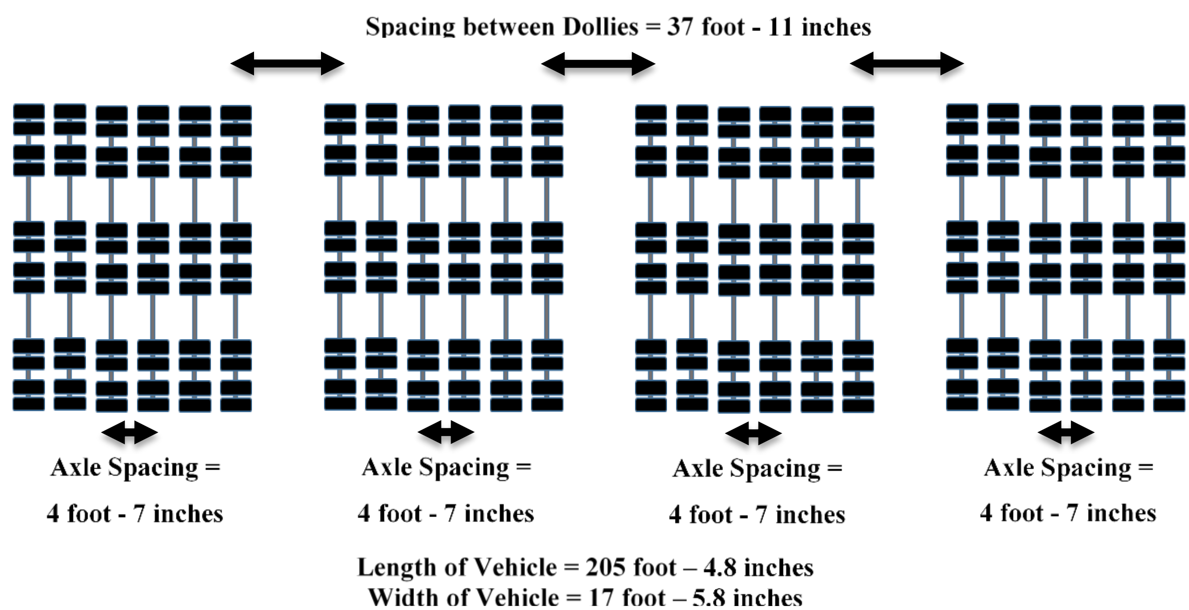

Figure 79. Illustration. Example configuration of a permitted SHL vehicle (LA-12T-16).

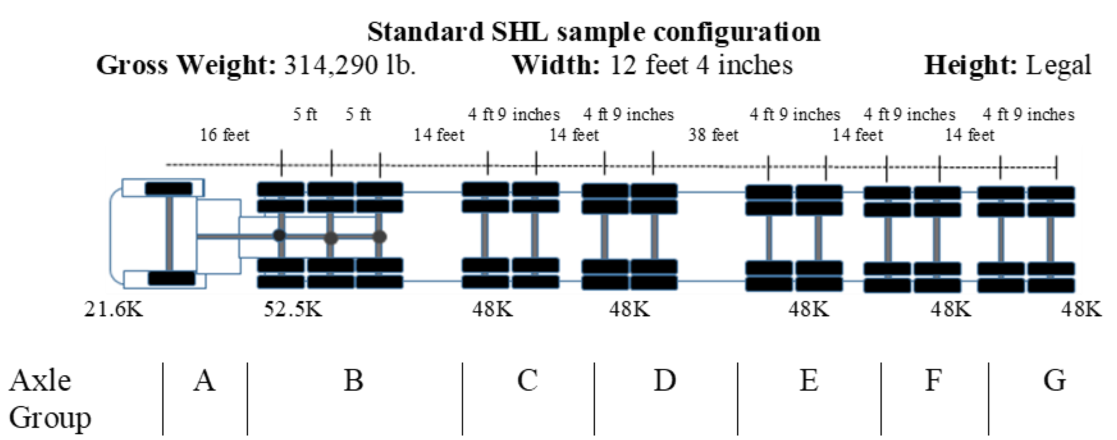

Figure 80. Illustration. Example configuration of a permitted SHL truck in Nevada.

In summary, axle grouping is used to define the groups within the SHL-vehicle domain that contain axle(s) with identical configurations and spacing between the axles of less than 60 inches. Subsequently, for each axle group, the associated nucleus that is the representative element of the axle group is determined. For instance, the axle configuration for the SHL vehicle shown in figure 80 is divided into seven axle groups: the steering single axle, a tridem axle, and five tandem axles.

The axle grouping and nucleus are the required inputs for the developed analysis procedures. The critical axle group, which is defined by the highest induced σ_v under its nucleus, is first determined. This critical axle group is subsequently employed to compute the state of stresses in the unbound layers, leading to the determination of representative material properties for these layers. The nucleus of each axle group is then used to investigate the likelihood of ultimate shear failure in the SG. However, service limit analyses, including localized shear failure analysis and deflection-based service limit analysis, are conducted for the critical axle group as a conservative measure. In addition, slope stability analysis as well as buried utility risk analysis use the stresses induced by the nucleus of the critical axle group. However, in the cost allocation analysis, the nuclei of all axle groups need to be considered, since the cost associated with each axle group needs to be accumulated.

CHAPTER 5. OVERALL SUMMARY

SHL hauling units require specialized trailers and components to suit the superheavy components being transported. Although the tires used in the transport are often conventional, the axle and tire configurations are variable. Examples of typical tire and axle loads and configurations for SHL vehicles were collected and summarized. A wide range of axle weights and spacing as well as tire widths and loads were observed.

To model SHL-vehicle movements on flexible pavements while considering the nonstandard axle and tire configurations, a novel approach to identifying element(s) of SHL configurations that can be regarded as representative of the entire SHL vehicle (referred to as the nucleus) has been presented. σ_v distribution (or any other pavement response) under the entire SHL configuration can be estimated by superimposing the stresses calculated under the nucleus, eliminating the need to model the entire SHL vehicle.

A factorial experiment has been presented to assess the procedure sensitivity to different pavement structures, SHL-vehicle cases, and pavement analysis temperatures. $\sigma_{v\ max}$ induced on top of SG due to the SHL vehicle's nucleus is the main focal point of this assessment. The value of the $\sigma_{v,max}$ on top of SG was observed to decrease with the increase in pavement structure thickness, the decrease in tire load(s), and the decrease in the AC analysis temperature.

Procedures for handling uniform axle and tire spacing of SHL vehicles as well as special SHL cases have been presented. Three categories of SHL vehicles were identified based on their axle and tire configurations: SHL vehicles with uniform axles (i.e., similar number of tires per axle, spacing between the tires, and tire load); SHL units consisting of two or more separate dollies where the gaps between the dollies are relatively large in comparison with the spacing between the axles present within the dollies; and general cases with any axle configuration. A case from each of the three categories has been presented.

REFERENCES

1. Hajj, E.Y., Siddharthan, R.V., Nabizadeh, H., Elfass, S., Nimeri, M., Kazemi, S.F., Batioja-Alvarez, D.D., and Piratheepan, M. (2018). *Analysis Procedures for Evaluating Superheavy Load Movement on Flexible Pavements, Volume I: Final Report,* Report No. FHWA-HRT-18-049, Federal Highway Administration, Washington, DC.

2. Nimeri, M., Nabizadeh, H., Hajj, E.Y., Siddharthan, R.V., Elfass, S, and Piratheepan, M. (2018). *Analysis Procedures for Evaluating Superheavy Load Movement on Flexible Pavements, Volume II: Appendix A, Experimental Program*, Report No. FHWA-HRT-18-050, Federal Highway Administration, Washington, DC.

3. Nabizadeh, H., Hajj, E.Y., Siddharthan, R.V., and Elfass, S. (2018). *Analysis Procedures for Evaluating Superheavy Load Movement on Flexible Pavements, Volume IV: Appendix C, Material Characterization for Superheavy Load Movement Analysis*, Report No. FHWA-HRT-18-052, Federal Highway Administration, Washington, DC.

4. Nabizadeh, H., Hajj, E. Y., Siddharthan, R. V., Nimeri, M., Elfass, S., and Piratheepan, M. (2018). *Analysis Procedures for Evaluating Superheavy Load Movement on Flexible Pavements, Volume V: Appendix D, Estimation of Subgrade Shear Strength Parameters Using Falling Weigh Deflectometer*, FHWA-HRT-18-053, Federal Highway Administration, Washington, DC.

5. Nabizadeh, H., Nimeri, M., Hajj, E.Y., Siddharthan, R.V., Elfass, S., and Piratheepan, M. (2018). *Analysis Procedures for Evaluating Superheavy Load Movement on Flexible Pavements, Volume VI: Appendix E, Ultimate and Service Limit Analyses,* Report No. FHWA-HRT-18-054, Federal Highway Administration, Washington, DC.

6. Nabizadeh, H., Siddharthan, R.V., Elfass, S., and Hajj, E.Y. (2018). *Analysis Procedures for Evaluating Superheavy Load Movement on Flexible Pavements, Volume VII: Appendix F, Failure Analysis of Sloped Pavement Shoulders*, Report No. FHWA-HRT-18-055, Federal Highway Administration, Washington, DC.

7. Nabizadeh, H., Elfass, S., Hajj, E.Y., Siddharthan, R.V., Nimeri, M., and Piratheepan, M. (2018). *Analysis Procedures for Evaluating Superheavy Load Movement on Flexible Pavements, Volume VIII: Appendix G, Risk Analysis of Buried Utilities Under SHL Vehicle Moves*, Report No. FHWA-HRT-18-056, Federal Highway Administration, Washington, DC.

8. Batioja-Alvarez, D.D., Hajj, E.Y., and Siddharthan, R.V. (2018). *Analysis Procedures for Evaluating Superheavy Load Movement on Flexible Pavements, Volume IX: Appendix H, Analysis of Cost Allocation Associated With Pavement Damage Under a Superheavy Load Vehicle Move*, Report No. FHWA-HRT-18-057, Federal Highway Administration, Washington, DC.

9. Kazemi, S.F., Nabizadeh, H., Nimeri, M., Batioja-Alvarez, D.D., Hajj, E.Y., Siddharthan, R.V., and Hand, A.J.T. (2018). *Analysis Procedures for Evaluating Superheavy Load Movement on Flexible Pavements, Volume X: Appendix I, Analysis Package for Superheavy Load Vehicle Move on Flexible Pavement (SuperPACK)*, Report No. FHWA-HRT-18-058, Federal Highway Administration, Washington, DC.

10. Arizona Department of Transportation. "Class C Permits." (website) Arizona Department of Transportation, Phoenix, AZ. Available online: https://www.azdot.gov/business/Permits/class-c-permits, last accessed October 23, 2018.

11. Far, B. (2015). *Policy for Evaluating the Colorado Bridge Weight Limit Map for Over-Wide Overweight Vehicles*, Memorandum, Colorado Department of Transportation, Division of Project Support, Denver, CO. Available online: https://www.codot.gov/business/permits/truckpermits/documents-1/DoubleDollyWeightChart.pdf, last accessed October 19, 2017.

12. 3D-Move Analysis software® V2.1. (2013). Developed by University of Nevada, Reno, NV. Available online: http://www.arc.unr.edu/Software.html#3DMove, last accessed September 19, 2017.

13. Siddharthan, R.V., Yao, J., and Sebaaly, P.E. (1998). "Pavement Strain From Moving Dynamic 3D Load Distribution." *Journal of Transportation Engineering*, *124*(6), pp. 557–566, American Society of Civil Engineers, Reston, VA.

14. Hajj, E.Y., Ulloa, A., Siddharthan, R., and Sebaaly, P.E. (2010). "Estimation of Stress Conditions for the Flow Number Simple Performance Test." *Transportation Research Record*, *2181*, pp. 67–78, Transportation Research Board, Washington, DC.

15. Luo, R., Gu, F., Luo, X., Lytton R.L., Hajj, E.Y., Siddharthan, R., Elfass, S., Piratheepan, M., and Pournoman, S. (2017). *Quantifying the Influence of Geosynthetics on Pavement Performance*, NCHRP Project 1-50, National Academy of Sciences, Washington, DC.

16. Rada, G.R., Nazarian, S., Visintine, B. A., Siddharthan, R., and Thyagarajan, S. (2016). *Pavement Structural Evaluation at the Network Level*, Report No. FHWA-HRT-15-074, Federal Highway Administration, Washington, DC.

HRDI-20/12-18(WEB)E